
Electronic Thesis and Dissertation Repository

7-21-2015 12:00 AM

The role of bone sialoprotein in the tendon-bone insertion

Ryan M. Marinovich, *The University of Western Ontario*


Supervisor: Dr. Harvey Goldberg, *The University of Western Ontario*

Joint Supervisor: Dr. Frank Beier, *The University of Western Ontario*

A thesis submitted in partial fulfillment of the requirements for the Master of Science degree in Biochemistry

© Ryan M. Marinovich 2015

Follow this and additional works at: <https://ir.lib.uwo.ca/etd>

 Part of the [Biochemistry Commons](#), [Medical Biochemistry Commons](#), [Musculoskeletal, Neural, and Ocular Physiology Commons](#), and the [Orthopedics Commons](#)

Recommended Citation

Marinovich, Ryan M., "The role of bone sialoprotein in the tendon-bone insertion" (2015). *Electronic Thesis and Dissertation Repository*. 2953.

<https://ir.lib.uwo.ca/etd/2953>

This Dissertation/Thesis is brought to you for free and open access by Scholarship@Western. It has been accepted for inclusion in Electronic Thesis and Dissertation Repository by an authorized administrator of Scholarship@Western. For more information, please contact wlsadmin@uwo.ca.

ROLE OF BONE SIALOPROTEIN IN THE TENDON-BONE INSERTION

(Thesis format: Integrated-Article)

By

Ryan Michael Marinovich

Graduate Program in Biochemistry

A thesis submitted in partial fulfillment

of the requirements for the degree of

Master of Science

The School of Graduate and Postdoctoral Studies

The University of Western Ontario

London, Ontario, Canada

© Ryan M. Marinovich 2015

ABSTRACT

Tendons and ligaments insert into bone through a transitional tissue termed the enthesis which is susceptible to injury and difficult to repair. Entheses contain a region of calcified fibrocartilage (CFC), however mineral-associated proteins in this tissue remain poorly characterized. Bone sialoprotein (BSP) is a phosphoprotein associated with mineralizing tissues. In these studies BSP was identified in the CFC of entheses by immunohistochemistry. Analysis of the entheses of *Bsp*^{-/-} mice indicate abnormalities in the CFC. Compared to controls, the CFC of the quadriceps tendon enthesis is 28% and 41% longer in 15 week and 14 month old *Bsp*^{-/-} mice, respectively. MicroCT and Raman spectroscopic analysis of the CFC in *Bsp*^{-/-} mice demonstrate that mineral content is similar between genotypes. Mechanical studies show that the *Bsp*^{-/-} patellar tendon is larger in cross-sectional area yet mechanically weaker. These data suggest BSP is involved in the regulation and growth of the CFC.

KEYWORDS

Bone sialoprotein, enthesis, calcified fibrocartilage, tendon-bone insertion, mineralization

STATEMENT OF CO-AUTHORSHIP

Chapter 2, entitled “Identification of bone sialoprotein in enthesis fibrocartilage and characterization of *Bsp*^{-/-} fibrocartilaginous enthesis” was adapted from Marinovich *et al.* (2015) (in preparation). MicroCT scanning and subsequent data analysis was performed by Yohannes Soenjaya. Raman spectroscopy on samples prepared by Ryan Marinovich were performed by Greg Wallace (Dr. F. Laguné-Labarhet). Mechanical studies, on specimens prepared by Yohannes Soenjaya, and subsequent data analysis was performed by Andrew Dunkman and Andrew Zuskov (Dr. Lou Soslowsky)

Chapter 3, entitled “Elucidating the role of bone sialoprotein in the murine enthesis during development and age”. All work and experiments were performed by Ryan Marinovich.

ACKNOWLEDGEMENTS

I would like to thank my family, Mom, Dad, Mitch and Baba for the constant love and support they have given me over the years. I wouldn't be the person I am today without their influence and guidance in life. Knowing that I'm making you proud in London has been a huge motivation for me to continue on, especially when times are difficult.

Nancy, your love and support have gotten me through some of my most difficult times. You've helped me accomplish things I never thought myself capable of and I wouldn't be the man I am today without you in my life. I love you very much.

I would like thank my supervisor, Dr. Harvey "The Boss" Goldberg for the mentorship and guidance he's given me over the years. Not only has he been an invaluable asset to my research, he has also provided me with numerous life lessons, and has had an undoubtable influence on me and my professional life as I move forward in my education.

I would like to acknowledge my co-supervisor, Dr. Frank Beier, and my advisory committee members Drs. Graeme Hunter and Alan Getgood for the advice and guidance they have provided to me during my graduate studies. I would also like to acknowledge Linda Jackson for her expertise in histology, and Wendy Dunn, who provided expertise in the care of our animals.

The members of the Goldberg lab, past and present: Kevin Bartman, Yohannes Soenjaya, Dr. Erik Holm, Vida Lam, Dorchester, Lim Tang, Rose Yee and last but certainly not least Heidi Liao, thank you for all the advice, memories and support. Grad

school would not have been what it was for me without you, and I'll always look back on our time together with fond memories.

TABLE OF CONTENTS

ABSTRACT.....	ii
STATEMENT OF CO-AUTHORSHIP	iii
ACKNOWLEDGEMENTS	iv
TABLE OF CONTENTS.....	vi
LIST OF FIGURES	ix
LIST OF TABLES	xi
LIST OF APPENDICES.....	xii
LIST OF ABBREVIATIONS.....	xiii
CHAPTER ONE: LITERATURE REVIEW	1
1.1 Mineralized Tissues.....	2
1.2 Biomineralization.....	4
1.3 SIBLINGs.....	4
1.4 Bone Sialoprotein.....	6
1.4.1 <i>Structure</i>	6
1.4.2 <i>Collagen Binding</i>	9
1.4.3 <i>Hydroxyapatite Binding and Nucleation</i>	10
1.4.4 <i>Cell Attachment and Signaling</i>	11
1.4.5 <i>Tissue Distribution and Expression</i>	12
1.4.6 <i>In Vivo Function</i>	13
1.5 The Enthesis	15
1.5.1 <i>Fibrous Entheses</i>	16
1.5.2 <i>Fibrocartilaginous Entheses</i>	16
1.5.3 <i>Development</i>	23
1.5.4 <i>Tissue Injury and Healing</i>	27
1.6 Purpose of Thesis	29
1.7 References	30
CHAPTER TWO: IDENTIFICATION OF BONE SIALOPROTEIN IN ENTESIS FIBROCARILAGE AND CHARACTERIZATION OF THE BSP-/ FIBROCARILAGINOUS ENTESIS	42
2.1 Chapter Summary.....	43

2.2	Introduction	45
2.3.	Materials and Methods	48
2.3.1	<i>Animals</i>	48
2.3.2	<i>Histology and Immunohistochemistry</i>	48
2.3.3	<i>Measurement of the calcified fibrocartilage zone</i>	50
2.3.4	<i>Mechanical testing</i>	51
2.3.5	<i>Microcomputed Tomography</i>	52
2.3.6	<i>Raman spectroscopy</i>	52
2.3.7	<i>Statistical analyses</i>	53
2.4	Results	54
2.4.1	<i>BSP and OPN are present in the mineralized tissues of fibrocartilaginous entheses</i> 54	
2.4.2	<i>Bsp^{-/-} mice exhibit defects in calcified fibrocartilage zone of the enthesis</i> . 54	
2.4.3	<i>Mechanical testing suggests a weakened enthesis in Bsp^{-/-} mice</i>	64
2.4.4	<i>Collagen organization is not affected by the loss of BSP</i>	64
2.5	Discussion	70
2.5.1	<i>Role of altered calcified fibrocartilage zone of the Bsp^{-/-} QCT enthesis</i>	70
2.5.2	<i>Bsp^{-/-} patellar tendon exhibit weakened mechanical properties under load</i> . 73	
2.6	References	75
CHAPTER THREE: ELUCIDATING THE ROLE OF BONE SIALOPROTEIN IN THE MURINE ENTHESIS DURING DEVELOPMENT AND AGEING		79
3.1	Chapter Summary.....	80
3.2	Introduction	82
3.3	Materials and Methods	84
3.3.1	<i>Animals</i>	84
3.3.1	<i>Histology and Immunohistochemistry</i>	84
3.4	Results	86
3.4.1	<i>Age 14 months</i>	86
3.4.2	<i>Age 14 and 21 days</i>	96
3.5	Discussion	117
3.5.1	<i>14 months</i>	117
3.5.2	<i>14 and 21 days</i>	119

3.6	References	122
CHAPTER FOUR: GENERAL DISCUSSIONS AND CONCLUSIONS		123
4.1	Summary and Perspectives.....	124
4.2	Limitations of Research and Future Directions.....	126
4.2.1	<i>Phenotypic differences in different entheses and the role of muscle loading</i> 126	
4.2.2	<i>Establishing the expression of BSP in the enthesis.....</i>	127
4.2.3	<i>Other potential mineralization factors in the enthesis.....</i>	130
4.3	Conclusions	133
4.4	References	134
APPENDIX A: Animal Use Ethics Statement.....		137
APPENDIX B: Copyright Holder Permissions		138
CURRICULUM VITAE.....		139

LIST OF FIGURES

Figure 1.1 Schematic of bone sialoprotein.....	8
Figure 1.2 Anatomical location of selected fibrocartilaginous entheses.....	19
Figure 1.3 The transitional zones of the fibrocartilaginous enthesis.....	21
Figure 2.1 SIBLING proteins are present in the calcified fibrocartilage of the SST and QCT entheses.....	56
Figure 2.2 Mineral is deposited in the calcified fibrocartilage of <i>Bsp</i> ^{-/-} mice however the morphology of the calcified fibrocartilage is altered.....	58
Figure 2.3 MicroCT analyses indicates similar levels of mineralization in wild type and <i>Bsp</i> ^{-/-} QCT entheses.....	61
Figure 2.4 Raman spectroscopy shows that the mineral content in the QCT enthesis is comparable between wild type and <i>Bsp</i> ^{-/-} mice.....	63
Figure 2.5 <i>Bsp</i> ^{-/-} mice exhibit alteration in patellar enthesis mechanical properties.....	67
Figure 2.6 Collagen organization is not affected by loss of BSP.....	69
Figure 3.1 BSP is present in the calcified fibrocartilage of 14 month-old mice.....	88
Figure 3.2 OPN is present in the calcified fibrocartilage of 14 month-old mice.....	90
Figure 3.3 Calcified fibrocartilage of <i>Bsp</i> ^{-/-} is further lengthened with age.....	92
Figure 3.4 At 14 months of age no differences in collagen organization are observed between wild type and <i>Bsp</i> ^{-/-} mice.....	95
Figure 3.5 No gross morphological differences are apparent in the entheses of 14 day-old wild type and <i>Bsp</i> ^{-/-} mice.....	98
Figure 3.6 No gross morphological differences are apparent in the entheses of 21 day-old wild type and <i>Bsp</i> ^{-/-} mice.....	100
Figure 3.7 Mineral is not present in the entheses of 14 day-old wild type and <i>Bsp</i> ^{-/-} mice.....	102
Figure 3.8 Mineral is not present in the QCT enthesis of 21 day-old wild type and <i>Bsp</i> ^{-/-} mice however small amounts are present in the SST enthesis.....	104
Figure 3.9 At 14 days of age no differences in collagen organization are observed between wild type and <i>Bsp</i> ^{-/-} mice.....	106
Figure 3.10 At 21 days of age no differences in collagen organization are observed between wild type and <i>Bsp</i> ^{-/-} mice.....	108
Figure 3.11 BSP is not present in the entheses of 14 day old wild type and <i>Bsp</i> ^{-/-} mice.....	110

Figure 3.12 BSP is localized to mineralized regions in 21 day old wild type mice.....112

Figure 3.13 OPN is not present in the entheses of 14 day old wild type and *Bsp*^{-/-} mice.....114

Figure 3.14 OPN is localized to mineralized regions in 21 day-old wild type and *Bsp*^{-/-} mice.....116

LIST OF TABLES

Table 3.1 CFC lengths of 15 week and 14 month old wild type and <i>Bsp</i> ^{-/-} QCT entheses.....	93
---	----

LIST OF APPENDICES

APPENDIX A: Statement of Permission for the Use of Animals for Experimental Research.....	137
APPENDIX B: Copyright Holder Permissions.....	138

LIST OF ABBREVIATIONS

Ala	Alanine
BMP	Bone Morphogenic Protein
BSP	Bone Sialoprotein
CFC	Calcified Fibrocartilage
CMV	Cytomegalovirus
CT	Critical Threshold
Da	Dalton
DAB	3,3'-Diaminobenzidine
DMP1	Dentin Matrix Protein 1
DSPP	Dentin Sialophosphoprotein
ECM	Extracellular Matrix
EDTA	Ethylenediaminetetraacetic acid
Glu	Glutamic Acid
Gly	Glycine
HA	Hydroxyapatite
IHC	Immunohistochemistry
IHH	Indian Hedgehog
KAE	Lysine-Alanine-Glutamic Acid
K _D	Dissociation Constant
kDa	Kilodalton
LCM	Laser Capture Microdissection
MALDI-TOF	Matrix Assisted Laser Desorption/Ionization Time of Flight
MEPE	Matrix Extracellular Phosphoglycoprotein
microCT	Micro-Computed Tomography
mRNA	Messenger Ribonucleic Acid
NMR	Nuclear Magnetic Resonance
OCT	Optimum Cutting Temperature

OPN	Osteopontin
PBS	Phosphate Buffered Saline
PBS-T	Phosphate Buffed Saline-Tween 20
PCR	Polymerase Chain Reaction
PDL	Periodontal Ligament
PHEX	Phosphate Regulating Endopeptidase Homolog, X-Linked
pI	Isoelectric point
PMMA	Polymethyl Methacrylate
Ptch	Patched
PTHrP	Parathyroid Hormone-Related Protein
QCT	Quadriiceps Femoris Tendon
qPCR	Quantitative Real-Time Polymerase Chain Reaction
RGD	Arginine-Glycine-Aspartic Acid
RNA	Ribonucleic Acid
RNAseq	Ribonucleic Acid Sequencing
ROI	Region of Interest
Runx2	Runt-Related Transcription Factor 2
Scx	Scleraxis
SIBLING	Small Integrin-Binding Ligand, N-Linked Glycoproteins
Smo	Smoothened
Sox	Sex Determining Region on Y-box
SST	Supraspinatus Tendon
TGF β	Transforming Growth Factor β
TGF β r	Transforming Growth Factor β Receptor
UFC	Uncalcified Fibrocartilage
VOI	Volume of Interest

CHAPTER ONE

LITERATURE REVIEW

1.1 Mineralized Tissues

Biom mineralization refers to the processes by which organisms form minerals (Lowenstam and Weiner, 1989). It requires the selective extraction and uptake of elements from the local environment and their incorporation into functional structures under strict biological control. The earliest fossil evidence of biom mineralization dates back 3.5 billion years (Lepot et al., 2008) and has since been observed in all five of the biological kingdoms (Lowenstam and Weiner, 1989). Mineralized tissues are biological matrices that have incorporated inorganic minerals such as calcium and phosphorus into their structure. Mineralized tissues serve a variety of functions. They can act as protective armor, such as a shell, they can be involved in cutting and grinding functions, such as teeth, and can offer support and stability, as in the skeleton. Perhaps the most recognizable, and by far the best characterized, mineralized tissue is that of mammalian bone, of which a brief description follows.

Bone is a complex connective tissue composed of three main phases: the cellular phase, the inorganic phase, and the organic phase. The major cell types in bone are osteoblasts, osteocytes and osteoclasts. Osteoblasts are anabolic cells associated with the secretion of matrix and the deposition of mineral. Osteocytes, derived from osteoblasts that have become entombed within the matrix of the bone, are associated with its regulation and homeostasis. Osteoclasts are catabolic cells involved in the resorption and remodeling of bone, releasing mineral and breaking down the extracellular matrix. The mineral content of bone, constituting the inorganic phase, is largely hydroxyapatite (HA), a stable crystal of calcium phosphate with unit formula $\text{Ca}_{10}(\text{PO}_4)_6(\text{OH})_2$. HA deposition is facilitated by osteoblasts into an organic matrix (the organic phase) primarily

comprised of type I collagen. Roughly 10% of this matrix consists of non-collagenous proteins which serve a variety of functions such as cell attachment and signaling, regulation of mineral formation, which includes nucleation, binding and inhibition, as well as structural functions.

Bones form through two major processes: intramembranous ossification and endochondral ossification. Flat bones, such as the components of the skull and scapula form through intramembranous ossification in which mesenchymal tissues become mineralized without a cartilage intermediate. Long bones, such as the femur and humerus, form through the process of endochondral ossification. Endochondral ossification begins embryonically when cells of the mesenchyme condense in regions that will eventually become the long bones of the skeleton. These cells differentiate into chondrocytes and form a cartilaginous anlage rich in type II collagen. Cells in the central region of this structure begin to exit the cell cycle and enter hypertrophy, in which they swell in size and excrete extracellular matrix. Hypertrophic chondrocytes secrete angiogenic factors which promotes the invasion of blood vessels into the tissue. These blood vessels deliver precursor cells which differentiate into osteoblasts and osteoclasts, as well as blood and bone marrow-forming hematopoietic cells, to the developing bone. This creates a primary ossification center in the middle of the anlage from which the mineralization process begins. Osteoblasts promote mineral deposition, while osteoclasts remodel the mineralized cartilage, facilitating the formation of lamellar bone. At the terminals of the developing long bones, the epiphysis, secondary ossification centers also form, creating a sandwich of resting, proliferative and hypertrophic chondrocytes termed the epiphyseal growth plate. Proliferation, hypertrophy and mineralization of the

chondrocytes of the growth plate drive the elongation and growth of the bone, until the plates fuse at the end of puberty

1.2 Biomineralization

The exact mechanism by which HA is deposited into the type I collagen matrix of bone is not fully understood. Serum concentrations of Ca^{2+} and PO_4^{3-} are above the solubility product constant of HA (Eidelman et al., 1987), however, they are kept from precipitating in the body by a variety of inhibitors of crystal formation. In bone, type I collagen fibrils are arranged in staggered arrays creating a periodic gap, call the hole zone, every 67 nm (Katz and Li, 1973). It is within these hole zones that the initiation of HA crystal formation takes place (Traub et al., 1992). It has been suggested that the aqueous compartment created by the collagen hole zone is sufficiently small to exclude large HA inhibitors, which leads to mineral deposition by the exclusion of inhibitors (Nudelman et al., 2010; Price et al., 2009). Despite this evidence, type I collagen fibrils themselves are not sufficient to nucleate HA formation (Blumenthal et al., 1990; Hunter et al., 1986), indicating that some additional factor must be present to initiate HA crystal formation. Acidic collagen binding proteins have long been speculated to fulfill this role (Glimcher and Muir, 1984), of which members of the SIBLING protein family are the prime examples.

1.3 SIBLINGs

Members of the Small Integrin Binding Ligand, N-linked Glycoprotein (SIBLING) family are small phosphoproteins, often associated with mineralized tissues.

The SIBLINGs have flexible structures and extensive post-translational modifications. All members of the SIBLING family contain an RGD integrin-binding motif (Fisher et al., 2001; George and Veis, 2008). The SIBLING genes are grouped in a 375 kbp cluster on human chromosome 4 (Fisher and Fedarko, 2003) and mouse chromosome 5 (Crosby et al., 1996). The family is comprised of 5 members: Osteopontin (OPN), Bone Sialoprotein (BSP), Dentin Matrix Protein 1 (DMP1), Matrix Extracellular Phosphoglycoprotein (MEPE) and Dentin Sialophosphoprotein (DSPP) (Fisher and Fedarko, 2003; Fisher et al., 2001). Although the SIBLING proteins do not share a high degree of sequence similarity, an examination of their exon structure reveals that the 5 genes are indeed related, likely resulting from gene duplication events and subsequent divergences, facilitated by their flexible structure (Fisher and Fedarko, 2003).

All members of the SIBLING family seem to be involved with the regulation and control of biological mineral deposition, although in different ways. The SIBLING proteins are largely acidic, with isoelectric points ranging from 3.4-4.3, however MEPE differs from the rest of the group as it is highly basic with a pI of 9.2 (Fisher and Fedarko, 2003) BSP, DMP1, DSPP are promoters of mineral deposition and are mostly found within mineralized tissues, with greater concentrations of BSP found in bone, while dentin contains greater amounts of DMP1 and DSPP (George and Veis, 2008). OPN and MEPE are potent inhibitors of HA formation and are expressed ubiquitously, likely to prevent ectopic calcification of soft tissues (George and Veis, 2008). Single knock-out animals for each of the SIBLINGs have been created, with each displaying alterations in the properties of their mineralized tissues, however the loss of a single SIBLING gene does not result in an inability to form mineralized tissue (George and Veis, 2008). This

suggests that the SIBLINGs work in concert with each other to control the process of biomineralization *in vivo* and a great deal of functional redundancy is present within the family. As the focus of this thesis is bone sialoprotein, an in depth discussion of BSP follows.

1.4 Bone Sialoprotein

BSP is an intrinsically disordered and extensively post-translationally modified phosphoprotein found in the mineralized tissues of bones and teeth. BSP was initially isolated from bone in 1963 as a 23-kDa sialic acid-containing glycoprotein (Herring and Kent, 1963)(Figure 1.1). By utilizing a dissociative extraction procedure, Fisher *et al.* isolated a 70-80 kDa variant from calf bone, representing full length native BSP complete with its post translational modifications (Fisher et al., 1983). The rat *Bsp* gene was first sequenced in 1988 by Oldberg *et al.* (Oldberg et al., 1988). The amino acid sequences of BSP have since been deduced in a variety of mammalian species and show a high level of conservation, with specific domains showing identity approaching 90% (Goldberg and Hunter, 2012).

1.4.1 Structure

Mammalian BSP contains an average of 300 amino acids, 20% of which are Glu and 11% are Gly. Additionally a 16-residue signal sequence is present at the N-terminus. Unmodified BSP has a pI of 3.9. BSP's calculated mass based on amino acid composition derived from the cDNA sequence is 33,549 Da; however, two independent MALDI-TOF

Figure 1.1 Schematic of bone sialoprotein. BSP is approximately 300 amino acids long. The collagen-binding sequence (yellow) spans residues 18-45. There are two poly-glutamic acid sequences (red) responsible for HA nucleation. Finally, there is an integrin-binding RGD sequence (blue) at the C-terminus.



mass spectroscopy studies of BSP found mean masses of 52.5 and 49.0 kDa (Wuttke et al., 2001; Zaia et al., 2001). Broad mass peaks were observed in both these studies, reflecting the significant heterogeneity of post-translation modifications on individual BSP molecules. Oligosaccharides comprise approximately 30% of BSP's weight and BSP contains 23 sialic acid residues (Zaia et al., 2001). BSP (bovine) also contains 11 identified phosphorylation sites, however not all of these sites appear to be phosphorylated on each molecule. MALDI-TOF mass spectroscopy studies on proteolytic digests of BSP indicate that on average BSP molecules contain 5.8 phosphorylated serine residues (Salih and Flückiger, 2004; Salih et al., 2002). BSP also contains several sulfated tyrosine residues located in the C-terminal region of the protein. Structural analyses of BSP utilizing circular dichroism spectropolarimetry, NMR and small-angle X-ray scattering indicate the loose, flexible structure of an intrinsically disordered protein (Fisher et al., 2001; Tye et al., 2003; Wuttke et al., 2001).

1.4.2 Collagen Binding

BSP binds to type I collagen fibrils with a high affinity ($K_D = 12.1$ nM) (Tye et al., 2005). The highly conserved collagen-binding domain of BSP encompasses residues 18-45 and is rich in hydrophobic and basic amino acids. The K_D of BSP₁₈₋₄₅ (150 nM) is weaker than that of native, full-length BSP however, indicating that other regions of the molecule are involved in stabilizing the interaction with collagen (Baht et al., 2008). Intermolecular forces involved in this binding appear to be comprised mostly of hydrophobic interactions, as elution of BSP with 1.0 M NaCl yielded little protein; however, elution with acetonitrile, which disrupts hydrophobic interactions, resulted in

the full release of BSP from a type I collagen affinity column (Baht et al., 2008). The exact location that BSP binds to on the collagen molecule remains unknown, however BSP appears to localize to the hole regions of type I collagen fibrils (Fujisawa et al., 1995), which as previously mentioned are associated with early mineral formation (Fratzl et al., 1991; Traub et al., 1992).

1.4.3 *Hydroxyapatite Binding and Nucleation*

BSP's many negatively charged groups confer HA binding properties. At physiological salt concentrations, native rat BSP bind ~60 Ca²⁺ ions per molecule with low affinity (Chen et al., 1992), however bone-derived porcine BSP's affinity for HA is higher with a K_D of ~0.9 μM (Goldberg et al., 2001). This affinity is largely attributed to the 2-3 contiguous Glu sequences present in the central region of the protein, as competitive binding studies using synthetic poly-Asp and poly-Glu peptides reduced BSP's affinity for HA by 90% and 68% respectively (Goldberg et al., 2001). Additionally, mutation of these poly-Glu sequences to poly-Ala sequences reduced *in vivo* HA adsorption 4-fold (Wazen et al., 2007).

BSP is also a potent nucleator of HA formation as demonstrated by Hunter and Goldberg using a steady-state agarose gel system (Hunter and Goldberg, 1993). This group went on to show that BSP's poly-Glu sequences are largely responsible for HA formation (Goldberg et al., 1996). Synthetic peptides spanning BSP poly-Glu sequences can mediate HA formation on its own, and a 2.5 fold increase in nucleation activity is observed when these peptides are phosphorylated (Baht et al., 2010). Correspondingly,

unmodified full length BSP also nucleates hydroxyapatite formation, however native BSP with its post translational modifications is ~100 fold more potent (Goldberg et al., 1996).

1.4.4 *Cell Attachment and Signaling*

Akin to its other SIBLING members, BSP contains an RGD integrin-binding motif, which is located towards its C-terminus. BSP's RGD sequence is recognized by the $\alpha_v\beta_3$ integrin (Oldberg et al., 1988), a receptor identified on the surfaces of osteoblasts (Prince et al., 1991) and osteoclasts (Miyachi et al., 1991; Ross et al., 1993) BSP-mediated attachment of these cell types has been demonstrated respectively by Somerman *et al.* and Helfrich *et al.* (Helfrich et al., 1992; Somerman et al., 1988). Cell attachment of osteoblasts, fibroblasts, and chondrocytes is abolished by alteration to a KAE sequence (Gill et al., 2008; Gordon et al., 2007; Harris et al., 2000). Eukaryotic cell binding via an RGD-independent mechanism has also been described (Mintz et al., 1993).

BSP has been shown to promote osteoblast differentiation and mineral formation in cell culture (Cooper et al., 1998; Zhou et al., 1995). Furthermore, a reduction in mineralized nodules was observed when osteoblast-like cell cultures were treated with an anti-BSP antibody (Boskey et al., 2008). Overexpression of BSP in primary rat calvarial cells increased mineral formation and markers of osteoblast differentiation (Gordon et al., 2007). Treatment with BSP and osteogenic media of human bone marrow-derived cells resulted in a decrease in cell proliferation and promoted differentiation into osteoblasts (Xia et al., 2011).

BSP mediates Ca^{2+} signaling in osteoclasts through the $\alpha_v\beta_3$ integrin receptor (Paniccia et al., 1995, 1993) and can modulate their activity. BSP is involved in the generation of osteoclasts (Valverde et al., 2005, 2008) and stimulates *in vitro* bone resorption (Raynal et al., 1996), however it is not critical for this process (Malaval et al., 2008).

1.4.5 *Tissue Distribution and Expression*

BSP expression is largely restricted to mineralized tissue. BSP has long been known to be expressed in osteoid tissue (Ganss et al., 1999) and has particularly strong expression in developing bone (Bianco et al., 1991). BSP is relatively uniform in its distribution throughout the bone, where it is likely bound to and entrapped by HA (Bianco et al., 1993; Chen et al., 1993; Kasugai et al., 1992; Riminucci et al., 1995) although BSP protein is particularly concentrated at the mineralization front (Bianco et al., 1993; Riminucci et al., 1995; Shapiro et al., 1993). Chen *et al.* showed BSP mRNA in rat tissue is abundant during times of *de novo* bone synthesis and mineralization in bone, dentin and cementum using northern blotting and *in situ* hybridization, however expression declines as the animals matured, with little mRNA detected in 100 day old rats (Chen et al., 1992). Thus, BSP's expression and localization coincides with the formation of a mineralized matrix. BSP mRNA is abundant and easily detected in mature osteoblasts and osteocytes, however it is not present in pre-osteoblastic cells, indicating that BSP expression is induced upon differentiation (Bianco et al., 1991; Chen et al., 1991). In line with its proposed role in *de novo* bone synthesis, BSP is also expressed by the hypertrophic chondrocytes within the epiphyseal growth plate (Bianco et al., 1991).

BSP expression has been detected in osteoclasts (Arai et al., 1995; Bianco et al., 1991), suggesting that it is involved in the modulation of mineral resorption.

BSP is expressed in a variety of dental tissues, and may have a role in the formation and maintenance of teeth. BSP protein and mRNA have been detected in both dentin and cementum where it is expressed by odontoblasts and cementoblasts, respectively (Chen et al., 1993; Somerman et al., 1991). Cementum in particular is rich in BSP and BSP appears to be critical to the formation of acellular cementum (Foster et al., 2013). Low levels of BSP have been detected in enamel and ameloblasts (Chen et al., 1998). BSP has also been detected in three non-mineralized tissues; the trophoblastic cells of the human placenta (Bianco et al., 1991), salivary glands (Ogbureke and Fisher, 2004) as well as platelets where it is probably endocytosed from the serum (Chenu and Delmas, 1992).

1.4.6 *In Vivo Function*

Due to its tissue distribution, expressional patterns and biochemical properties, BSP is thought to be involved in *de novo* bone synthesis. Specifically, BSP is believed to bind to collagen fibers and nucleate HA formation, while also recruiting osteogenic cells to sites of mineral formation (Ganss et al., 1999). A variety of *in vivo* studies support this hypothesis. When BSP and type I collagen are implanted into calvarial defects of rats, cell proliferation, osteoblast differentiation and mineral deposition are observed (Wang et al., 2006; Xu et al., 2007). BSP implantation into the pulp of rat molars may also stimulate dentinogenesis (Decup et al., 2000).

Mice lacking the *Bsp* gene (*Bsp*^{-/-}) demonstrate reduced body size and weight with undermineralized fetal bones compared to wild-type littermates. At 4 months of age *Bsp*^{-/-} mice display thinner cortical bones than wild type mice and have increased trabecular bone volume, however at 12 months few differences are apparent (Malaval et al., 2008). This suggests that the defects are transient, and mutant mice eventually "catch up" with their wild-type counterparts. Interestingly, mice which overexpress BSP via a CMV promoter also display thinner cortical bone and mild dwarfism, although trabecular bone volume is decreased in these animals (Valverde et al., 2008). Bone formation rate is decreased in *Bsp*^{-/-} mice, as is bone resorption and osteoclastogenesis (Boudiffa et al., 2010; Malaval et al., 2008). Conversely, BSP overexpressing mice display increased osteoclast activity and bone resorption (Valverde et al., 2008). Osteoblasts isolated from *Bsp*^{-/-} mice form fewer mineralizing colonies and express decreased levels of osteoblastic cell markers (Malaval et al., 2008); however BSP overexpressing mice also display decreased osteoblast populations and differentiation markers (Valverde et al., 2008).

Repair of cortical defects drilled into the femur of *Bsp*^{-/-} mice is slowed compared to wild type animals (Malaval et al., 2009), and marrow ablation models indicate primary bone formation is also delayed (Wade-Gueye et al., 2012). Embryonic mice at 15.5 days gestation display a delay in primary ossification (Holm et al., 2015). In newborn *Bsp*^{-/-} mice, microCT analysis of the skull revealed wider cranial sutures (Bouleftour et al., 2014), suggesting a delay in membranous ossification.

Recent studies suggest that there are alterations in the growth plates of these animals as well. Bouleftour *et al.* reported a thinner hypertrophic zone in the epiphyseal plate of 6 day old *Bsp*^{-/-} mice and a thinner proliferative zone and thicker hypertrophic

zone at 3 weeks of age (Boulefour et al., 2014). Holm *et al.* also report growth plate abnormalities in the *Bsp*^{-/-} mouse however this group observed an increase in the size of the resting zone with a reciprocal decrease in the size of the proliferative zone in newborn animals (Holm et al., 2015).

A significant periodontal phenotype has recently been uncovered in the *Bsp*^{-/-} mouse. The alveolar bone, into which the teeth are set, displays significant resorption in *Bsp*^{-/-} mice (Foster et al., 2013). Briefly mentioned previously, acellular cementum is a thin mineralized tissue found along the apical portion of the root of the tooth, into which the periodontal ligament (PDL) inserts and anchors the tooth into alveolar bone. Immunohistochemical staining has demonstrated that acellular cementum is rich in BSP, and this tissue is significantly reduced in *Bsp*^{-/-} mice (Foster et al., 2013). Additionally, the PDL in *Bsp*^{-/-} mice is disorganized, with poorly aligned collagen fibers that do not properly insert into the tooth root (Foster et al., 2013). This phenotype spurred us to investigate other junctions between hard and soft tissues.

1.5 The Enthesis

Tendons and ligaments attach to bones through a transitional structure known as the enthesis, however authors have given the structure several other names such as osteotendinous junction or simply the tendon-bone insertion (Benjamin and McGonagle, 2001; Benjamin et al., 2002). Entheses are vital to locomotion and movement as they transmit the contractile force of skeletal muscles to their corresponding structures of the skeleton proper. Due to the immense loads these structures bear, as well as the large

differences in the mechanical properties of the two tissues they connect, entheses possess unique mechanics and biology.

Entheses fall under two distinct categories which again have been called a variety of different names including periosteal-diaphyseal and chondroapophyseal attachments as well as indirect and direct attachments. For the purposes of this thesis we shall use the terms fibrous enthesis and fibrocartilaginous enthesis, respectively, for these structures since these are the consensus terms in the literature (Benjamin and McGonagle, 2001).

1.5.1 *Fibrous Entheses*

Fibrous insertions originating from tendon/ligaments usually occur over large areas where they connect either directly with the osteoid tissue of the bone or indirectly through the periosteum via perforating mineralized collagen fibers. When they attach to long bones, fibrous entheses usually occur at the diaphysis (Benjamin et al., 2002). Two examples of fibrous entheses are the tibial attachment of the medial collateral ligament of the knee and the deltoid attachment to the humerus in the shoulder. Fibrous entheses have received little research attention when compared to the fibrocartilaginous enthesis, which is likely due to the latter's clinical relevance. Indeed, the focus of this thesis too, is the fibrocartilaginous enthesis.

1.5.2 *Fibrocartilaginous Entheses*

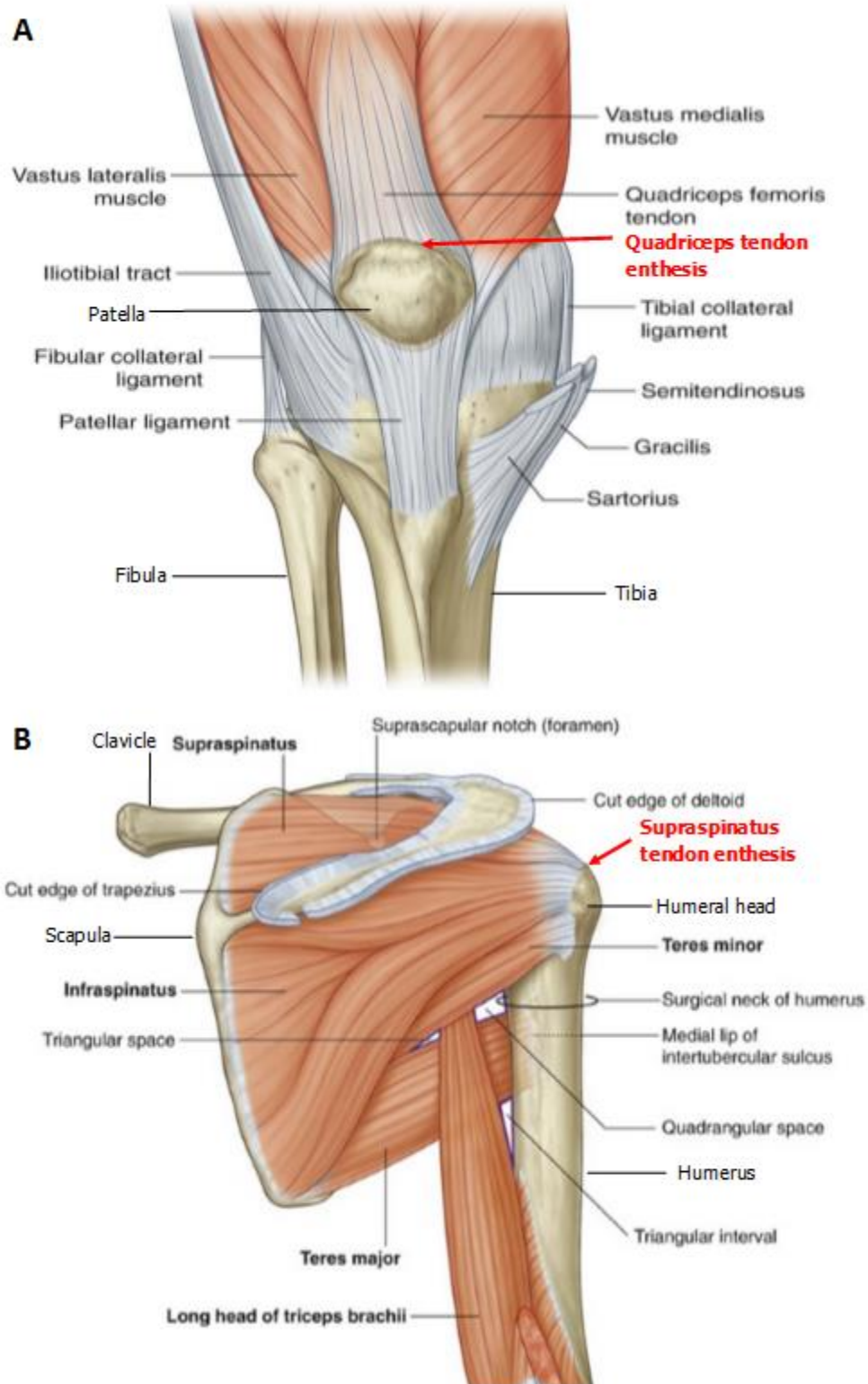
The far more common fibrocartilaginous enthesis is distinguished from the fibrous enthesis by the presence of fibrocartilage in the transition from tendon/ligament to bone and is of key clinical relevance as these are the structures most commonly damaged

in tears of the rotator cuff and ligaments of the knee. Examples of fibrocartilaginous entheses include the humeral attachment of the supraspinatus tendon (SST) and the insertion of the quadriceps femoris tendon (QCT) into the back of the patella (Figure 1.2). The fibrocartilaginous enthesis has traditionally been described as having four transitional zones: dense fibrous connective tissue of the tendon, uncalcified fibrocartilage, calcified fibrocartilage, and bone (Benjamin and McGonagle, 2001)(Figure 1.3).

The first zone of the fibrocartilaginous entheses is pure dense connective tissue of the tendon/ligament. This zone is primarily composed of linear type I collagen fibers with additional type III collagen, as well as small amounts of elastin and the proteoglycans biglycan and decorin. The major cells of this tissue are the elongated spindle-shaped fibroblasts which are responsible for the creation and maintenance of the tissue (Benjamin and Ralphs, 2000).

Next follows a region of fibrocartilage, part of which is mineralized and part of which is not, the calcified fibrocartilage (CFC) and uncalcified fibrocartilage (UFC). Tendon gradually gives way to the UFC, which is composed mainly of type II collagen, although type I and III collagen are also present. Proteoglycans that have been identified in the UFC include decorin, biglycan, lumican, versican, and aggrecan and the cells that populate this region referred to as fibrochondrocytes (Fukuta et al., 1998; Kumagai et al., 1994; Waggett et al., 1998). Fibrochondrocytes are isolated from one another and do not communicate with each other via gap junctions as the cells of the tendon and bone do, thus creating a barrier to communication between tenocytes and osteocytes

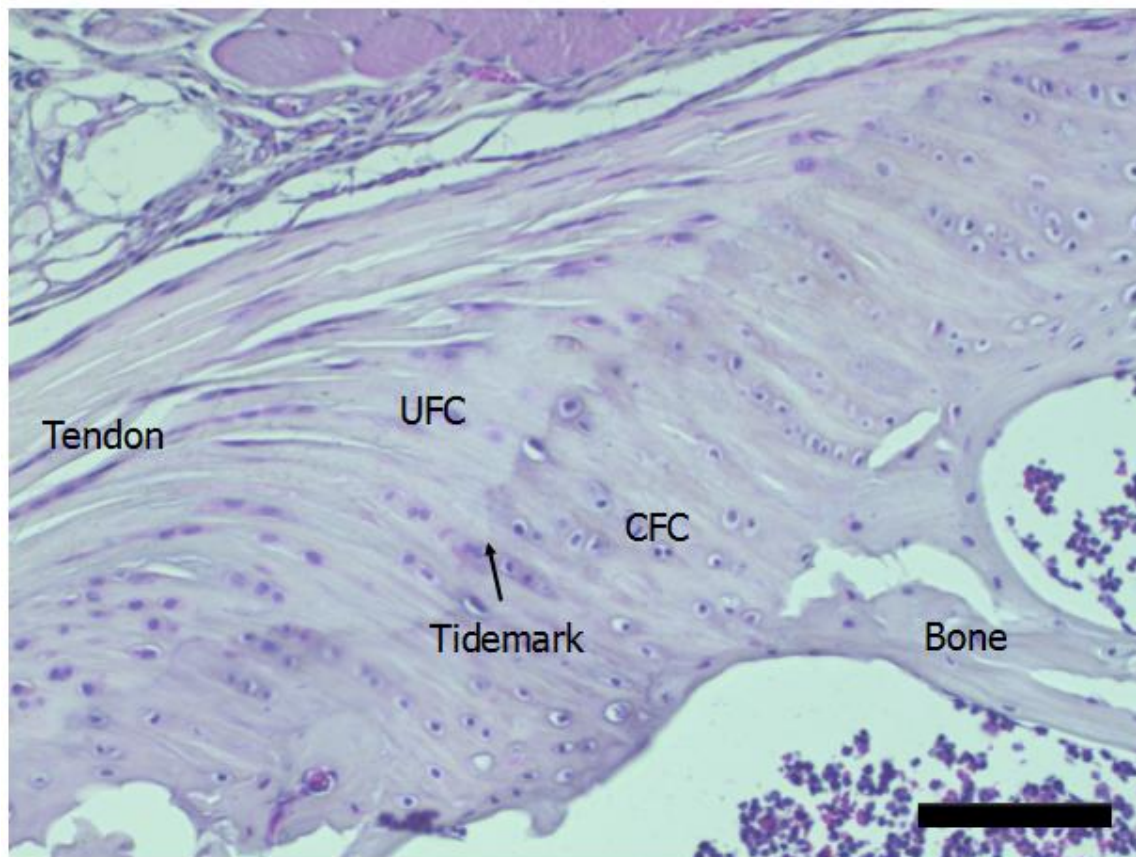
Figure 1.2 Anatomical location of selected fibrocartilaginous entheses. (A) Anterior view of the bones, muscles, tendons and ligaments of the knee. Insertion of the quadriceps femoris tendon into the back of the patella indicate (red arrow). (B) Posterior view of the muscles and bones of the shoulder. Insertion of the supraspinatus tendon into the humeral head indicated (red arrow).



This figure was adapted from *Gray's Anatomy for Students, Third Edition*, Drake RL, Vogl AW, Mitchell AWM, Copyright Churchill Livingstone Elsevier (2015). Reproduced with permission from the publisher.

Figure 1.3 The transitional zones of the fibrocartilaginous enthesis.

Fibrocartilaginous entheses have been classically divided into four zones: tendon, uncalcified fibrocartilage (UFC), calcified fibrocartilage (CFC), and bone. The tendon proper, made mostly of type I collagen, a region of fibrocartilage composed of type II collagen that is divided into an uncalcified and calcified region. The boundary is called the tidemark and indicates the edge of the mineralized tissue. The calcified fibrocartilage gives way to bone. Bar = 100 μm



(Ralphs et al., 1998). The UFC is more pliable than either the tendon or the CFC and it is thought that its primary function is stress dissipation and force dampening. This is evidenced by larger regions of UFC in entheses which vary more in their insertion angles during joint movement (Benjamin and McGonagle, 2001; Benjamin and Ralphs, 1998).

A sharp boundary exists between the UFC and the CFC, termed the tidemark, and represents the maximum extent of the mineralized zone of the fibrocartilaginous enthesis. Using Raman spectroprobe analysis Schwartz *et al.* characterized the mineral gradient that occurs between the UFC and CFC at the tidemark in the mouse supraspinatus tendon insertion (Schwartz et al., 2012). Mineral increases from zero to maximal levels over a length of approximately 20 μm , a relatively narrow band as the total length of the calcified fibrocartilage of the murine supraspinatus tendon enthesis is roughly 100 μm . Furthermore, although the length of the CFC increases as the animal ages, the length of the mineral gradient remains the same. A separate study on the rat supraspinatus tendon enthesis found a gradient with length of roughly 100 μm (Wopenka et al., 2008), however it is not clear how the span of the gradient scales with the size of the animal.

The mineral content of the CFC beyond the gradient zone is constant across its length (Schwartz et al., 2012), and the CFC has a slightly different matrix composition than the UFC. Type II collagen is much more abundant here, although type I collagen can still be detected. Furthermore, type X collagen is present in small amounts and its expression is not transient, as it is in the growth plate (Fujioka et al., 1997).

The major proteoglycan of the CFC is aggrecan, and notably this is the only region of the fibrocartilaginous enthesis where decorin is absent (Waggett et al., 1998).

Interestingly no mineral associated proteins have yet been described in the CFC, although

Liu *et al.* observed asporin mRNA in the developing insertion of the patellar ligament to the tibia (Liu *et al.*, 2013). Asporin is a member of the leucine rich repeat family of proteins, which includes the proteoglycans decorin and biglycan with collagen binding and HA binding properties (Kalamajski *et al.*, 2009; Lorenzo *et al.*, 2001). The CFC is intermediate in stiffness between tendon and bone and this characteristic is also thought to assist in stress dissipation during movement and loading (Benjamin *et al.*, 2002; Fujioka *et al.*, 1997).

The final zone of the fibrocartilaginous enthesis is bone, which has been described previously. The junction between the CFC and the lamellae of the bone is highly irregular, in contrast to the smooth straight line of the tidemark. This interdigitating of bone and CFC is thought to create a firm joining of these tissues, ultimately anchoring the tendon/ligament to the bone.

1.5.3 Development

The developmental pathways of the fibrocartilaginous enthesis are still being explored. The structure can first be identified in mice at embryonic day 13.5 while an apparently mature enthesis can be observed histologically as early as 21 days post-natal (Zelzer *et al.*, 2014). As discussed previously, the fibrocartilaginous enthesis is a transitional tissue between bone and tendon, and as such, the origin of the enthesis is likely to include developmental components from the two tissues it eventually unites. Mentioned above, bone initially develops as a cartilaginous anlage composed of a condensation of mesenchymal cells that differentiate into chondrocytes. A key regulator of chondrocyte differentiation is the transcription factor Sox9 that is continually

expressed by all chondroprogenitors and chondrocytes during chondrogenesis (Akiyama et al., 2002; Dy et al., 2012; Ng et al., 1997; Zhao et al., 1997). Tenocyte differentiation is largely controlled by a basic helix loop helix transcription factor known as scleraxis (*Scx*) (Cserjesi et al., 1995; Murchison et al., 2007; Schweitzer et al., 2001).

Generally tendons and ligaments insert into bone at bony eminences or protrusions, thus initial studies of the development of fibrocartilaginous entheses began with these structures. Intriguingly, cell lineage tracing indicates that bone eminences are not derived from the cartilaginous anlage of the bone but rather arise as a distinct unit derived from a pool of progenitors which are appended onto the developing bone (Blitz et al., 2013). Gene expression analysis of these progenitors reveals that they are positive for both *Sox9* and *Scx* (Blitz et al., 2013; Sugimoto et al., 2013). This observation has led Zelzer *et al.* to propose the segregation model of enthesis development and cell differentiation (Zelzer et al., 2014). In this model, the bone eminence, *Sox9 Scx* double positive, progenitor cells differentiate and segregate into either the *Sox9* positive cells of the enthesis fibrocartilage, or the *Scx* positive cells of the incoming tendon, uniting the two tissues without the need for a complex homing mechanism to direct a tendon to its proper attachment point.

Other molecules have been identified to participate in the development of entheses. Transforming growth factor β (TGF β) is necessary for tenocyte differentiation as evidenced by a lack of all tendinous tissue in mice which lack either the genes for Tgf β 1 and Tgf β 2, or its receptor Tgf β rII (Pryce et al., 2009). The role of TGF β in bone is poorly understood, as overexpression triggers chondrogenesis (Carrington et al., 1991; Chimal-Monroy and Díaz de León, 1997; Kulyk et al., 1989; Leonard et al., 1991;

Merino et al., 1998; Verrecchia and Mauviel, 2002) while lack of expression results in mild phenotypes (Seo and Serra, 2007; Spagnoli et al., 2007; Verrecchia and Mauviel, 2002). At the developing enthesis, deletion of *Tgfb β II* results in mice which lack bone eminence progenitor cells (Blitz et al., 2013), indicating that the TGF β signaling pathway is required to commit mesenchymal cells to the enthesis development pathway. In contrast, the *Scx*/bone morphogenic protein 4 (BMP4) pathway does not seem to be involved in the specification of cells to enthesis development, as mice that lack these genes still possess *Sox9* positive bone eminence progenitors. However, this pathway is involved in their differentiation as the bone eminence progenitors in both *Scx*^{-/-} and *Bmp4*^{-/-} mice fail to differentiate and do not express type II collagen (Blitz et al., 2013). Other BMPs may be involved in enthesis development as well, as loss of the receptor for BMP2 and BMP7 results in the failure of bone eminences of the humerus to form (Ovchinnikov et al., 2006). Dominant negative mutations in *Bmp5* also cause alterations in bone eminence formation (Ho et al., 2008).

The mechanism by which the developing enthesis mineralizes is largely unknown however the process is speculated to be similar to endochondral ossification of the long bones. Endochondral ossification is regulated in part by the Indian hedgehog (IHH) pathway, which also seems to play a role in enthesis development. IHH is expressed by hypertrophic chondrocytes as they terminally differentiate. IHH stimulates further chondrocyte proliferation by binding to the membrane receptor Patched (Ptch) which activates the membrane receptor Smoothed (Smo), resulting in the expression of parathyroid hormone-related protein (PTHrP). PTHrP inhibits chondrocyte maturation and mineralization and exercises negative feedback control on IHH, resulting in a loop in

which chondrocyte proliferation and hypertrophy can be finely controlled, based on the distance between the hypertrophic and proliferating chondrocytes. Expression of PTHrP and IHH has been detected in the developing enthesis, suggesting a developmental role for this pathway (Chen et al., 2006; Liu et al., 2012). Deletion of PTHrP in Scx expressing cells appears to deleteriously effect the ability of osteoclasts to excavate insertions for fibrous entheses (Wang et al., 2013). Constitutive expression of IHH in Scx-expressing cells leads to enthesis marker expression in the central region of the tendon (tendon midsubstance), such as type II collagen, where it is not normally expressed (Liu et al., 2013). Deletion of *Smo* in Scx-expressing cells results in chondrocyte impairment such that they fail to form fibrocartilage at the insertion. Furthermore, adult animals lacking *Smo* in these cells lack a tidemark, indicating mineralization is impaired (Liu et al., 2013). Although several studies have investigated the role of classical endochondral ossification signaling pathways in enthesis development, to date, protein regulators of mineralization remain wholly uncharacterized in the development and function fibrocartilaginous enthesis.

Mechanical load has a significant influence on enthesis development. The role of physical cues in the development of the musculoskeletal system has been extensively studied (Galloway et al., 2013; Gkiatas and Lykissas, 2015). In the absence of muscle forces, defects in bone size, shape and mineralization can occur (Gomez et al., 2007; Mikic et al., 2000; Osborne et al., 2002; Sharir et al., 2011). Bone eminences too require mechanical force to fully mature as evidenced by transplantation experiments (Hamburger and Waugh, 1940; Hamburger, 1939, 1938). However, force is not required for the initiation of eminence formation as mice with induced muscle paralysis possess

stunted versions of these structures. It appears that instead, mechanical force drives growth and cell proliferation (Blitz et al., 2009; Kahn et al., 2009), and as a result, maturation of these structures in the absence of muscle force is delayed, with little or no fibrocartilage present at 8 weeks of age (Das et al., 2011; Schwartz et al., 2013; Thomopoulos et al., 2007). Disorganization of enthesis collagen fibres was also apparent at 8 weeks of age (Schwartz et al., 2013). Mineralization of the enthesis is also severely impaired by a loss of mechanical loading, causing an overall reduction in mineral content as well as altering the characteristics of the mineral crystals (Thomopoulos et al., 2007). Together these defects ultimately lead to a mechanically inferior tissue that failed under lower loads (Schwartz et al., 2013).

1.5.4 Tissue Injury and Healing

Tearing in tendons and ligaments is a common orthopedic injury, however, when the damage sustained involves enthesal tissue significant morbidity can occur. The muscles involved in the movement of the shoulder are collectively termed the rotator cuff and tears in these structures due to work and sports related injuries and aging are common (Ricchetti et al., 2012; Rothrauff and Tuan, 2014). Between 30,000 and 75,000 rotator cuff repairs are performed annually in the United States (relevant Canadian statistics could not be identified) however the outcome of these surgeries remains poor (Ricchetti et al., 2012). Post-surgical repair failure rates for minor tears are as high as 20% while the re-tear rate for massive rotator cuff tears are reported to reach a staggering 94% (Derwin et al., 2012; Galatz et al., 2004). Repair failure is due in large part to a lack of tendon reintegration back into the bone.

Various studies using animal models have demonstrated that reattachment of a torn tendon/ligament to bone does not result in the regeneration of an enthesis, but rather the formation of a fibrovascular scar (Aoki et al., 2001; Fujioka et al., 1998; Rodeo et al., 1993; Thomopoulos and Williams, 2003). Although these therapies elicited a robust healing response, the resulting scar tissue did not have the same mechanical integrity as a true enthesis (Pierre et al., 1995; Thomopoulos and Williams, 2003). A detailed study using a rat rotator cuff injury model by Thomopoulos and Williams showed that a sharp boundary forms between the hard and soft tissues, and the continuous collagen fibers spanning the length of the native enthesis were absent and replaced by a disorganized matrix rich in type III collagen. Also absent was the gradation of mineral between soft tissue and bone, thought to be so crucial to stress dissipation. The authors report a tenfold reduction in the mechanical properties of this tissue (Thomopoulos and Williams, 2003).

Numerous therapies have been developed to overcome this problem, yet none so far have succeeded in creating a tissue with the same or greater mechanical properties of the native fibrocartilaginous enthesis. Further study of the composition and development of this structure, especially in regards to its mineralized portions, are required to develop better methods of reattaching tendons and ligaments to bones.

1.6 Purpose of Thesis

A common joint injury is the avulsion or tear of a tendon or ligament from its attachment point on the skeleton, the fibrocartilaginous enthesis. These injuries cause significant morbidity, yet surgical and regenerative techniques fail to restore the full biomechanical properties of the original tissue. Our knowledge of the enthesis is incomplete, with the specifics of its composition and development still being elucidated. The calcified fibrocartilage in particular is poorly characterized. Although the presence and distribution of mineral in the CFC is vital to the mechanical properties and function of the tissue, a great void in our knowledge exists with regards to the mechanism of mineral deposition and the regulation of this process within it. Rationale for studying bone sialoprotein in the fibrocartilaginous enthesis is abundant. BSP's presence in mineralizing tissues and its abilities to bind collagen, nucleate HA formation and interact with osteogenic cells are applicable and transferrable to the development of the fibrocartilaginous enthesis. In fact, numerous researchers have already highlighted the similarities and parallels present in the development of growth plates and fibrocartilaginous entheses. Furthermore, a significant defect caused by the loss of BSP has been identified at the site where the periodontal ligament attaches to the root of the tooth. The purpose of this thesis is to establish the presence of BSP in the fibrocartilaginous enthesis and to characterize the phenotype of this enthesis in the *Bsp*^{-/-} mouse. It is hoped that a better understanding of the role BSP plays in the mineralization of this structure will further our understanding of its development and ultimately lead to more effective therapeutic and biomimetic techniques in the regeneration of the fibrocartilaginous enthesis.

1.7 References

- Akiyama, H., Chaboissier, M.-C.C., Martin, J.F., Schedl, A., Crombrughe, B. de, 2002. The transcription factor Sox9 has essential roles in successive steps of the chondrocyte differentiation pathway and is required for expression of Sox5 and Sox6. *Genes Dev.* 16, 2813–28.
- Aoki, M., Oguma, H., Fukushima, S., Ishii, S., Ohtani, S., 2001. Fibrous connection to bone after immediate repair of the canine infraspinatus: the most effective bony surface for tendon attachment. *J. Shoulder Elbow Surg.* 10, 123-8.
- Arai, N., Ohya, K., Kasugai, S., 1995. Expression of bone sialoprotein mRNA during bone formation and resorption induced by colchicine in rat tibial bone marrow cavity. *J. Bone Miner. Res.* 10, 1209-17.
- Baht, G.S., O'Young, J., Borovina, A., Chen, H., Tye, C.E., Karttunen, M., Lajoie, G.A., Hunter, G.K., Goldberg, H.A., 2010. Phosphorylation of Ser136 is critical for potent bone sialoprotein-mediated nucleation of hydroxyapatite crystals. *Biochem. J.* 428, 385–95.
- Baht, G.S., Hunter, G.K., Goldberg, HA, 2008. Bone sialoprotein–collagen interaction promotes hydroxyapatite nucleation. *Matrix Biol.* 27, 600–608.
- Benjamin, M., McGonagle, D., 2001. The anatomical basis for disease localisation in seronegative spondyloarthritis at entheses and related sites. *J. Anat.* 199, 503-26.
- Benjamin, M., Ralphs, J.R., 2000. The cell and developmental biology of tendons and ligaments. *International review of cytology.* 196, 85-130.
- Benjamin, M., Kumai, T., Milz, S., Boszczyk, B.M., Boszczyk, A.A., Ralphs, J.R., 2002. The skeletal attachment of tendons--tendon “entheses”. *Comp. Biochem. Physiol., Part A Mol. Integr. Physiol.* 133, 931–45.
- Benjamin, M., Ralphs, J.R., 1998. Fibrocartilage in tendons and ligaments--an adaptation to compressive load. *J. Anat.* 193(Pt 4), 481–94.
- Bianco, P., Fisher, L.W., Young, M.F., Termine, J.D., 1991. Expression of bone sialoprotein (BSP) in developing human tissues. *Calcif. Tissue Int.* 49, 421-26.
- Bianco, P., Riminucci, M., Bonucci, E., 1993. Bone sialoprotein (BSP) secretion and osteoblast differentiation: relationship to bromodeoxyuridine incorporation, alkaline phosphatase, and matrix deposition. *J. Histochem. Cytochem.* 41(2), 183-91.
- Blitz, E., Sharir, A., Akiyama, H., Zelzer, E., 2013. Tendon-bone attachment unit is formed modularly by a distinct pool of Scx- and Sox9-positive progenitors. *Development* 140(13), 2680-90.

Blitz, E., Viukov, S., Sharir, A., Shwartz, Y., Galloway, J., Pryce, B., Johnson, R., Tabin, C., Schweitzer, R., Zelzer, E., 2009. Bone Ridge Patterning during Musculoskeletal Assembly Is Mediated through SCX Regulation of Bmp4 at the Tendon-Skeleton Junction. *Developmental Cell* 17, 861-73.

Blumenthal, N., Cosma, V., Gomes, E., 1990. Regulation of hydroxyapatite formation by gelatin and type I collagen gels. *Calcif. Tissue Int.* 48, 440–442.

Boskey, A.L., Doty, S.B., Kudryashov, V., Mayer-Kuckuk, P., 2008. Modulation of extracellular matrix protein phosphorylation alters mineralization in differentiating chick limb-bud mesenchymal cell micromass cultures. *Bone* 42, 1061-71.

Boudiffa, M., Wade- Gueye, N., Guignandon, A., Vanden- Bossche, A., Sabido, O., Aubin, J., Jurdic, P., Vico, L., Lafage- Proust, M., Malaval, L., 2010. Bone sialoprotein deficiency impairs osteoclastogenesis and mineral resorption in vitro. *J. Bone Miner. Res.* 25, 2669–2679.

Bouleftour, W., Boudiffa, M., Wade-Gueye, N., Bouët, G., Cardelli, M., Laroche, N., Vanden-Bossche, A., Thomas, M., Bonnelye, E., Aubin, J., 2014. Skeletal Development of Mice Lacking Bone Sialoprotein (BSP)-Impairment of Long Bone Growth and Progressive Establishment of High Trabecular Bone Mass. *PloS one* 9(5), e95144.

Carrington, J.L., Chen, P., Yanagishita, M., Reddi, A.H., 1991. Osteogenin (bone morphogenetic protein-3) stimulates cartilage formation by chick limb bud cells in vitro. *Dev. Biol.* 146, 406–15.

Chen, J., McCulloch, C., Sodek, J., 1993. Bone sialoprotein in developing porcine dental tissues: cellular expression and comparison of tissue localization with osteopontin and osteonectin. *Arch. Oral. Biol.* 38(3), 241-9.

Chen, J., Sasaguri, K., Sodek, J., 1998. Enamel epithelium expresses bone sialoprotein (BSP). *Eur. J. Oral. Sci.* 106(Supp 1), 331-6.

Chen, J., Shapiro, H.S., Wrana, J.L., Reimers, S., 1991. Localization of bone sialoprotein (BSP) expression to sites of mineralized tissue formation in fetal rat tissues by in situ hybridization. *Matrix.* 11(2), 133-43.

Chen, J., Shapiro, H., Sodek, J., 1992. Developmental expression of bone sialoprotein mRNA in rat mineralized connective tissues. *Journal of Bone and Mineral Research* 7, 987–997.

Chen, X., Macica, C., Dreyer, B., Hammond, V., Hens, J., Philbrick, W., Broadus, A., 2006. Initial Characterization of PTH- Related Protein Gene- Driven lacZ Expression in the Mouse. *J. Bone. Miner. Res.* 21, 113–123.

- Chenu, C., Delmas, P.D., 1992. Platelets contribute to circulating levels of bone sialoprotein in human. *J. Bone. Miner. Res.* 7(8), 987-97.
- Chimal-Monroy, J., Díaz de León, L., 1997. Differential effects of transforming growth factors beta 1, beta 2, beta 3 and beta 5 on chondrogenesis in mouse limb bud mesenchymal cells. *Int. J. Dev. Biol.* 41, 91–102.
- Cooper, L.F., Yliheikkilä, P.K., Felton, D.A., 1998. Spatiotemporal assessment of fetal bovine osteoblast culture differentiation indicates a role for BSP in promoting differentiation. *J. Bone. Miner. Res.* 13(4), 620-32.
- Crosby, A.H., Lyu, M.S., Lin, K., McBride, O.W., Kerr, J.M., Aplin, H.M., Fisher, L.W., Young, M.F., Kozak, C.A., Dixon, M.J., 1996. Mapping of the human and mouse bone sialoprotein and osteopontin loci. *Mammalian Genome* 7, 149–151.
- Cserjesi, P., Brown, D., Ligon, K.L., Lyons, G.E., Copeland, N.G., Gilbert, D.J., Jenkins, N.A., Olson, E.N., 1995. Scleraxis: a basic helix-loop-helix protein that prefigures skeletal formation during mouse embryogenesis. *Development* 121, 1099–110.
- Das, R., Rich, J., Kim, M., McAlinden, A., Thomopoulos, S., 2011. Effects of botulinum toxin-induced paralysis on postnatal development of the supraspinatus muscle. *J. Orthop. Res.* 29, 281–288.
- Decup, F., Six, N., Palmier, B., Buch, D., Lasfargues, J.J., Salih, E., Goldberg, M., 2000. Bone sialoprotein-induced reparative dentinogenesis in the pulp of rat's molar. *Clin. Oral. Investig.* 4, 110–119.
- Derwin, K.A., Milks, R.A., Davidson, I., Iannotti, J.P., 2012. Low-dose CT imaging of radio-opaque markers for assessing human rotator cuff repair: Accuracy, repeatability and the effect of arm position. *J. Biochem.* 45(3), 614-8.
- Dy, P., Wang, W., Bhattaram, P., Wang, Q., Wang, L., Ballock, T., Lefebvre, V., 2012. Sox9 Directs Hypertrophic Maturation and Blocks Osteoblast Differentiation of Growth Plate Chondrocytes. *Developmental Cell* 22, 597–609.
- Eidelman, N., Chow, L.C., Brown, W.E. 1987. Calcium phosphate saturation levels in ultrafiltered serum. *Calcif. Tissue Int.* 41(1), 18-26.
- Fisher, L., Fedarko, N., 2003. Six Genes Expressed in Bones and Teeth Encode the Current Members of the SIBLING Family of Proteins. *Connect. Tissue Res.* 44, 3340.
- Fisher, L.W., Torchia, D.A., Fohr, B., Young, M.F., Fedarko, N.S., 2001. Flexible structures of SIBLING proteins, bone sialoprotein, and osteopontin. *Biochem. Biophys. Res. Commun.* 280, 460–5.

Fisher, L.W., Termine, J.D., Dejter, S.W., Whitson, S.W., Yanagishita M., Kimura J.H., Hascall V.C., Kleinman H.K., Hassell J.R., Nilsson B., 1983., Proteoglycans of developing bone. *J. Biol. Chem.* 258(10), 6588-94.

Foster, B.L., Soenjaya, Nociti, F.H., Holm, Zerfas, P.M., Wimer, H.F., Holdsworth, D.W., Aubin, J.E., Hunter, G.K., Goldberg, H.A., Somerman, M.J., 2013. Deficiency in Acellular Cementum and Periodontal Attachment in Bsp Null Mice. *J. Dent. Res.* 92, 166–72.

Fratzl P., Fratzl-Zelman N., Klaushofer K., Vogl G., Koller K., 1991. Nucleation and growth of mineral crystals in bone studied by small-angle X-ray scattering. *Calcif. Tissue Int.* 48(6), 407-13.

Fujioka, H., Thakur, R., Wang, G.J., 1998. Comparison of surgically attached and non-attached repair of the rat Achilles tendon-bone interface. Cellular organization and type X collagen expression. *Connect. Tissue Res.* 37(3-4), 205-18.

Fujioka, H., Wang, G., Mizuno, K., Balian, G., Hurwitz, S., 1997. Changes in the expression of type- X collagen in the fibrocartilage of rat Achilles tendon attachment during development. *J. Orthop. Res.* 15(5): 675-81.

Fujisawa R., Nodasaka Y., Kuboki Y., 1995. Further characterization of interaction between bone sialoprotein (BSP) and collagen. *Calcif. Tissue Int.* 56, 140–144.

Fukuta, S., Oyama, M., Kavalkovich, K., Fu, F.H., Niyibizi, C., 1998. Identification of types II, IX and X collagens at the insertion site of the bovine achilles tendon. *Matrix Biol.* 17(1), 65-73.

Galatz, L.M., Ball, C.M., Teefey, S.A., Middleton, W.D., 2004. The outcome and repair integrity of completely arthroscopically repaired large and massive rotator cuff tears. *J. Bone Joint Surg. Am.* 86-A(2), 219-24.

Galloway, M.T., Lalley, A.L., Shearn, J.T., 2013. The role of mechanical loading in tendon development, maintenance, injury, and repair. *J. Bone Joint Surg. Am.* 95, 1620–8.

Ganss, B., Kim, R.H., Sodek, J.S., 1999. Bone Sialoprotein. *Crit. Rev. Oral Biol. Med.* 10, 79–98.

George, A., Veis, A., 2008. Phosphorylated proteins and control over apatite nucleation, crystal growth, and inhibition. *Chemical Reviews* 108, 4670–93.

Gill, K.S., Beier, F., Goldberg, H.A., 2008. Rho-ROCK signaling differentially regulates chondrocyte spreading on fibronectin and bone sialoprotein. *Am. J. Physiol. Cell Physiol.* 295(1), C38-49.

- Gkiatas, I., Lykissas, M., 2015. Factors Affecting Bone Growth. *Am. J. Orthop.* 44(2), 61-7.
- Glimcher, M.J., Muir, H., 1984. Recent Studies of the Mineral Phase in Bone and Its Possible Linkage to the Organic Matrix by Protein-Bound Phosphate Bonds. *Phil. Trans. R. Soc. Lond.* 304, 479-508.
- Goldberg, H.A., Warner, K.J., Li, M.C., Hunter, G.K., 2001. Binding of bone sialoprotein, osteopontin and synthetic polypeptides to hydroxyapatite. *Connect. Tissue Res.* 42(1), 25-37.
- Goldberg, H.A., Warner, K.J., Stillman, M.J., Hunter, G.K., 1996. Determination of the hydroxyapatite-nucleating region of bone sialoprotein. *Connect. Tissue Res.* 35(1-4), 385-92.
- Goldberg, H.A., Hunter, G.K., 2012. Functional domains of bone sialoprotein. In: Goldberg M., ed. *Phosphorylated extracellular matrix proteins of bone and dentin*. Vol. 2. Oak Park (IL): Bentham Science Publishers. p. 266–282.
- Gomez, C., David, V., Peet, N., Vico, L., Chenu, C., Malaval, L., Skerry, T., 2007. Absence of mechanical loading in utero influences bone mass and architecture but not innervation in Myod-Myf5-deficient mice. *J. Anat.* 210, 259–271.
- Gordon, J., Tye, C., Sampaio, A., Underhill, M., Hunter, G., Goldberg, H., 2007. Bone sialoprotein expression enhances osteoblast differentiation and matrix mineralization in vitro. *Bone* 41, 462473.
- Hamburger, V., Waugh, M., 1940. The primary development of the skeleton in nerveless and poorly innervated limb transplants of chick embryos. *Physiol. Zool.* 13(4), 367-82.
- Hamburger, V., 1938. Morphogenetic and axial self-differentiation of transplanted limb primordia of 2-day chick embryos. *Journal of Experimental Zoology* 77, 379–399.
- Hamburger, V., 1939. The development and innervation of transplanted limb primordia of chick embryos. *J. Exp. Zool.* 80, 347–389.
- Harris, N.L., Rattray, K.R., Tye, C.E., Underhill, T.M., 2000. Functional analysis of bone sialoprotein: identification of the hydroxyapatite-nucleating and cell-binding domains by recombinant peptide expression and site-directed mutagenesis. *Bone* 27(6), 795-802.
- Helfrich, M.H., Nesbitt, S.A., Dorey, E.L., 1992. Rat osteoclasts adhere to a wide range of rgd (arg- gly- asp) peptide- containing proteins, including the bone sialoproteins and fibronectin, via a β 3 integrin. *J. Bone Miner. Res.* 7(3), 335-43.

- Herring, G.M., Kent, P.W., 1963. Some studies on mucosubstances of bovine cortical bone. *Biochem. J.* 89, 405-14.
- Ho, A.M., Marker, P.C., Peng, H., Quintero, A.J., Kingsley, D.M., Huard, J., 2008. Dominant negative Bmp5 mutation reveals key role of BMPs in skeletal response to mechanical stimulation. *BMC Dev. Biol.* 8, 35.
- Holm, E., Aubin, J.E., Hunter, G.K., Beier, F., Goldberg, H.A., 2015. Loss of bone sialoprotein leads to impaired endochondral bone development and mineralization. *Bone* 71, 145-54.
- Hunter, G.K., Nyburg, S.C., Pritzker, K., 1986. Hydroxyapatite formation in collagen, gelatin, and agarose gels. *Coll. Relat. Res.* 6(3), 229-38.
- Hunter, G.K., Goldberg, H.A., 1993. Nucleation of hydroxyapatite by bone sialoprotein. *Proc. Natl. Acad. Sci. U.S.A.* 90, 8562-5.
- Kahn, J., Shwartz, Y., Blitz, E., Krief, S., Sharir, A., Breitel, D.A., Rattenbach, R., Relaix, F., Maire, P., Rountree, R.B., Kingsley, D.M., Zelzer, E., 2009. Muscle contraction is necessary to maintain joint progenitor cell fate. *Dev. Cell* 16, 734-43.
- Kalamajski, S., Aspberg, A., Lindblom, K., Heinegård, D., Oldberg, Å., 2009. Asporin competes with decorin for collagen binding, binds calcium and promotes osteoblast collagen mineralization. *Biochem. J.* 423(1), 53-9.
- Kasugai, S., Nagata, T., Sodek, J., 1992. Temporal studies on the tissue compartmentalization of bone sialoprotein (BSP), osteopontin (OPN), and SPARC protein during bone formation in vitro. *J. Cell Physiol.* 152(3), 467-77.
- Katz, E.P., Li, S.T., 1973. The intermolecular space of reconstituted collagen fibrils. *J. Mol. Biol.* 80(1), 1-15.
- Kulyk, W.M., Rodgers, B.J., Greer, K., Kosher, R.A., 1989. Promotion of embryonic chick limb cartilage differentiation by transforming growth factor-beta. *Dev. Biol.* 135, 424-30.
- Kumagai, J., Sarkar, K., Uthoff, H.K., Okawara, Y., 1994. Immunohistochemical distribution of type I, II and III collagens in the rabbit supraspinatus tendon insertion. *J. Anat.* 185(Pt 2), 279-84.
- Leonard, C.M., Fuld, H.M., Frenz, D.A., Downie, S.A., Massagué, J., Newman, S.A., 1991. Role of transforming growth factor-beta in chondrogenic pattern formation in the embryonic limb: stimulation of mesenchymal condensation and fibronectin gene expression by exogenous TGF-beta and evidence for endogenous TGF-beta-like activity. *Dev. Biol.* 145, 99-109.

- Lepot, K., Benzerara, K., Brown, G.E., Philippot, P., 2008. Microbially influenced formation of 2,724-million-year-old stromatolites. *Nature Geoscience* 1, 118–121.
- Liu, C.F., Aschbacher-Smith, L., Barthelery, N., Dymont, N., Butler, D., Wylie, C., 2012. Spatial and Temporal Expression of Molecular Markers and Cell Signals During Normal Development of the Mouse Patellar Tendon. *Tissue Eng. Part A* 18, 598–608.
- Liu, C.F., Breidenbach, A., Aschbacher-Smith, L., Butler, D., Wylie, C., 2013. A Role for Hedgehog Signaling in the Differentiation of the Insertion Site of the Patellar Tendon in the Mouse. *PLoS ONE* 8, e65411.
- Lorenzo, P., Aspberg, A., Önerfjord, P., Bayliss, M., Neame, P., Heinegård, D., 2001. Identification and Characterization of Asporin. A novel member of the leucine-rich repeat protein family closely related to decorin and biglycan. *J. Biol. Chem.* 276, 12201–11.
- Lowenstam, H.A., Weiner, S., 1989. *On Biomineralization*. Oxford University Press, Oxford.
- Malaval, L., Monfoulet, L., Fabre, T., Pothuau, L., Bareille, R., Miraux, S., Thiaudiere, E., Raffard, G., Franconi, J.-M., Lafage-Proust, M.-H., Aubin, J., Vico, L., Amédée, J., 2009. Absence of bone sialoprotein (BSP) impairs cortical defect repair in mouse long bone. *Bone* 45(5), 853-61.
- Malaval, L., Wade-Guéye, N., Boudiffa, M., Fei, J., Zirngibl, R., Chen, F., Laroche, N., Roux, J.-P., Burt-Pichat, B., Duboeuf, F., Boivin, G., Jurdic, P., Lafage-Proust, M.-H., Amédée, J., Vico, L., Rossant, J., Aubin, J., 2008. Bone sialoprotein plays a functional role in bone formation and osteoclastogenesis. *J. Exp. Med.* 205(5), 1145-53.
- Merino, R., Gañan, Y., Macias, D., Economides, A.N., Sampath, K.T., Hurle, J.M., 1998. Morphogenesis of digits in the avian limb is controlled by FGFs, TGFbetas, and noggin through BMP signaling. *Dev. Biol.* 200, 35–45.
- Mikic, B., Johnson, T.L., Chhabra, A.B., 2000. Differential effects of embryonic immobilization on the development of fibrocartilaginous skeletal elements. *J. Rehabil. Res. Dev.* 37(2), 127-33.
- Mintz, K.P., Grzesik, W.J., Midura, R.J., 1993. Purification and fragmentation of nondenatured bone sialoprotein: Evidence for a cryptic, RGD- resistant cell attachment domain. *J. Bone Miner. Res.* 8(8), 985-95.
- Miyauchi, A., Alvarez, J., Greenfield, E.M., Teti, A., 1991. Recognition of osteopontin and related peptides by an alpha v beta 3 integrin stimulates immediate cell signals in osteoclasts. *J. Biol. Chem.* 266(30), 20369-74.

Murchison, N.D., Price, B.A., Conner, D.A., Keene, D.R., Olson, E.N., Tabin, C.J., Schweitzer, R., 2007. Regulation of tendon differentiation by scleraxis distinguishes force-transmitting tendons from muscle-anchoring tendons. *Development* 134, 2697–708.

Ng, L.J., Wheatley, S., Muscat, G.E., Conway-Campbell, J., Bowles, J., Wright, E., Bell, D.M., Tam, P.P., Cheah, K.S., Koopman, P., 1997. SOX9 binds DNA, activates transcription, and coexpresses with type II collagen during chondrogenesis in the mouse. *Dev. Biol.* 183, 108–21.

Nudelman, F., Pieterse, K., George, A., Bomans, PH., Friedrich, H., Brylka, LJ., Hilbers, PA., de With, G., Sommerdijk, NA. 2010. The role of collagen in bone apatite formation in the presence of hydroxyapatite nucleation inhibitors. *Nat. Mater.* 9(12), 1004-9.

Ogbureke, K., Fisher, L.W., 2004. Expression of SIBLINGs and their partner MMPs in salivary glands. *J. Dent. Res.* 83(9), 664-70.

Oldberg, A., Franzen, A., Heinegaard, D., 1988. The primary structure of a cell-binding bone sialoprotein. *J. Biol. Chem.* 263(36), 19340-2.

Osborne, A.C., Lamb, K.J., Lewthwaite, J.C., Dowthwaite, G.P., Pitsillides, A.A., 2002. Short-term rigid and flaccid paralyses diminish growth of embryonic chick limbs and abrogate joint cavity formation but differentially preserve pre-cavitated joints. *J Musculoskelet. Neuronal Interact.* 2, 448–56.

Ovchinnikov, D.A., Selever, J., Wang, Y., Chen, Y.-T.T., Mishina, Y., Martin, J.F., Behringer, R.R., 2006. BMP receptor type IA in limb bud mesenchyme regulates distal outgrowth and patterning. *Dev. Biol.* 295, 103–15.

Paniccia, R., Colucci, S., Grano, M., 1993. Immediate cell signal by bone-related peptides in human osteoclast-like cells. *Am. J. Physiol.* 165(5 Pt 1), C1289-97.

Paniccia, R., Riccioni, T., Zani, B.M., Zigrino, P., 1995. Calcitonin down-regulates immediate cell signals induced in human osteoclast-like cells by the bone sialoprotein-IIA fragment through a postintegrin receptor mechanism. *Endocrinology.* 136(3), 1177-86.

Pierre, S.P., Olson, E.J., Elliott, J.J., O’Hair, K.C., 1995. Tendon-healing to cortical bone compared with healing to a cancellous trough. A biomechanical and histological evaluation in goats. *J. Bone Joint Surg. Am.* 77(12), 1858-66.

Price, P., Toroian, D., Lim, J., 2009. Mineralization by Inhibitor Exclusion The Calcification of Collagen with Fetuin. *J. Biol.Chem.* 284, 17092–17101.

Prince, C.W., Dickie, D., Krumdieck, C.L., 1991. Osteopontin, a substrate for transglutaminase and factor XIII activity. *Biochem. Biophys. Res. Commun.* 177, 1205–1210.

Pryce, B.A., Watson, S.S., Murchison, N.D., Staverosky, J.A., Dünker, N., Schweitzer, R., 2009. Recruitment and maintenance of tendon progenitors by TGFbeta signaling are essential for tendon formation. *Development* 136, 1351–61.

Ralphs, J.R., Benjamin, M., Waggett, A.D., Russel, D.C., Messner, K., Gao, J., 1998. Regional differences in cell shape and gap junction expression in rat Achilles tendon: relation to fibrocartilage differentiation. *J. Anat.* 193(Pt 2), 215-22.

Raynal, C., Delmas, P.D., Chenu, C., 1996. Bone sialoprotein stimulates in vitro bone resorption. *Endocrinology* 137(6), 2347-54.

Ricchetti, E.T., Aurora, A., Iannotti, J.P., Derwin, K.A., 2012. Scaffold devices for rotator cuff repair. *J. Shoulder Elbow Surg.* 21(2), 251-65.

Riminucci, M., Silvestrini, G., Bonucci, E., Fisher, L.W., 1995. The anatomy of bone sialoprotein immunoreactive sites in bone as revealed by combined ultrastructural histochemistry and immunohistochemistry. *Calcif. Tissue Int.* 57(4), 277-84.

Rodeo, S.A., Arnoczky, S.P., Torzilli, P.A., Hidaka, C., 1993. Tendon-healing in a bone tunnel. A biomechanical and histological study in the dog. *J. Bone Joint Surg. Am.* 75(12), 1795-803.

Ross, F.P., Chappel, J., Alvarez, J.I., Sander, D., 1993. Interactions between the bone matrix proteins osteopontin and bone sialoprotein and the osteoclast integrin alpha v beta 3 potentiate bone resorption. *J. Biol. Chem.* 268(13), 9901-7.

Rothrauff, B.B., Tuan, R.S., 2014. Cellular therapy in bone-tendon interface regeneration. *Organogenesis* 10, 13–28.

Salih, E., Flückiger, R., 2004. Complete topographical distribution of both the in vivo and in vitro phosphorylation sites of bone sialoprotein and their biological implications. *The J. Biol. Chem.* 279, 19808–15.

Salih, E., Wang, J., Mah, J., Fluckiger, R., 2002. Natural variation in the extent of phosphorylation of bone phosphoproteins as a function of in vivo new bone formation induced by demineralized bone matrix in soft tissue and bony environments. *Biochem. J.* 364, 465–74.

Schwartz, A.G., Lipner, J.H., Pasteris, J.D., Genin, G.M., 2013. Muscle loading is necessary for the formation of a functional tendon enthesis. *Bone* 55(1), 44-51.

Schwartz, A.G., Pasteris, J.D., Genin, G.M., Daulton, T.L., Thomopoulos, S., 2012. Mineral distributions at the developing tendon enthesis. *PloS One* 7, e48630.

- Schweitzer, R., Chyung, J.H., Murtaugh, L.C., Brent, A.E., Rosen, V., Olson, E.N., Lassar, A., Tabin, C.J., 2001. Analysis of the tendon cell fate using Scleraxis, a specific marker for tendons and ligaments. *Development* 128, 3855–66.
- Seo, H.-S.S., Serra, R., 2007. Deletion of *Tgfb2* in *Prx1*-cre expressing mesenchyme results in defects in development of the long bones and joints. *Dev. Biol.* 310, 304–16.
- Shapiro, HS, Chen, J, Wrana, JL, Zhang, Q, Blum, M, 1993. Characterization of porcine bone sialoprotein: primary structure and cellular expression. *Matrix* 13(6), 431-40.
- Sharir A., Stern T., Rot C., Shahar R., Zelzer E., 2011. Muscle force regulates bone shaping for optimal load-bearing capacity during embryogenesis. *Development* 138, 3247–3259.
- Somerman, M.J., Fisher, L.W., Foster, R.A., 1988. Human bone sialoprotein I and II enhance fibroblast attachment in vitro. *Calcif. Tissue Int.* 43(1), 50-3.
- Somerman, M.J., Sauk, J.J., Foster, R.A., 1991. Cell attachment activity of cementum: bone sialoprotein II identified in cementum. *J. Periodontal Res.* 26(1), 10-16.
- Spagnoli, A., O'Rear, L., Chandler, R.L., Granero-Molto, F., Mortlock, D.P., Gorska, A.E., Weis, J.A., Longobardi, L., Chytil, A., Shimer, K., Moses, H.L., 2007. TGF-beta signaling is essential for joint morphogenesis. *J. Cell Biol.* 177, 1105–17.
- Sugimoto Y., Takimoto A., Akiyama H., Kist R., Scherer G., Nakamura T., Hiraki Y., Shukunami C., 2013. *Scx*+/*Sox9*+ progenitors contribute to the establishment of the junction between cartilage and tendon/ligament. *Development* 140, 2280–2288.
- Thomopoulos, S., Williams, G.R., Soslowky, L.J., 2003. Tendon to bone healing: differences in biomechanical, structural, and compositional properties due to a range of activity levels. *J. Biomech. Eng.* 125(1), 106-13.
- Thomopoulos, S., Kim, H., Rothermich, S., Biederstadt, C., Das, R., Galatz, L., 2007. Decreased muscle loading delays maturation of the tendon enthesis during postnatal development. *J. Orthop. Res.* 25, 1154–63.
- Traub, W., Arad, T., Weiner, S. 1992. Origin of mineral crystal growth in collagen fibrils. *Matrix* 12(4), 251-5.
- Tye, C.E., Hunter, G.K., Goldberg, H.A., 2005. Identification of the type I collagen-binding domain of bone sialoprotein and characterization of the mechanism of interaction. *J. Biol. Chem.* 280(4), 13487-92.
- Tye, C.E., Rattray, K.R., Warner, K.J., Gordon, J.A., Sodek, J., Hunter, G.K., Goldberg H.A., 2003. Delineation of the hydroxyapatite-nucleating domains of bone sialoprotein. *J. Biol. Chem.* 278(10), 7949-55.

- Valverde, P., Tu, Q., Chen, J., 2005. BSP and RANKL induce osteoclastogenesis and bone resorption synergistically. *J. Bone Miner. Res.* 20(9), 1669-79.
- Valverde, P., Zhang, J., Fix, A., Zhu, J., Ma, W., Tu, Q., Chen, J., 2008. Overexpression of Bone Sialoprotein Leads to an Uncoupling of Bone Formation and Bone Resorption in Mice. *J. Bone Miner. Res.* 23, 1775–1788.
- Verrecchia, F., Mauviel, A., 2002. Transforming Growth Factor- β ; Signaling Through the Smad Pathway: Role in Extracellular Matrix Gene Expression and Regulation. *J. Invest. Dermatol.* 118, 211–215.
- Wade-Gueye, N., Boudiffa, M., Vanden-Bossche, A., Laroche, N., Aubin, J., Vico, L., Lafage-Proust, M.-H., Malaval, L., 2012. Absence of bone sialoprotein (BSP) impairs primary bone formation and resorption: The marrow ablation model under PTH challenge. *Bone* 50(5), 1064-73.
- Waggett, A.D., Ralphs, J.R., Kwan, A.P., Woodnutt, D., Benjamin, M., 1998. Characterization of collagens and proteoglycans at the insertion of the human Achilles tendon. *Matrix Biol.* 16(8), 457-70.
- Wang, J., Zhou, H.-Y., Salih, E., Xu, L., Wunderlich, L., Gu, X., Hofstaetter, J., Torres, M., Glimcher, M., 2006. Site-Specific In Vivo Calcification and Osteogenesis Stimulated by Bone Sialoprotein. *Calcif. Tissue Int.* 79, 179–89.
- Wang, M., VanHouten, J., Nasiri, A., Johnson, R., Broadus, A., 2013. PTHrP regulates the modeling of cortical bone surfaces at fibrous insertion sites during growth. *J. Bone Miner. Res.* 28(3), 598-607.
- Wazen, R.M., Tye, C.E., Goldberg, H.A., 2007. In vivo functional analysis of polyglutamic acid domains in recombinant bone sialoprotein. *J. Histochem. Cytochem.* 55(1), 35-42.
- Wopenka, B., Kent, A., Pasteris, J.D., Yoon, Y., 2008. The tendon-to-bone transition of the rotator cuff: a preliminary Raman spectroscopic study documenting the gradual mineralization across the insertion in rat tissue samples. *Appl. Spectrosc.* 62(12), 1285-94.
- Wuttke, M., Müller, S., Nitsche, D.P., Paulsson, M., 2001., Structural characterization of human recombinant and bone-derived bone sialoprotein functional implications for cell attachment and hydroxyapatite binding. *J. Biol. Chem.* 276(39), 36839-48.
- Xia, B., Wang, J., Guo, L., Jiang, Z., 2011. Effect of bone sialoprotein on proliferation and osteodifferentiation of human bone marrow-derived mesenchymal stem cells in vitro. *Biologicals* 39(4), 217-23.

Xu, L., Anderson, A., Lu, Q., Wang, J., 2007. Role of fibrillar structure of collagenous carrier in bone sialoprotein-mediated matrix mineralization and osteoblast differentiation. *Biomaterials* 28, 750–61.

Zaia, J., Boynton, R., Heinegård, D., Barry, F., 2001. Posttranslational modifications to human bone sialoprotein determined by mass spectrometry. *Biochemistry*. 40(43), 12983-91.

Zelzer, E., Blitz, E., Killian, M., Thomopoulos, S., 2014. Tendon- to- bone attachment: From development to maturity. *Birth Defects Res. C. Embryo Today* 102, 101–12.

Zhao, Q.I., Eberspaecher, H., Lefebvre, V., 1997. Parallel expression of Sox9 and Col2a1 in cells undergoing chondrogenesis. *Dev. Dyn.* 209(4), 377-86.

Zhou, H.Y, Takita, H., Fujisawa, R., Mizuno, M., 1995. Stimulation by bone sialoprotein of calcification in osteoblast-like MC3T3-E1 cells. *Calcif. Tissue Int.* 56(5), 403-7.

CHAPTER TWO

IDENTIFICATION OF BONE SIALOPROTEIN IN ENTESIS
FIBROCARILAGE AND CHARACTERIZATION OF THE *BSP*^{-/-}
FIBROCARILAGINOUS ENTESIS

2.1 Chapter Summary

Tendons/ligaments insert into bone via a transitional structure, the enthesis, which is susceptible to injury and difficult to repair. Fibrocartilaginous entheses contain fibrocartilage in their transitional zone, part of which is mineralized. Mineral associated proteins within this zone have not been adequately characterized. Members of the Small Integrin Binding Ligand N-Linked Glycoprotein (SIBLING) family are acidic phosphoproteins expressed in mineralized tissues. Here we show two SIBLING proteins, bone sialoprotein (BSP) and osteopontin (OPN), are present in the enthesis. Histological analysis indicate that the calcified zone of *Bsp*^{-/-} mice is 28% longer in the quadriceps tendon enthesis, however no difference is apparent in the supraspinatus tendon enthesis. In an analysis of mineral content within the calcified zone, microCT and Raman spectroscopy indicate that more mineral is present at the mineralization front of the quadriceps tendon enthesis in *Bsp*^{-/-} mice, resulting in a steeper mineral gradient at the transition between soft and hard tissue. Mechanical testing of the patellar tendon indicate that while the tendons fail under similar loads, the *Bsp*^{-/-} patellar tendon is 7.5% larger in cross sectional area than wild type tendons, resulting in a 16.5% reduction in mechanical strength. However, picrosirius red staining shows no difference in collagen organization. Data collected here indicate that BSP and OPN are present in the calcified fibrocartilage of murine entheses and suggest that BSP plays a regulatory role at the mineralization front in this structure. BSP appears to be involved in modulating the deposition of mineral at the mineralization front, ultimately controlling the extent to which the tissue grows and due to this, loss of BSP may cause a weakening of the tendon mechanical properties. BSP's ability to modulate mineral deposition at the enthesis may ultimately

prove it to be a useful therapeutic molecule in the reattachment of tendons and ligaments to bone.

2.2 Introduction

Members of the Small Integrin Binding Ligand N-linked Glycoprotein (SIBLING) protein family are associated with the mineralized tissues of the skeleton and dentition (Fisher and Fedarko, 2003). SIBLINGs are anionic phosphoproteins with a flexible structure and extensive post-translational modifications. The family consists of 5 members: bone sialoprotein (BSP), osteopontin (OPN), dentin matrix protein 1 (DMP1), dentin sialophosphoprotein (DSPP) and matrix extracellular phosphoglycoprotein (MEPE), with the encoding genes located in a syntenic gene locus on murine chromosome five (Fisher and Fedarko, 2003).

BSP is a heavily glycosylated and phosphorylated protein that is expressed at the onset of mineralization in hard connective tissues (Goldberg and Hunter, 2012). In cell-free systems, BSP has been demonstrated to be a potent nucleator of hydroxyapatite (HA), the principal mineral component of bone (Hunter and Goldberg, 1993). Nucleation and binding to HA by BSP is conferred by poly-glutamic acid sequences found in the central region of the protein (Hunter and Goldberg, 1993; Tye et al., 2003). BSP also contains an N-terminal collagen-binding domain and it is proposed that binding of BSP to collagen promotes HA nucleation (Baht et al., 2008; Tye et al., 2005). Finally, BSP contains an integrin-binding RGD motif, located towards the C-terminus, which promotes osteoblast differentiation and matrix mineralization (Gordon et al., 2007).

Mice in which the *Bsp* gene has been ablated (*Bsp*^{-/-}) have a variety of skeletal and dental defects. At 4 months of age, these mice display reduced long bone length and cortical thickness, and a lower rate of bone formation, but have higher trabecular bone density than wild type mice (Malaval et al., 2008). However, due to an incisor

malocclusion phenotype on hard diet, some of these defects are ameliorated if *Bsp*^{-/-} mice are fed a soft food diet (Soenjaya et al., 2015). Further studies by the Malaval group showed that the *Bsp*^{-/-} mouse displays a delay of bone repair in cortical injury models (Monfoulet et al., 2010) and impaired bone formation and resorption in marrow ablation models (Wade-Gueye et al., 2012).

More recently, a significant periodontal phenotype has been uncovered in the *Bsp*^{-/-} mouse. Acellular cementum is a thin mineralized tissue found along the apical portion of the root of the tooth, into which the periodontal ligament (PDL) inserts. Immunohistochemistry shows that acellular cementum is rich in BSP, however in the *Bsp*^{-/-} mouse there is a striking reduction in the amount of this tissue (Foster et al., 2013). Additionally, the *Bsp*^{-/-} mouse PDL is disorganized, with poorly aligned collagen fibers that do not properly insert into the tooth root (Foster et al., 2015, 2013; Soenjaya et al., 2015). However, insertion of the PDL collagen into alveolar bone appears normal (Foster et al., 2015).

The defects observed in the PDL of the *Bsp*^{-/-} mouse have spurred us to investigate other junctions between soft and mineralized tissue. Of particular interest is the enthesis, the transition site of tendon and ligament insertion into bone. Fibrocartilaginous entheses are found where tendons or ligaments attach to the epiphysis or apophysis of long bones (Benjamin and McGonagle, 2001). As such, they are present at several key sites involved in locomotion, such as where the supraspinatus tendon (SST) of the rotator cuff meets the epiphysis of the humerus, and where the quadriceps femoris tendon (QCT) inserts into the back of the patella.

Fibrocartilaginous entheses contain a fibrocartilage zone containing type II collagen and fibrochondrocytes at the interface between tendon and bone. As such, fibrocartilaginous entheses display 4 transitional zones: the dense connective tissue of the tendon, uncalcified fibrocartilage (UFC), calcified fibrocartilage (CFC), and bone. A sharp boundary occurs between the calcified and uncalcified fibrocartilage which is known as the tidemark. Entheses are largely avascular and as such have a limited potential for regeneration (Benjamin and McGonagle, 2001; Benjamin et al., 2002). Once torn away from bone, reattachment of a tendon or ligament is difficult. Indeed, the failure rates for repairs of massive rotator cuff tears remain high despite advances in surgical technique (Galatz et al., 2004).

Given its HA nucleating and collagen binding properties, and the phenotype observed in the *Bsp*^{-/-} mouse PDL, we hypothesize that BSP is present in fibrocartilaginous entheses and is involved in directing the mineralization and organization of these structures. In this study we show for the first time that the mineralized zones of murine fibrocartilaginous entheses contain the SIBLING proteins BSP and OPN, and that the loss of BSP results in structural, mineral and mechanical alterations in these entheses and attached tendons.

2.3. Materials and Methods

2.3.1 *Animals*

Animal care followed guidelines of the Canadian Council on Animal Care and Veterinary Services at the University of Western Ontario. Preparation and genotyping of *Bsp*^{-/-} and wild-type mice, maintained on a mixed 129/CD1 background, were performed as described previously (Malaval et al., 2008). *Opn*^{-/-} mice were obtained from Jackson Laboratory (JAX Stock number 004936, Sacramento, USA) and handled as described previously (Holm et al., 2014). All mice used in this study were fed a soft diet as outlined by Soenjaya *et al.* (Soenjaya et al., 2015). Animals used in this study were sacrificed by CO₂ asphyxiation. All comparisons between genotypes were performed on male mice born in the same litter.

2.3.2 *Histology and Immunohistochemistry*

Wild type and *Bsp*^{-/-} shoulder and knee joints from 15 week old mice were harvested and prepared for histology as described previously with alterations (Wang et al., 2007) . Briefly, tissue was fixed in neutral buffered formalin (10%) overnight at 4°C and were then decalcified in 0.65 M EDTA pH 7.4 at 37 °C for three weeks. Tissues were processed by University Hospital Pathology Core, London, ON, Canada, then embedded in paraffin and sectioned into 5 µm sections.

Immunohistochemical analysis used in this study is as described previously (Foster et al., 2013; Holm et al., 2015). Briefly, following standard histological deparaffinization and rehydration, samples were treated with 3% hydrogen peroxide in methanol. Heat mediated antigen retrieval was performed in 0.1 M sodium citrate, pH 6.0. Non-specific interactions were blocked using 5% goat serum in PBS for 1 hour at

room temperature. Sections were then treated with rabbit anti-mouse BSP serum (courtesy of Dr. Renny Franceschi, University of Michigan School of Dentistry, Ann Arbor, MI) or rabbit anti-mouse OPN serum (Courtesy of Dr. Larry Fisher, Bethesda, MD) overnight at 4°C. Antibodies used in the study have been described previously (Foster et al., 2013; Ogbureke and Fisher, 2004). 1:200 dilutions in phosphate buffered saline with 5% goat serum were used for both the OPN and BSP antibodies. In the morning, sections were washed in PBS-T (0.1% Tween 20, Sigma-Aldrich) then treated with horseradish peroxidase-conjugated goat anti-rabbit IgG for 1 hour at room temperature. Sections were again washed with PBS-T, then treated with hydrogen peroxide and 3,3'-diaminobenzidine (DAB) (Vector Labs). Following DAB development, sections were counterstained with methyl green, dehydrated, cleared then mounted in xylene-based mounting medium.

A basic hematoxylin and eosin staining technique was used for this study. Sections were stained for 10 seconds in Harris's Hematoxylin (Sigma-Aldrich), then washed in running tap water for 10 min. Sections were then rinsed briefly in deionized water and stained with Eosin Y (Sigma-Aldrich) for 1 min. After another rinse in deionized water, sections were dehydrated and cleared, and then mounted in xylene-based mounting medium.

Von Kossa staining was performed as follows. Tissues were incubated in 2% silver nitrate for 48 hours. After the silver nitrate solution had permeated the tissues in their entirety silver ions were precipitated by reduction with sodium hypophosphite (0.6 M) over the course of three days. By this method, elemental silver is deposited as a black precipitate in areas where hydroxyapatite is present. Tissues were then decalcified in 10%

formic acid over the course of 10 hours, followed by histological processing and sectioning as described above. After sectioning, tissues were incubated with 5% sodium thiosulfate to remove excess nonspecific staining. Sections were counterstained in alcian blue for 30 min, washed with deionized water, and then stained with nuclear fast red for 10 min. Sections were then dehydrated and cleared followed by mounting in xylene-based mounting medium.

Picrosirius red staining was performed as follows. Tissues were stained with Sirius red (Sigma-Aldrich) in saturated picric acid for 1 hour. Following staining, sections were washed in two changes of acidified water, then dehydrated and cleared. Specimens were imaged using circularly polarized light and collagen organization was characterized using the methods outlined by Rich and Whittaker (Rich and Whittaker, 2005).

All solutions used in these protocols were made with Milli-Q deionized water unless otherwise indicated.

2.3.3 Measurement of the calcified fibrocartilage zone

The distance between the tidemark and bone of the SST and QCT entheses were measured across three transverses drawn parallel to the orientation of the collagen fibres, by two blinded individuals, in five 15 week-old male wild type and *Bsp*^{-/-} litter mate pairs. The lengths of the triplicate measurements in each enthesis were averaged and these averages were compared between wild type and *Bsp*^{-/-} mice using a parametric unpaired t-test.

2.3.4 *Mechanical testing*

Immediately after euthanization, the hind limbs of 15 week old mice were removed and wrapped in PBS soaked gauze, then stored at -20°C prior to mechanical testing at the University of Pennsylvania. After thawing, the skin of the contralateral limbs was removed and the patella-patellar ligament-tibia complexes were carefully dissected under magnification, as described previously (Dunkman et al., 2013). The tendon cross-sectional area was measured using a custom laser-based device. The anterior surface of each tendon was speckle-coated with Verhoeff's stain to facilitate optical strain measurement. Prior to mechanical testing, the tibia was potted in polymethyl methacrylate (PMMA) and the patella was gripped with a custom aluminum fixtures. The specimens were then loaded into a materials testing system (Instron, Model 5848; Norwood, MA, USA) with a 10 N load cell. Throughout the testing, the system was submerged in a PBS bath maintained at 37°C . All specimens were tested using a modified version of the protocol outlined in (Dunkman et al., 2013). Briefly, the protocol consisted of preloading and preconditioning followed by 300 second hold and stress relaxation at 5% strain. After a return to gauge length, a ramp to failure at $0.1\%/s$ was performed to measure the failure load of the specimens. For data analysis, modulus was calculated using optical tracking software for each tendon at three regions: (1) the patellar origin (1 mm distal to the patella), (2) tendon mid-substance and (3) tibial insertion (1 mm proximal to tibial insertion).

2.3.5 *Microcomputed Tomography*

Microcomputed tomography (microCT) analysis of the patella was performed using the eXplore Locus SP scanner (GE Healthcare, London, ON, Canada). 2D images were acquired using an X-ray tube with a voltage of 80 kVP and a current of 80 mA, with a 0.508 mm Al filter. The exposure interval time of the scanner was 1600 msec/frame at 4 frames/view. In total, 900 views were obtained at 0.4 degrees angular increments. The data were reconstructed at a spatial resolution of 13.5 μm . All reconstructed data were calibrated with a cortical bone phantom (SB3; Gammex RMI, Milwaukee, WI, USA) with a hydroxyapatite equivalent of 1,100 mg/cc (White 1978), as well as water and air. Data were analyzed with MicroView ABA version 2.2 (GE Healthcare).

For patellar analysis, 5 mice per genotype were used. Quantification of mineral density was performed on 3D cubical volumes of interest (VOIs; 20 isotropic voxel size) identified at the base area, where attachment of the quadriceps tendon occurred.

For measurement of mineral density distribution along the tendon-to-bone insertion, three parallel transverse line measurements were obtained and averaged for each region of interest (ROI). The lines were defined manually along the CFC of the QCT enthesis.

2.3.6 *Raman spectroscopy*

Three pairs of male wild type and *Bsp*^{-/-} littermates aged 15 weeks were euthanized, and the patellae were carefully dissected out following death. Patellae were then immersed in O.C.T (Tissuetek) and snap frozen. Sagittal sections (10 μm) of the patellae were cut in a cryostat using a tungsten carbide blade. Sections were quickly

fixed, washed and dehydrated using an ethanol gradient, and then stored at -80°C until scanning.

The apparatus used for Raman spectroscopy was a LabRAM HR (Horiba-Jobin-Yvon, Kyoto Japan) connected to an inverted optical microscope (IX71, Olympus, Tokyo, Japan) and interfaced with an atomic force microscope system stage (NanoWizard II Bioscience, JPK Instruments Inc., Berlin, Germany). The protocols used are as described by (Schwartz et al. 2012). Peak intensity (height) was measured at 960 cm^{-1} , representing the P-O bonds of hydroxyapatite, and 2940 cm^{-1} , representing the C-H bonds of collagen and other proteins. After baseline correction, the P-O peak was normalized to the C-H peak, based on the assumption that the collagen content of the sample was constant at all points measured. Normalized 960 cm^{-1} hydroxyapatite P-O peak intensities were then compared between wild type and *Bsp*^{-/-} samples. For each individual QCT enthesis, three separate linear measurements were made per enthesis, as described in the figure legends, lines of measurement were drawn from tidemark to bone in the orientation of the collagen fibres of the CFC.

2.3.7 Statistical analyses

Quantitative data are expressed as mean \pm standard error. For enthesis length and mechanical comparisons, statistical analyses between experimental groups were performed using an unpaired parametric t-test. For microCT and Raman spectroscopy, differences between wild type and *Bsp*^{-/-} mice was performed using repeated measures two way ANOVA. All statistical analysis were performed with Prism version 6.00 (GraphPad Software, La Jolla, CA).

2.4 Results

2.4.1 *BSP and OPN are present in the mineralized tissues of fibrocartilaginous entheses*

Immunohistochemistry was performed to determine whether the SIBLING proteins BSP and OPN are present in the murine fibrocartilaginous entheses. BSP and OPN were detected in the calcified fibrocartilage of the QCT and SST entheses as well as the adjacent bone (Fig. 2.1). The absence of BSP and OPN immunostaining was confirmed in *Bsp*^{-/-} and *Opn*^{-/-} mice, respectively (Fig. 2.1).

2.4.2 *Bsp*^{-/-} mice exhibit defects in calcified fibrocartilage zone of the enthesis

Von Kossa staining of the QCT and SST enthesis indicate approximately equivalent mineral content in the CFC of the wild type and *Bsp*^{-/-} enthesis (Fig. 2.2C,D,G,H). However, the CFC is extended in QCT enthesis of *Bsp*^{-/-} mice (Fig. 2.2A-D). The tidemark-to-bone length in the QCT enthesis measured at 178.8 ±15.5 μm for wild type and 229.1±17.5 μm for *Bsp*^{-/-} mice (p<0.05, n=5). Surprisingly, no differences in the length of the CFC was observed in the SST enthesis of *Bsp*^{-/-} and wild type mice (Fig. 2.2E-H).

Due to the alteration in the CFC length of the *Bsp*^{-/-} QCT enthesis, we analyzed the degree of mineralization along the length of the QCT enthesis. We initially utilized microCT in order to analyze the mineral distribution along the CFC of the *Bsp*^{-/-} QCT enthesis. MicroCT analysis demonstrated that radiodensity in the region corresponding to the CFC of the QCT enthesis increased rapidly then plateaued (Fig. 3A,B). No statistically significant difference was observed in radiodensity of the QCT CFC

Figure 2.1 SIBLING proteins are present in the calcified fibrocartilage of the SST and QCT entheses. Immunohistochemistry was performed to detect the presence of BSP and OPN protein (diaminobenzidine staining, brown) in the quadriceps tendon enthesis (QCT) and supraspinatus tendon enthesis (SST). BSP and OPN were detected in the calcified fibrocartilage of these entheses and are not present beyond a sharp boundary representing the tidemark between the CFC and UFC. Negative controls for BSP and OPN immunostaining of the SST and QCT entheses were performed on *Bsp*^{-/-} and *Opn*^{-/-} mice respectively. No nonspecific staining in the CFC on control mice was detected. Wild type and *Bsp*^{-/-} animals are 15 week old, male, 129/CD1 mice; *Opn*^{-/-} animals at 15 week old, male, C57Bl/6 mice. CFC: calcified fibrocartilage, UFC: uncalcified fibrocartilage, bar = 100 μm

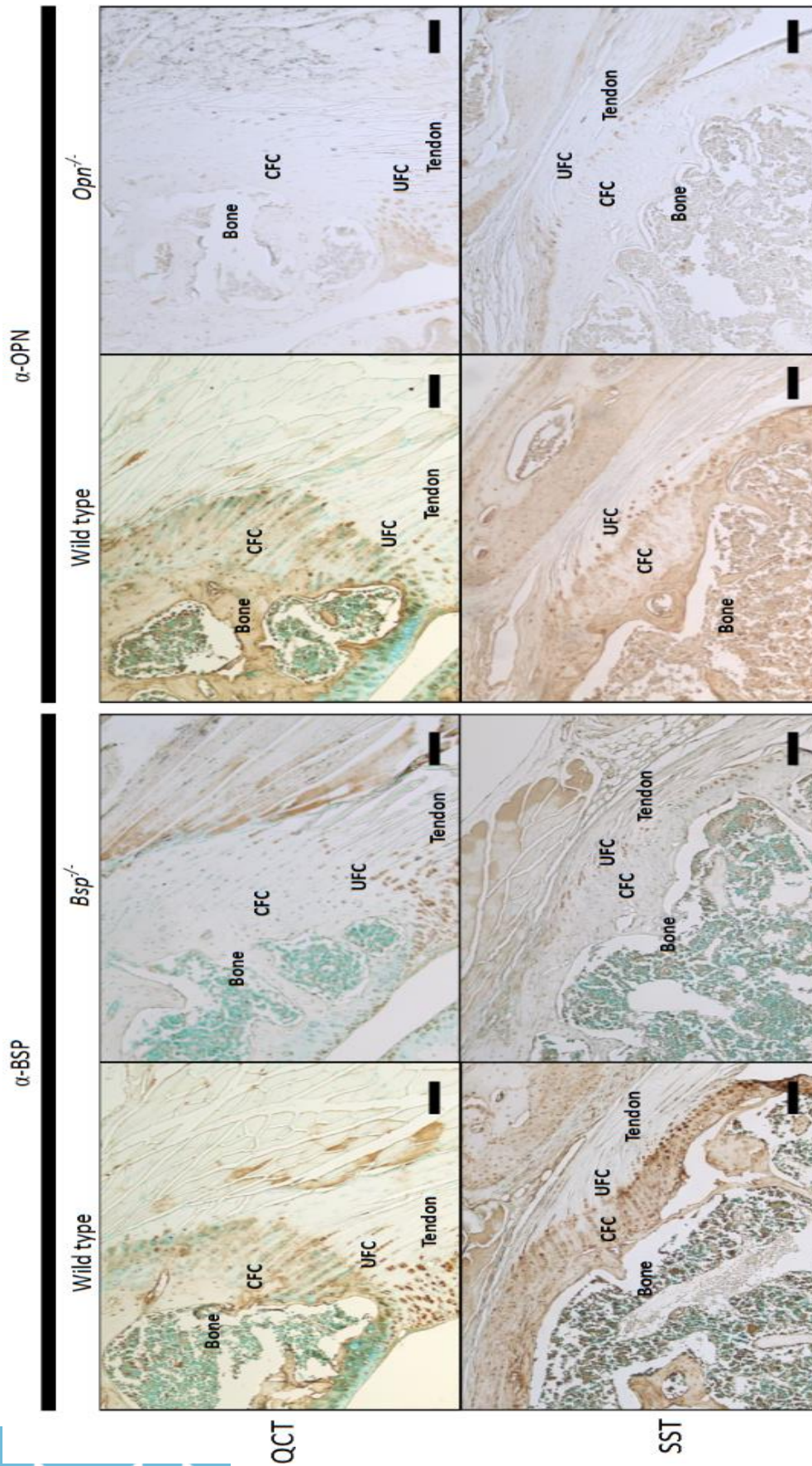
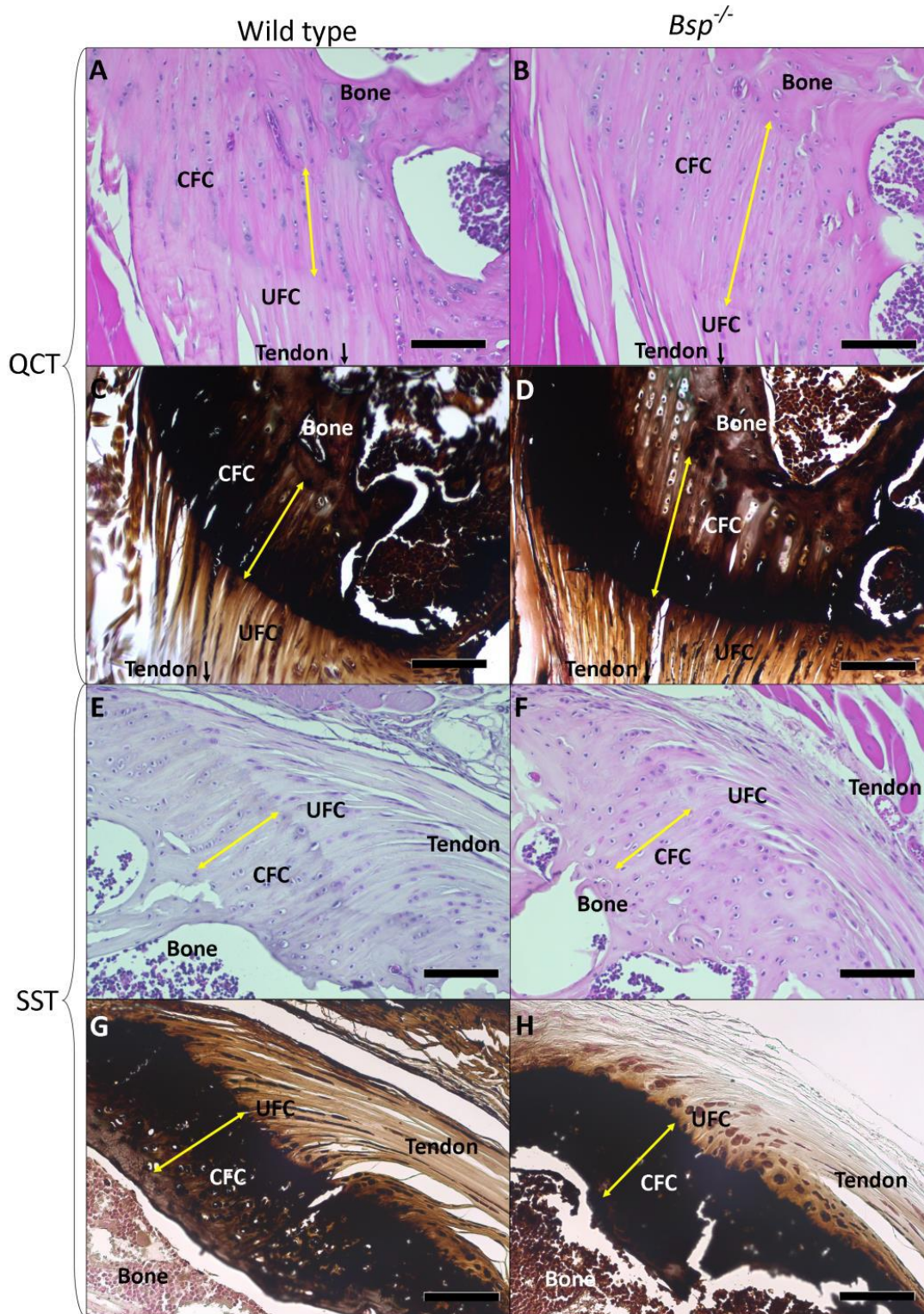


Figure 2.2 Mineral is deposited in the calcified fibrocartilage of *Bsp*^{-/-} mice however the morphology of the calcified fibrocartilage is altered. (C,D,G,H) Von Kossa staining of the QCT and SST entheses indicate approximately equivalent mineral content in the CFC of the wild type and *Bsp*^{-/-} entheses. (A,B,E,F) Staining with haematoxylin and eosin was used to assess gross morphology. An extension of the calcified fibrocartilage was observed, as measured from tidemark to bone (yellow arrow) in the QCT entheses (n=5). CFC: calcified fibrocartilage, UFC: uncalcified fibrocartilage, bar = 100 μ m



between wild type and *Bsp*^{-/-} mice, suggesting that mineral content in the enthesis is similar (Fig. 3C,D). A slight increase in radiodensity was observed in the region immediately after the tidemark of the *Bsp*^{-/-} QCT enthesis compared to wild type, suggesting that higher levels of mineral are present in this region in the *Bsp*^{-/-} mouse, however the difference was not statistically significant (Fig. 3A and B).

Previously, the mineral gradient that occurs at the tidemark was measured to be approximately 20 μm in length (Schwartz et al., 2012). Of relevance, past studies have shown that a gradient of mineral is present along the enthesis where it is believed to play a role in stress dissipation (Genin et al., 2009; Schwartz et al., 2012). Since the resolution of the microCT analysis was limited to 11.5 μm , to obtain more definitive analysis, Raman spectroscopy, which has a resolution of approximately 0.5-0.75 μm , was used to determine the gradient of mineral content. We used Raman spectroscopy to analyse the relative difference in intensity between the P-O bonds (peak at 960 cm^{-1}) of phosphate ions of HA to the organic C-H bonds (peak at 2940 cm^{-1}) of the organic matter present in the tissue (mostly collagen), in *Bsp*^{-/-} and wild type mice (Fig. 4A). Raman analysis mirrored our microCT findings. Mineral content increases rapidly at the tidemark in both *Bsp*^{-/-} and wild type mice then plateaued, with relatively equal levels of mineral being present in both sets of animals (Fig. 4B). Similar to microCT analysis, a minor increase in mineral is present near the tidemark in *Bsp*^{-/-} mice (Fig. 4C,D) however due to the highly variable nature of Raman signals, statistical significance was not found ($p > 0.05$).

Figure 2.3 MicroCT analyses indicates similar levels of mineralization in wild type and *Bsp*^{-/-} QCT entheses. (A) Three parallel lines (yellow arrows) per individual were drawn along the orientation of the collagen fibers inserting into bone to analyze changes in mineral density across the CFC, then averaged. Lines span from points before the tidemark across the QCT enthesis and patellar bone into the marrow space. Position 0.00 indicates where radiodensity crossed a threshold of 800 HU, which was estimated to be the tidemark. (B) Radiodensity, which is an estimate of mineral content, across the length of the QCT enthesis was similar between wild type and *Bsp*^{-/-} mice. Radiodensity trended towards an increase in the region adjacent to the tidemark in *Bsp*^{-/-} mice. (C) MicroCT analysis was also performed to determine the overall radiodensity within a 20 voxel region (isotropic voxel size of 11.5 μm) region of the CFC. However, (D) the results showed no apparent changes in the overall mineral density of the *Bsp*^{-/-} CFC zone compared to wild type. HU: Hounsfield units.

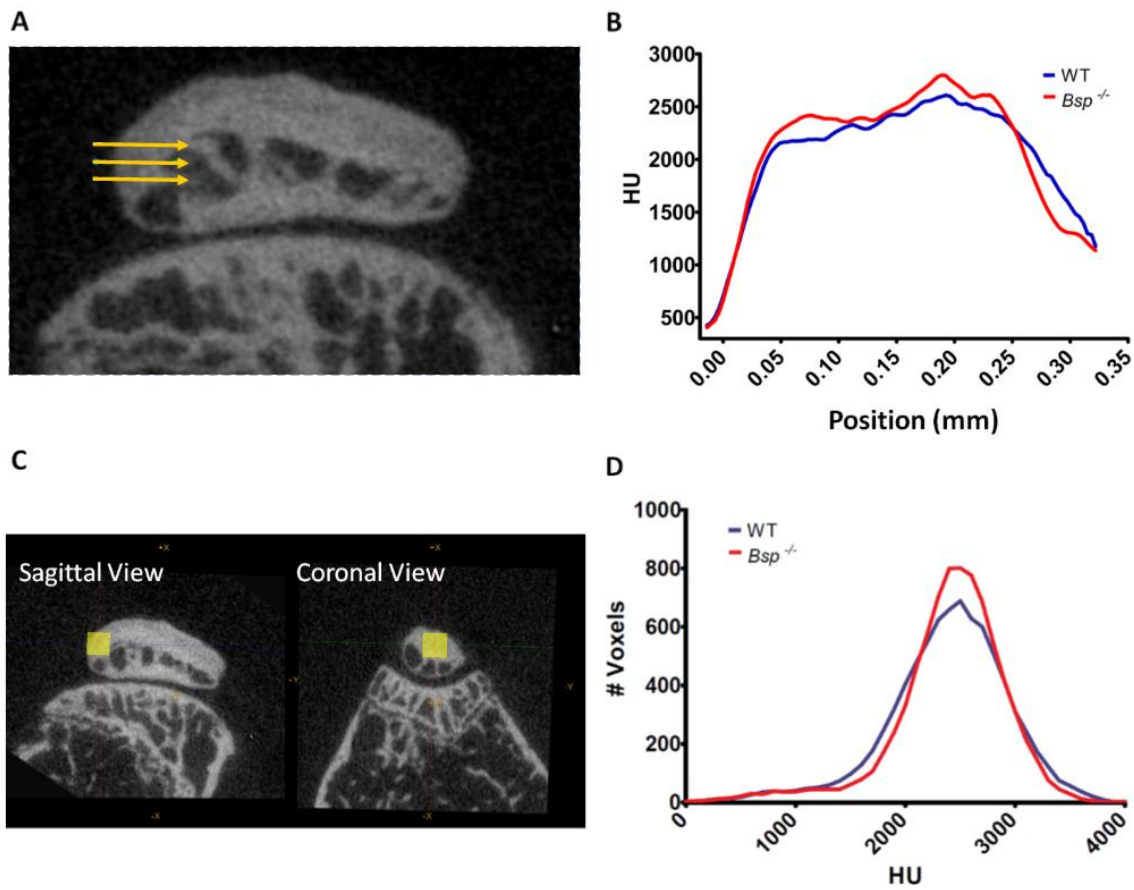
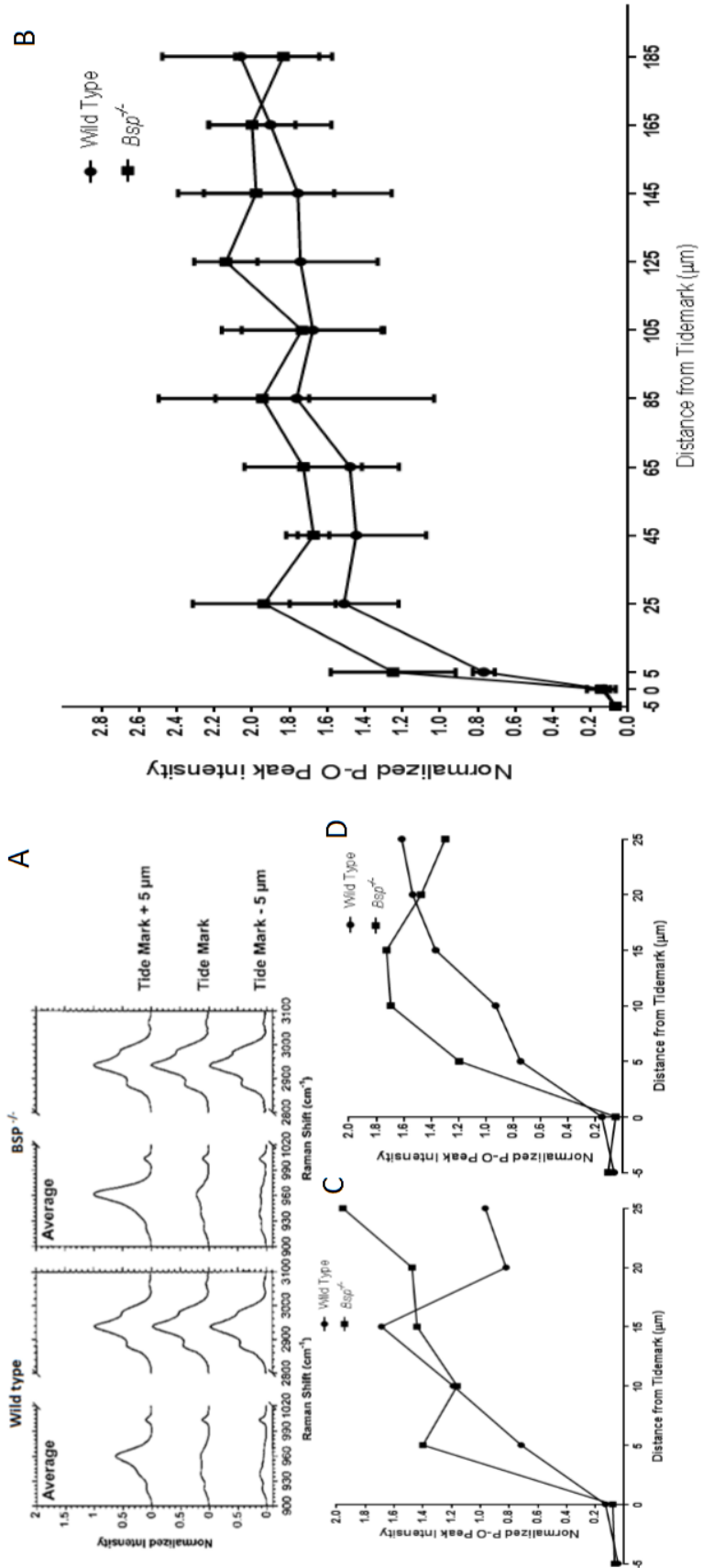


Figure 2.4 Raman spectroscopy shows that the mineral content in the QCT enthesis is comparable between wild type and *Bsp*^{-/-} mice. (A) 960 cm⁻¹ hydroxyapatite peak intensities and 2940 cm⁻¹ collagen peak intensities were analyzed at the tidemark and 5 μm to either side. 960 cm⁻¹ peaks are normalized to the 2940 cm⁻¹ peak at each position measured. (B) Overall mineral content across the length of the the QCT enthesis is similar between *Bsp*^{-/-} and wild type mice. (C,D) Differences in mineral gradients are more apparent in comparisons of single transverses from individual wild type and *Bsp*^{-/-} littermate pairs due to high variability in mineral to collagen ratios.



2.4.3 *Mechanical testing suggests a weakened enthesis in $Bsp^{-/-}$ mice*

Defects noted in the CFC of the QCT enthesis prompted us to determine whether the strength of $Bsp^{-/-}$ enthesis is compromised. Mechanical testing performed on the patellar ligament, which links the patella to the proximal end of the tibia, indicated that its cross-sectional area was approximately 7.5% larger in $Bsp^{-/-}$ mice than wild type (Fig. 2.5); however, the load required to fail the patellar tendon is similar for both genotypes, indicating that $Bsp^{-/-}$ mice have a weaker patellar tendon with a 16.5% lower failure stress compared to wild type (Fig. 2.5). Regardless of genotype, the patellar tendon failed at different positions along its length, with some failures occurring at the enthesis while others occurring at the tendon midsubstance and, in some cases, failing at more than one location. Unexpectedly, the local elastic moduli of $Bsp^{-/-}$ patellar tendon at three different regions: 1) patellar insertion, 2) midsubstance, and 3) tibial insertion were found to be similar to wild type (data not shown). In addition, the overall percent relaxation and stiffness of the $Bsp^{-/-}$ patellar tendon were not affected (data not shown).

2.4.4 *Collagen organization is not affected by the loss of BSP*

Given the mechanical defect observed, as well as the disorganization seen in the periodontal ligament (Foster et al., 2013), collagen organization was assessed by picrosirius red staining. Images of wild type and $Bsp^{-/-}$ SST entheses and QCT entheses were taken using circularly polarized light (Fig. 2.6A). No striking difference in collagen organization was observed. Hue values, which are an index of collagen fiber thickness, were quantified using the protocol outlined by Rich and Whittaker (MacKenna and

Omens, 1994; Rich and Whittaker, 2005)(Fig. 2.6B). The proportions of pixels with specific hue values is not significantly shifted in *Bsp*^{-/-} entheses when compared to wildtype in either the SST or QCT entheses.

Figure 2.5 *Bsp*^{-/-} mice exhibit alteration in patellar enthesis mechanical properties.

At 15 weeks, *Bsp*^{-/-} mice (n=11) revealed greater cross-sectional area compared to wild type. During tensile mechanical test, the *Bsp*^{-/-} mice (n=10) patellar enthesis failed at a lower stress compared to wild type (n=12). Values shown represent means \pm SEM; *p < 0.05.

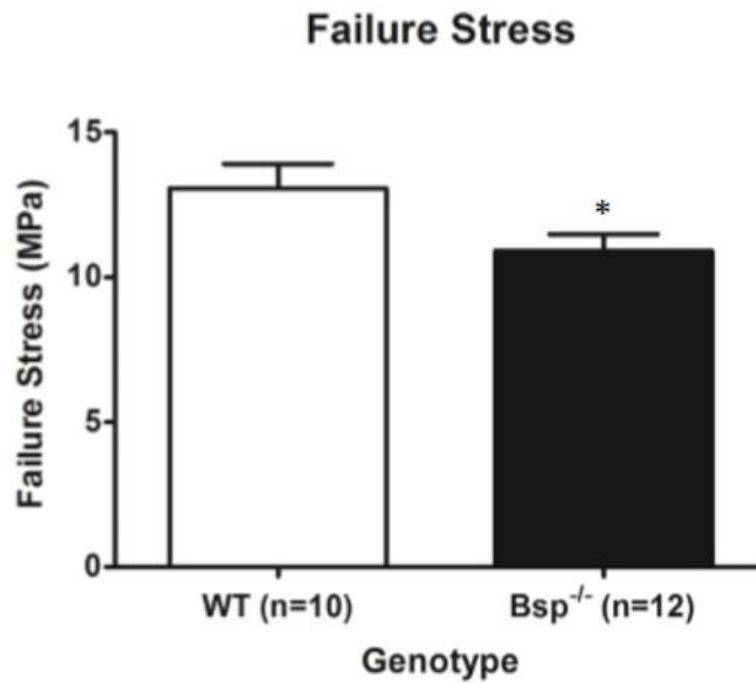
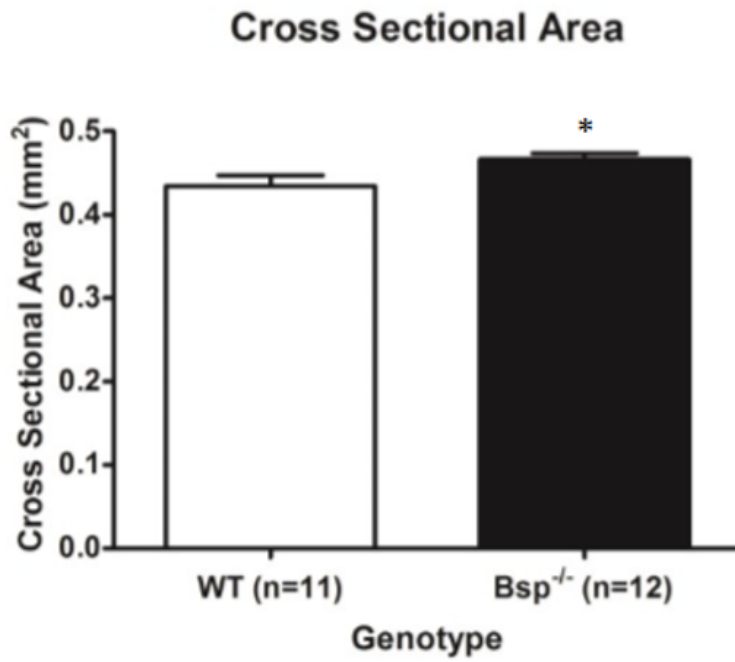
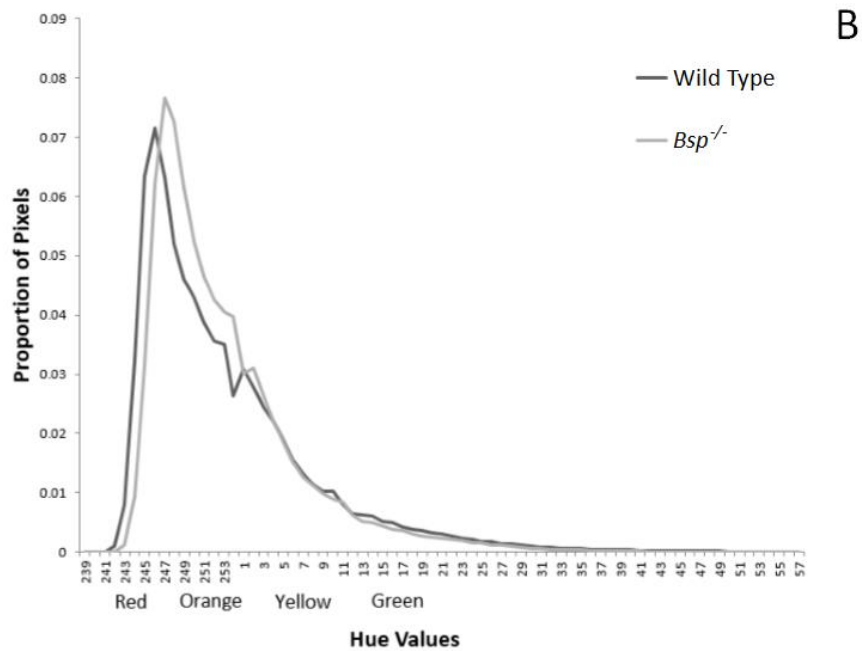
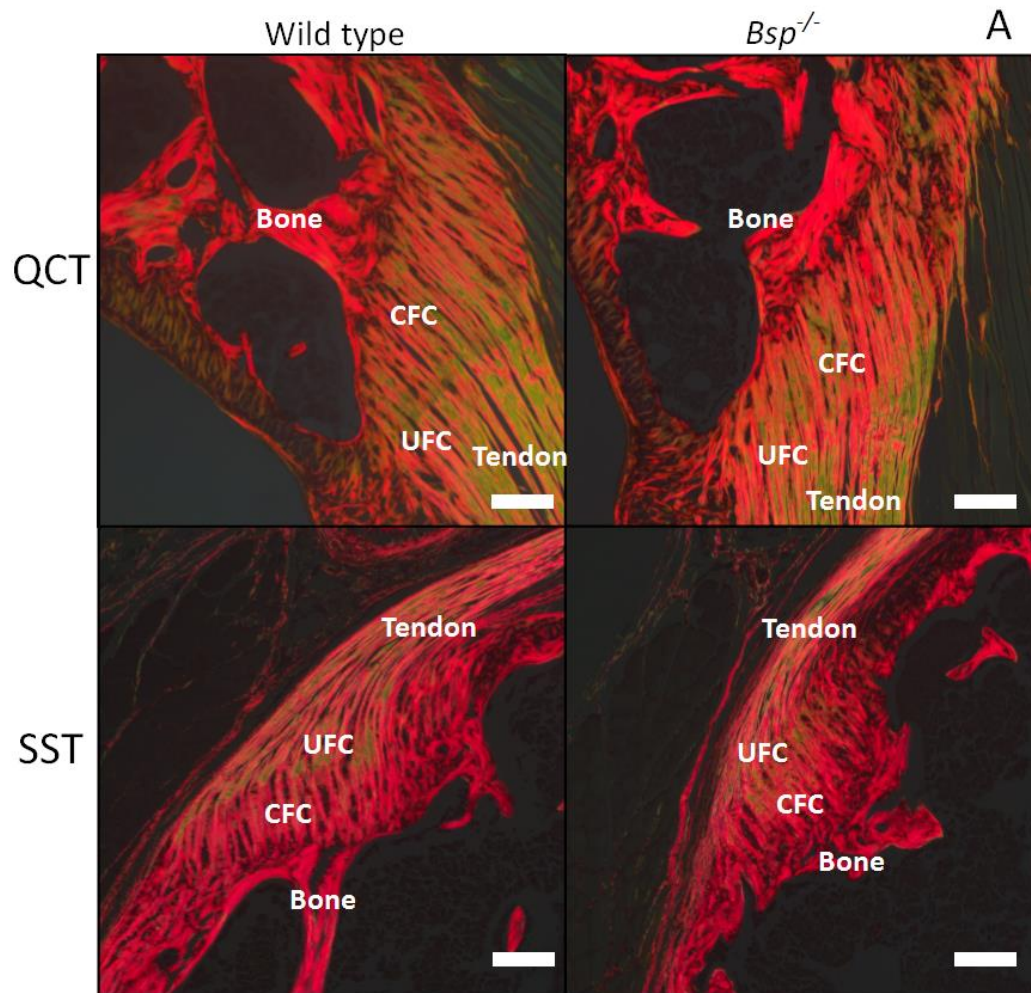


Figure 2.6 Collagen organization is not affected by loss of BSP. (A) SST and QCT entheses of wild type and *Bsp*^{-/-} animals were stained using picosirius red and viewed under circularly polarized light. Red-orange hues represent densely packed collagen fibers while greenish hues represent more loosely packed collagen fibers. CFC: calcified fibrocartilage, UFC: uncalcified fibrocartilage, bar = 100µm (B) Hue values for the SST were quantified. Each image (n=7 for wild type and *Bsp*^{-/-}) was resolved into 256 bit colour. The calcified fibrocartilage was manually selected in each image and the number of pixels with each hue value was counted and divided by the total number of pixels in the selected area to determine the proportion of pixels with each hue. Hue proportions were then averaged. Red hues correspond to values between 240-250, orange 251-254 and 1-3, yellow 4-12, green 13-56. Black pixels are given a value of 0 and white pixels a value of 255 and were omitted from analysis. Note that hues values of interest span the high and low end of the spectrum, but are presented here as a single peak.



2.5 Discussion

BSP is an extracellular matrix protein present in mineralized tissues such as bone and tooth. Here we demonstrate for the first time that BSP is also present in the CFC zone of the fibrocartilaginous enthesis. OPN was identified for the first time in this structure as well. The absence of BSP resulted in a lengthening of the CFC in the QCT enthesis. Furthermore, the *Bsp*^{-/-} patellar tendon has an increased cross-sectional area and lower failure stress, however, the overall collagen organization and mineral content of the *Bsp*^{-/-} enthesis appeared to be normal. Our findings suggest that BSP plays a role in the calcified fibrocartilage of the fibrocartilaginous enthesis.

2.5.1 Role of altered calcified fibrocartilage zone of the *Bsp*^{-/-} QCT enthesis.

In this study, we have shown that BSP, a protein with demonstrated potency to promote mineral formation *in vitro* (Hunter and Goldberg, 1993), is present in the CFC zone of the enthesis. In the same tissue, we also demonstrated the presence of OPN, a close relative of BSP with inhibitory activity on HA formation (Hunter et al., 1994). The extracellular matrix composition of fibrocartilaginous entheses has been investigated previously (Gao et al., 1996; Waggett et al., 1998), however these studies primarily focused on the various collagens and proteoglycans. The distribution of mineral and orientation of the collagen fibers in the enthesis has been shown to influence its mechanical properties (Genin et al., 2009; Liu et al., 2012, 2011; Thomopoulos and Williams, 2003; Thomopoulos et al., 2005). However, there has been limited attempt to identify the mechanism by which the CFC is mineralized. To our knowledge, the presence of mineral associated proteins has never been reported in the enthesis, although

recently asporin mRNA was identified in the enthesis fibrocartilage of 14-day-old mice (Liu et al., 2013).

Our previous studies have shown that *Bsp*^{-/-} mice lack acellular cementum, which led to PDL detachment and disorganization, and associated periodontal tissue breakdown such as resorption of alveolar bone and tooth surface (Foster et al., 2013). Minimizing the mechanical load during mastication, by changing to a soft diet, was not successful in ameliorating the rate of periodontal breakdown. In spite of this, reducing the mechanical load has significantly reduced the rate of incisor malocclusion, which affects the *Bsp*^{-/-} mice ability to feed normally. By 8 weeks, long bone lengths normalize when *Bsp*^{-/-} mice are fed a soft diet as does overall weight and serum alkaline phosphatase activity (Soenjaya et al., 2015). Based on the disorganization and detachment in the PDL, we initially hypothesized that the loss of BSP would have a negative effect on the collagen structure of the enthesis. However, no changes in the organization of collagen structure in the CFC of *Bsp*^{-/-} mouse enthesis was observed. This observation suggests that BSP does not have a role in collagen organization.

In the absence of BSP, the calcified fibrocartilage of the enthesis still forms and becomes mineralized. Thus, it is likely that other factors are compensating for the lack of BSP. Of relevance, our own studies have shown that in contrast to the poor PDL insertion into acellular cementum, insertion into the alveolar bone was not affected by the absence of BSP (Foster et al., 2015). It is of interest that at 15 weeks, the *Bsp*^{-/-} QCT enthesis is greater in length (28% increase over wild type) compared to wild type at 15 weeks of age. In contrast, microCT and Raman spectroscopy analysis revealed that there is little

difference in the level of mineralization within the CFC between *Bsp*^{-/-} and wild type mice.

These results indicate mineral deposition and CFC growth are dysregulated in BSP's absence. Recently it was shown that active mineralization occurs in a narrow band of Indian hedgehog (IHH) producing cells at the tidemark and that there is little turnover in enthesis fibrocartilage once formed (Dyment et al., 2015). Thus it seems likely that BSP is active at the tidemark. Interestingly, although BSP is thought to be a pro-mineralization factor, the mineralized tissue in the *Bsp*^{-/-} enthesis is larger in size. It is possible that in BSP's absence another pro-mineralization factor is compensating for BSP and driving excess mineralization in the CFC. Another possibility is that BSP is involved in cell proliferation through its integrin-binding RGD motif and acts as a regulatory molecule on enthesis fibrochondrocytes.

Extensions of the mineralized zones of entheses have been documented in other studies. Polisson *et al.* have reported lengthening of the mineralized tissues of tendon and ligament insertions in humans suffering from X-linked hypophosphatemic osteomalacia (Polisson et al., 1985). Utilizing a murine model of this disorder in which *PHEX*, a gene involved in phosphate regulation, has been inactivated, Liang *et al.* have shown lengthening of the CFC in the QCT enthesis as well as in the Achilles tendon insertion into the calcaneus and the attachment of the patellar ligament to the tibial tubercle (Liang et al., 2009). Interestingly, a related disorder, autosomal recessive hypophosphatemia, is caused by a loss of function mutation in *DMP1* (Lorenz-Depiereux et al., 2006), which is a close relative of BSP and part of the SIBLING protein family (Fisher and Fedarko

2003). Characterization of the *Dmp1*^{-/-} fibrocartilaginous enthesis, however, has not yet been described.

2.5.2 *Bsp*^{-/-} patellar tendon exhibit weakened mechanical properties under load.

Interestingly, the *Bsp*^{-/-} patellar tendon cross-sectional area is greater than the wild type; however, under mechanical testing, the *Bsp*^{-/-} patellar tendon failed at a similar applied load compared to wild type. This implies that the *Bsp*^{-/-} patellar tendon is weaker since it requires lower stress, which is a function of both load and cross-sectional area, to fail. It is possible that a larger patellar tendon cross-sectional area observed in the *Bsp*^{-/-} mouse is a compensatory mechanism which ensures that although the tendon is weaker, it can withstand the same loads. Similarly, Gao and Messer have hypothesized that the size of the CFC in an enthesis is related to the tensile load under which it is placed during its use (Gao and Messner, 1996). The increased size of the QCT CFC in the *Bsp*^{-/-} mouse may also be compensating for a weakened tendon. Challenge experiments in which greater stress is placed on the *Bsp*^{-/-} enthesis may provide insight as to how mechanical factors impact BSP's role in enthesis mineralization.

Furthermore, challenge experiments may reveal a more profound defect caused by the loss of BSP due to compromised repair processes in the enthesis. BSP has been implicated in the repair of several mineralized tissues. When BSP and collagen (prepared by crosslinking BSP to collagen, personal communication E. Salih) are implanted into calvarial defects of 7-8 week old rats, new bone formation is observed (Wang et al., 2006). Cortical defects drilled into the femurs of *Bsp*^{-/-} mice heal slowly when compared to wild type counterparts (Malaval et al., 2009; Monfoulet et al., 2010). Indeed, given

BSP's collagen binding domain, hydroxyapatite nucleating properties and cell attachment and migration functions, BSP may be an attractive molecule to promote remineralization in common enthesal injuries such as rotator cuff tears, however further characterization of BSP's role in enthesis development is required.

Interestingly, there are many similarities between the development of fibrocartilaginous entheses and growth plates involved in endochondral ossification (Zelzer et al., 2014). We and others have recently identified abnormalities in the growth plates of *Bsp*^{-/-} mice as well as a delay in mineral deposition during endochondral ossification (Bouleftour et al., 2014; Holm et al., 2015). By 8 weeks however, *Bsp*^{-/-} mice display a normal bone phenotype when fed a soft food diet (Soenjaya et al., 2015). This suggests that a more pronounced phenotype may be present during the development of *Bsp*^{-/-} fibrocartilaginous entheses.

In combination, these data suggest that BSP may play a role in the mineralization of the CFC of the enthesis. Specifically, BSP seems to be acting at the mineralization front, the tidemark, of the fibrocartilaginous enthesis where it controls mineral deposition within a larger regulatory network. In BSP's absence, other pro-mineralization factors appear to be compensating, resulting in excess mineralization at the tidemark and a dysregulation of CFC growth. These defects may ultimately contribute to the weakening of patellar tendon observed in the *Bsp*^{-/-} mouse.

2.6 References

- Baht, G.S., Hunter, G.K., Goldberg, HA, 2008. Bone sialoprotein–collagen interaction promotes hydroxyapatite nucleation. *Matrix Biol.* 27, 600–608.
- Benjamin, M., McGonagle, D., 2001. The anatomical basis for disease localisation in seronegative spondyloarthropathy at entheses and related sites. *J. Anat.* 199(Pt5), 503-26.
- Benjamin, M., Kumai, T., Milz, S., Boszczyk, B.M., Boszczyk, A.A., Ralphs, J.R., 2002. The skeletal attachment of tendons--tendon “entheses”. *Comp. Biochem. Physiol., Part A Mol. Integr. Physiol.* 133, 931–45.
- Bouleftour, W., Boudiffa, M., Wade-Gueye, N., Bouët, G., Cardelli, M., Laroche, N., Vanden-Bossche, A., Thomas, M., Bonnelye, E., Aubin, J., 2014. Skeletal Development of Mice Lacking Bone Sialoprotein (BSP)-Impairment of Long Bone Growth and Progressive Establishment of High Trabecular Bone Mass. *PloS One* 9, e95144.
- Dunkman, A.A., Buckley, M.R., Meinaltowski, M.J., Adams, S.M., Thomas, S.J., Satchell, L., Kumar, A., Pathmanathan, L., Beason, D.P., Iozzo, R.V., Birk, D.E., Soslowsky, L.J., 2013. Decorin expression is important for age-related changes in tendon structure and mechanical properties. *Matrix Biol.* 32(1), 3-13.
- Dyment N.A., Breidenbach A.P., Schwartz A.G., Russell R.P., Aschbacher-Smith L., Liu H., Hagiwara Y., Jiang R., Thomopoulos S., Butler D.L., Rowe D.W., 2015. GDF5 Progenitors Give Rise To Fibrocartilage Cells That Mineralize Via Hedgehog Signaling To Form The Zonal Entesis. *Dev. Biol.* doi: 10.1016/j.ydbio.2015.06.020 [Epub ahead of print].
- Fisher, L., Fedarko, N., 2003. Six Genes Expressed in Bones and Teeth Encode the Current Members of the SIBLING Family of Proteins. *Connect Tissue Res.* 44, 3340.
- Foster, B.L., Ao, M., Willoughby, C., Soenjaya, Y., Holm, E., 2015. Mineralization defects in cementum and craniofacial bone from loss of bone sialoprotein. *Bone* 78, 150-64.
- Foster, B.L., Soenjaya, Nociti, F.H., Holm, Zerfas, P.M., Wimer, H.F., Holdsworth, D.W., Aubin, J.E., Hunter, G.K., Goldberg, H.A., Somerman, M.J., 2013. Deficiency in Acellular Cementum and Periodontal Attachment in Bsp Null Mice. *J. Dent. Res.* 92, 166–72.
- Galatz, L.M., Ball, C.M., Teefey, S.A., Middleton, W.D., 2004. The outcome and repair integrity of completely arthroscopically repaired large and massive rotator cuff tears. *The J. Bone Joint Surg. Am.* 86-A(2), 219-24.
- Gao, J., Messner, K., 1996. Quantitative comparison of soft tissue-bone interface at chondral ligament insertions in the rabbit knee joint. *J. Anat.* 188 (Pt 2), 367–73.

Gao J., Messner K., Ralphs J.R., Benjamin M., 1996. An immunohistochemical study of entheses development in the medial collateral ligament of the rat knee joint. *Anat. Embryol.* 194(4), 399-406.

Genin, G.M., Kent, A., Birman, V., Wopenka, B., Pasteris, J.D., Marquez, P.J., Thomopoulos, S., 2009. Functional grading of mineral and collagen in the attachment of tendon to bone. *Biophys. J.* 97, 976–85.

Goldberg, H.A., Hunter, G.K., 2012. Functional domains of bone sialoprotein. In: Goldberg M., ed. *Phosphorylated extracellular matrix proteins of bone and dentin*. Vol. 2. Oak Park (IL): Bentham Science Publishers. p. 266–282.

Gordon, J., Tye, C., Sampaio, A., Underhill, M., Hunter, G., Goldberg, H., 2007. Bone sialoprotein expression enhances osteoblast differentiation and matrix mineralization in vitro. *Bone* 41, 462-73.

Holm, E., Aubin, J.E., Hunter, G.K., Beier, F., Goldberg, H.A., 2015. Loss of bone sialoprotein leads to impaired endochondral bone development and mineralization. *Bone* 71, 145-54.

Holm, E., Gleberzon, J.S., Liao, Y., Sørensen, E.S., Beier, F., 2014. Osteopontin mediates mineralization and not osteogenic cell development in vitro. *Biochem. J.* 464(3), 355–364.

Hunter, G.K., Goldberg, H.A., 1993. Nucleation of hydroxyapatite by bone sialoprotein. *Proc. Natl. Acad. Sci. U.S.A.* 90, 8562–5.

Hunter, G.K., Kyle, C.L., Goldberg, H.A., 1994. Modulation of crystal formation by bone phosphoproteins: structural specificity of the osteopontin-mediated inhibition of hydroxyapatite formation. *Biochem. J.* 300(Pt 3), 723-8.

Liang, G., Katz, L., Insogna, K., Carpenter, T., Macica, C., 2009. Survey of the Enthesopathy of X-Linked Hypophosphatemia and Its Characterization in Hyp Mice. *Calcif. Tissue Int.* 85(3), 235-46.

Liu, C.F., Aschbacher-Smith, L., Barthelery, N., Dymont, N., Butler, D., Wylie, C., 2012. Spatial and Temporal Expression of Molecular Markers and Cell Signals During Normal Development of the Mouse Patellar Tendon. *Tissue Eng. Part A* 18, 598–608.

Liu, C.F., Breidenbach, A., Aschbacher-Smith, L., Butler, D., Wylie, C., 2013. A Role for Hedgehog Signaling in the Differentiation of the Insertion Site of the Patellar Tendon in the Mouse. *PLoS One.* 8, e65411.

Liu, Y., Thomopoulos, S., Chen, C., Birman, V., Buehler, M.J., Genin, G.M. 2013. Modelling the mechanics of partially mineralized collagen fibrils, fibres and tissue. *J. R. Soc. Interface.* 11(92), 20130835.

Liu, Y., Birman, V., Chen, C., Thomopoulos, S., Genin, G., 2011. Mechanisms of Bimaterial Attachment at the Interface of Tendon to Bone. *J. Eng. Mater. Technol.* 133, 011006.

Lorenz-Depiereux, B., Bastepe, M., Benet-Pagès, A., Amyere, M., Wagenstaller, J., Müller-Barth, U., Badenhop, K., Kaiser, S.M., Rittmaster, R.S., Shlossberg, A.H., Olivares, J.L., Loris, C., Ramos, F.J., Glorieux, F., Vikkula, M., Jüppner, H., Strom, T.M., 2006. DMP1 mutations in autosomal recessive hypophosphatemia implicate a bone matrix protein in the regulation of phosphate homeostasis. *Nat. Genet.* 38, 1248–50.

MacKenna, D.A., Omens, J.H., 1994. Contribution of collagen matrix to passive left ventricular mechanics in isolated rat hearts. *Am. J. Physiol.* 266(3 Pt 2), H1007-18.

Malaval, L., Monfoulet, L., Fabre, T., Pothuaud, L., Bareille, R., Miraux, S., Thiaudiere, E., Raffard, G., Franconi, J.-M., Lafage-Proust, M.-H., Aubin, J., Vico, L., Amédée, J., 2009. Absence of bone sialoprotein (BSP) impairs cortical defect repair in mouse long bone. *Bone* 45(5), 853-61.

Malaval, L., Wade-Guéye, N., Boudiffa, M., Fei, J., Zirngibl, R., Chen, F., Laroche, N., Roux, J.P., Burt-Pichat, B., Duboeuf, F., Boivin, G., Jurdic, P., Lafage-Proust, M.H., Amédée, J., Vico, L., Rossant, J., Aubin, J., 2008. Bone sialoprotein plays a functional role in bone formation and osteoclastogenesis. *J. Exp. Med.* 205(5), 1145-53.

Monfoulet, L., Malaval, L., Aubin, J.E., Rittling, S.R., Gadeau, A.P., Fricain, J.C., Chassande, O. 2010. Bone sialoprotein, but not osteopontin, deficiency impairs the mineralization of regenerating bone during cortical defect healing. *Bone* 46(2), 447-52.

Polisson, R.P., Martinez, S., Khoury, M., Harrell, R.M., Lyles, K.W., Friedman, N., Harrelson, J.M., Reisner, E., Drezner, M.K., 1985. Calcification of entheses associated with X-linked hypophosphatemic osteomalacia. *N. Engl. J. Med.* 313, 1–6.

Rich, L., Whittaker, P., 2005. Collagen and picosirius red staining: a polarized light assessment of fibrillar hue and spatial distribution. *Braz. J. Morphol. Sci.* 22, 97–104.

Schwartz, A.G., Pasteris, J.D., Genin, G.M., Daulton, T.L., Thomopoulos, S., 2012. Mineral distributions at the developing tendon enthesis. *PloS One* 7, e48630.

Soenjaya, Y., Foster, B.L., Nociti Jr., F.H., Ao, M., Holdsworth, D.W., Hunter, G.K., Somerman, M.J., Goldberg, H.A., 2015. Mechanical Forces Exacerbate Periodontal Defects in BSP-null mice. *J. Dent. Res.* pii: 0022034515592581. [Epub ahead of print]

Thomopoulos, S., Williams, G.R., 2003. Tendon to bone healing: differences in biomechanical, structural, and compositional properties due to a range of activity levels. *J. Biochem. Eng.* 125(1), 106-13.

Thomopoulos, S., Marquez, J., Weinberger, B., Birman, V., Genin, G., 2005. Collagen fiber orientation at the tendon to bone insertion and its influence on stress concentrations. *J. Biomech.* 39, 1842–51.

Tye, C.E., Hunter, G.K., Goldberg, H.A. 2005. Identification of the type I collagen-binding domain of bone sialoprotein and characterization of the mechanism of interaction. *J. Biol. Chem.* 280(14), 13487-92.

Tye, C.E., Rattray, K.R., Warner, K.J., Gordon, J.A., Sodek, J., Hunter, G.K., Goldberg, H.A. 2003. Delineation of the hydroxyapatite-nucleating domains of bone sialoprotein. *J. Biol. Chem.* 278(10), 7949-55.

Wade-Gueye, N., Boudiffa, M., Vanden-Bossche, A., Laroche, N., Aubin, J., Vico, L., Lafage-Proust, M.-H., Malaval, L., 2012. Absence of bone sialoprotein (BSP) impairs primary bone formation and resorption: The marrow ablation model under PTH challenge. *Bone* 50(5), 1064-73.

Waggett, A.D., Ralphs, J.R., Kwan, A.P., Woodnutt, D., Benjamin, M. 1998. Characterization of collagens and proteoglycans at the insertion of the human Achilles tendon. *Matrix Biol.* 16(8), 457-70.

Wang, G., Woods, A., Agoston, H., Ulici, V., Glogauer, M., Beier, F., 2007. Genetic ablation of *Rac1* in cartilage results in chondrodysplasia. *Dev. Biol.* 306, 612–623.

Wang, J., Zhou, H.Y., Salih, E., Xu, L., Wunderlich, L., Gu, X., Hofstaetter, J., Torres, M., Glimcher, M., 2006. Site-Specific In Vivo Calcification and Osteogenesis Stimulated by Bone Sialoprotein. *Calcif. Tissue. Int.* 79, 179–89.

Zelzer, E., Blitz, E., Killian, M., Thomopoulos, S., 2014. Tendon- to- bone attachment: From development to maturity. *Birth Defects Res. C Embryo Today* 102, 101–12.

CHAPTER THREE

ELUCIDATING THE ROLE OF BONE SIALOPROTEIN IN THE
MURINE ENTHESES DURING DEVELOPMENT AND AGEING

3.1 Chapter Summary

Tendons and ligaments insert into bone through a transitional structure termed the enthesis which features a region of fibrocartilage, part of which is mineralized. The mechanism by which this tissue becomes mineralized, however, is poorly characterized. Recently, bone sialoprotein (BSP), an acidic phosphoprotein associated with mineralizing tissues, was identified in the calcified fibrocartilage (CFC) of the enthesis, and loss of BSP resulted in alterations in this tissue in 15 week-old mice. The calcified fibrocartilage of *Bsp*^{-/-} mice is 28% longer than wild type in the quadriceps tendon enthesis (QCT) although overall mineral content within the CFC is similar between genotypes. *Bsp*^{-/-} mice possess defects in endochondral ossification and have abnormal growth plates. Enthesis development has been suggested to parallel growth plate development in a number of ways. As such, characterization of the *Bsp*^{-/-} enthesis in juvenile animals is warranted to elucidate BSP's role in this tissues development. Presented is a histological characterization of the supraspinatus tendon (SST) enthesis and the QCT enthesis of wild type and *Bsp*^{-/-} mice at ages of 14 days, 21 days and 14 months. BSP and OPN are not present in either enthesis at 14 days of age. Small amounts of both proteins were detected by immunohistochemistry in the SST enthesis at 21 days of age. No differences in the general morphology were observed between *Bsp*^{-/-} and wild type tissues in the QCT and SST entheses at either 14 or 21 days of age. Mineral content, as shown by von Kossa staining, and collagen organization, as assayed by picrosirius red staining, were also unaffected. At 14 months of age the *Bsp*^{-/-} QCT CFC is longer than in wild type mice and the difference between *Bsp*^{-/-} and wild type is larger than at 15 weeks, however no other differences were apparent. Data presented here indicate that loss of BSP has little effect

on the 14 and 21 day old enteses however loss of BSP appears to cause a dysregulation of CFC growth that continues well into adulthood.

3.2 Introduction

Tendons and ligaments transition into bone through a specialized tissue termed the enthesis. Fibrocartilaginous entheses are the most common category of entheses in the body and are commonly found at the insertions of tendons, which are connected to muscles involved in locomotion, into the epiphysis of long bones. As such, fibrocartilaginous entheses are of critical importance in efficient force transduction from skeletal muscles to the limbs. In order to effectively connect the soft, pliable material that makes up tendons and ligaments to the rigid structure of bone, fibrocartilaginous entheses transition through a region of fibrocartilage, part of which is mineralized. Thus fibrocartilaginous entheses have been classically described as have four zones: the tendon proper, uncalcified fibrocartilage (UFC), calcified fibrocartilage (CFC), and bone (Benjamin and McGonagle, 2001).

Bone sialoprotein (BSP) is an acidic phosphoprotein with a flexible structure and belongs to the Small Intergrin Binding Ligand N-Linked Glycoprotein (SIBLING) family of proteins (Fisher and Fedarko, 2003; Ganss et al., 1999). BSP has potent hydroxyapatite nucleating properties (Hunter and Goldberg, 1993), and binding of BSP to collagen is thought to promote matrix mineralization (Baht et al., 2008). Previously, BSP was detected in enthesis CFC and defects were identified in the 15 week old *Bsp*^{-/-} mouse quadriceps tendon (QCT) enthesis. The calcified fibrocartilage (CFC) of the enthesis was 28% longer in the *Bsp*^{-/-} mouse, as measured from tidemark to bone. No changes were evident in the supraspinatus tendon (SST) enthesis. The *Bsp*^{-/-} patellar tendon is 7.5% larger in cross-sectional area than the wild type; however, this tendon has a failure stress

that is 16.5% lower than wild type indicating that while *Bsp*^{-/-} tendons are larger, they are also mechanically weaker.

BSP's expression and localization coincides with the initial formation of a mineralized matrix in both intramembranous and endochondral ossification (Bianco et al., 1991), and BSP is expressed by the hypertrophic chondrocytes within the epiphyseal growth plate (Chen et al., 1992), among other mineralized tissue associated cells. Interestingly, there are many similarities between the development of fibrocartilaginous entheses and growth plates involved in endochondral ossification (Zelzer et al., 2014). We and others have recently identified abnormalities in the growth plates of *Bsp*^{-/-} mice as well as a delay in mineral deposition during endochondral ossification (Bouleftour et al., 2014; Holm et al., 2015). This suggests that a more pronounced phenotype may be present during the early development of *Bsp*^{-/-} fibrocartilaginous entheses. Additionally, the extension in the QCT CFC observed at 15 weeks suggests that entheses mineralization continues over a longer time period in the *Bsp*^{-/-} mouse. An examination of an older time point beyond 15 weeks of age would provide additional insight into this observation. Presented is a histological characterization of *Bsp*^{-/-} entheses at three additional time points, 14 days post-natal, 21 days post-natal, representing developmental time points, and 14 months of age, representing a time point well into adulthood.

3.3 Materials and Methods

3.3.1 *Animals*

Mice were prepared and handled as outlined in Section 2.3.1. Mice aged 14 months and 21 days were all males, however animals 14 days of age used in this study were male and female. It was assumed that effects on estrogen on the mineralized tissues under study would be negligible at this age because mice do not reach sexual maturity until roughly 6 weeks of age (Vandenbergh, 1967) and no gender based differences in enthesal tissue have been described.

3.3.1 *Histology and Immunohistochemistry*

Histological techniques used in this study are as described in Section 2.3.2 with alterations. Fourteen month old mouse limbs were decalcified in 0.650M EDTA at 37 °C for 3 weeks, 21 day old animals were decalcified in the same solution for 2 weeks and 14 day old animals were decalcified over the course of 7 days using this solution.

In order to decrease background staining of the OPN and BSP antibodies at the 14 and 21 day time points, an adaptation of the immunohistochemistry (IHC) protocol described in Section 2.3.2 was used. Antigen retrieval was not used on 14 and 21 day old samples. Antigen blocking was performed in 10% goat serum in phosphate buffer saline overnight at 4°C. In the morning primary antibody treatment with either rabbit anti-mouse BSP serum (courtesy of Dr. Renny Franceschi, University of Michigan School of Dentistry, Ann Arbor, MI) or rabbit anti-mouse OPN serum (Courtesy of Larry Fisher, Bethesda, MD) was performed for 1 hour at room temperature and half the amount of antiserum was used.

Von Kossa staining was performed as described in Section 2.3.2, however, toluidine blue was used as a counterstain in these studies rather than alcian blue and nuclear fast red.

3.4 Results

To better characterize the phenotype of the *Bsp*^{-/-} murine enthesis, tissues from older mice, 14 months, and two juvenile time points, 14 and 21 days, were examined via histology.

3.4.1 Age 14 months

At age 14 months BSP and OPN can still be readily detected in the CFC of the QCT and SST enthesis and no differences in the distribution of OPN was observed in the *Bsp*^{-/-} enthesis (Fig. 3.1 and 3.2). As previously shown, at age 15 weeks a 28% increase in the length of the QCT enthesis CFC was observed, measured tidemark to bone, in the *Bsp*^{-/-} enthesis, while no differences were apparent in the morphology of the SST enthesis. At age 14 months, the QCT enthesis is further lengthened in the *Bsp*^{-/-} mouse, while the size of the wild type CFC in the QCT enthesis did not change between 15 weeks and 14 months of age (Table 3.1). The 14 month wild type CFC of the QCT enthesis displays an average increase of 30.2 μm from the 15 week *Bsp*^{-/-} QCT enthesis and a 41% increase in size over wild type ($p < 0.05$, $n=3$) (Fig. 3.3). No changes were noted in the size of the SST CFC of *Bsp*^{-/-} mice, aged 14 month. Collagen organization, as demonstrated by picrosirius red staining, remains unaffected by the loss of *Bsp* (Fig. 3.4).

Figure 3.1 BSP is present in the calcified fibrocartilage of 14 month-old mice.

Immunohistochemistry using anti-BSP antiserum was performed on the QCT and SST entheses of 14 month old male wild type and *Bsp*^{-/-} mice (n=3). Diaminobenzidine staining (brown) indicates the presence of BSP protein. CFC: calcified fibrocartilage, UFC: uncalcified fibrocartilage, bar = 100 μ m

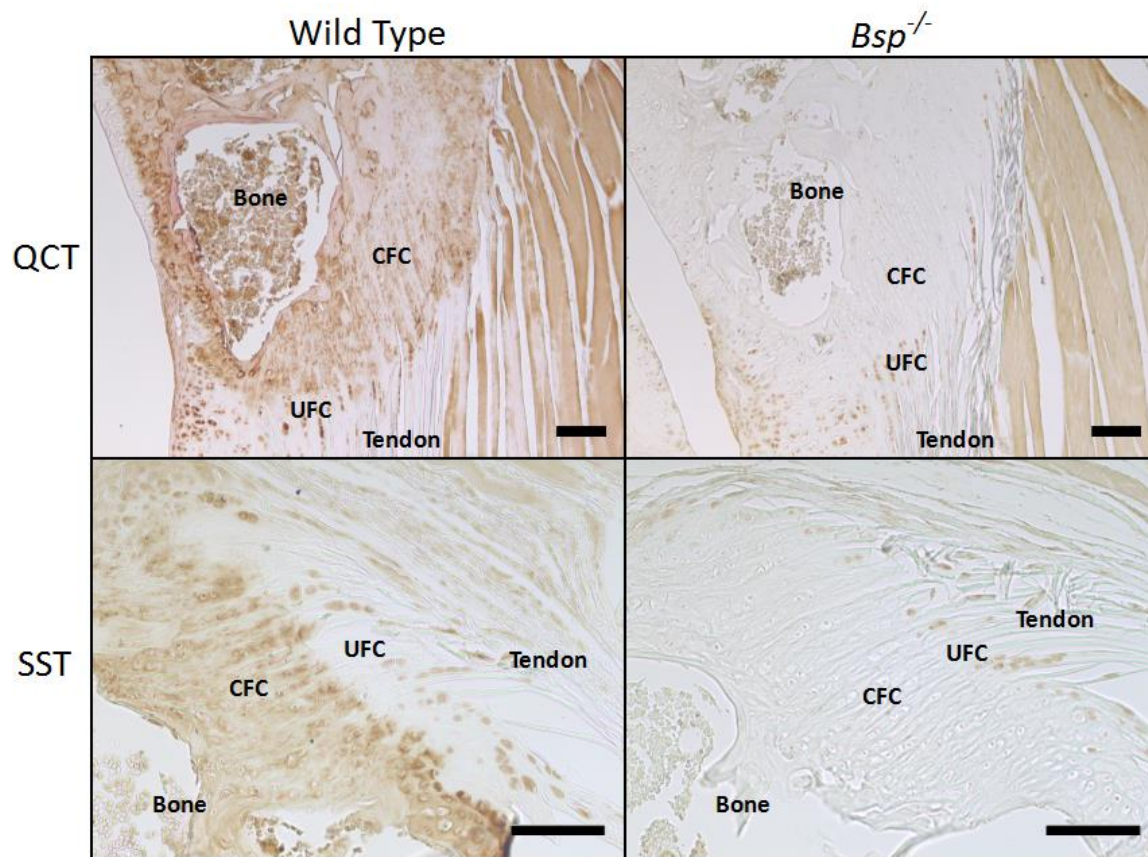


Figure 3.2 OPN is present in the calcified fibrocartilage of 14 month-old mice.

Immunohistochemistry using anti-OPN antiserum was performed on the QCT and SST entheses of 14 month old male wild type and *Bsp*^{-/-} mice (n=3). Diaminobenzidine staining (brown) indicates the presence of OPN protein. CFC: calcified fibrocartilage, UFC: uncalcified fibrocartilage, bar = 100 μ m

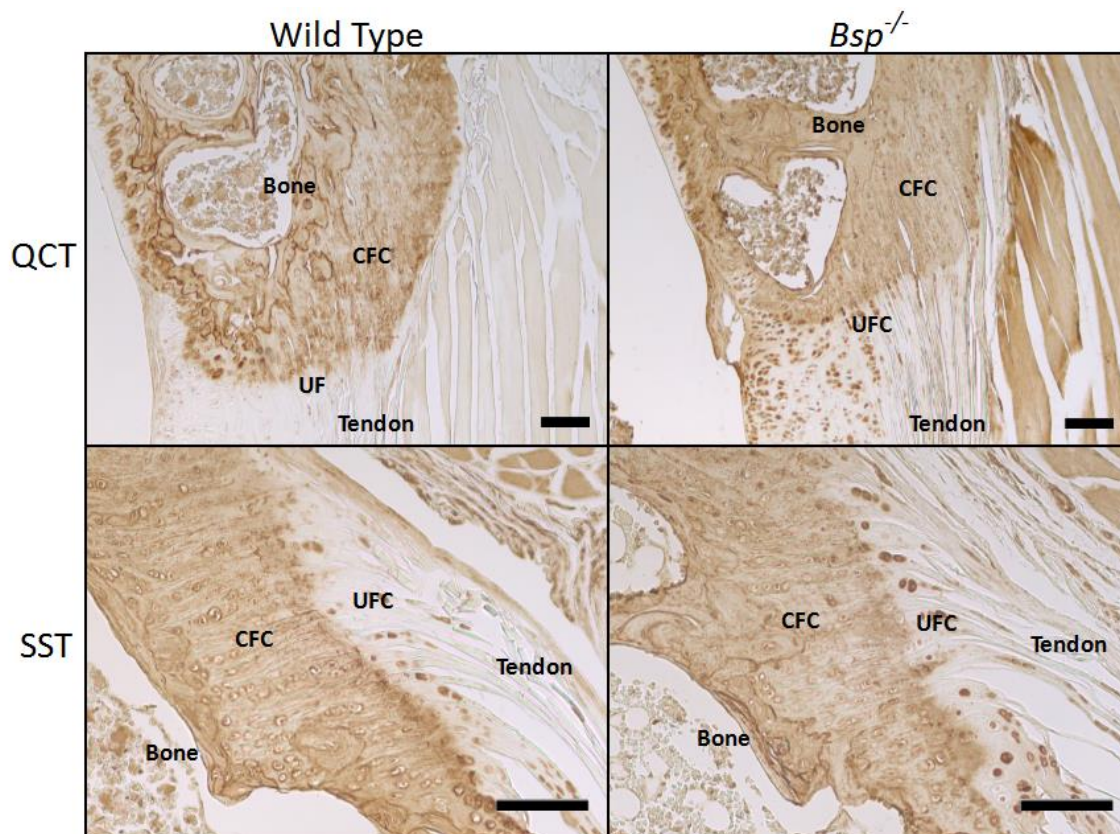


Figure 3.3 Calcified fibrocartilage of *Bsp*^{-/-} is further lengthened with age.

Hematoxylin and eosin staining of the QCT enthesis of male 14 month old wild type and *Bsp*^{-/-} mice. CFC length (yellow arrow) is increased in the *Bsp*^{-/-} mouse QCT enthesis compared to wild type (Table 3.1). CFC: calcified fibrocartilage, UFC: uncalcified fibrocartilage, T: tidemark, bar = 100 μ m

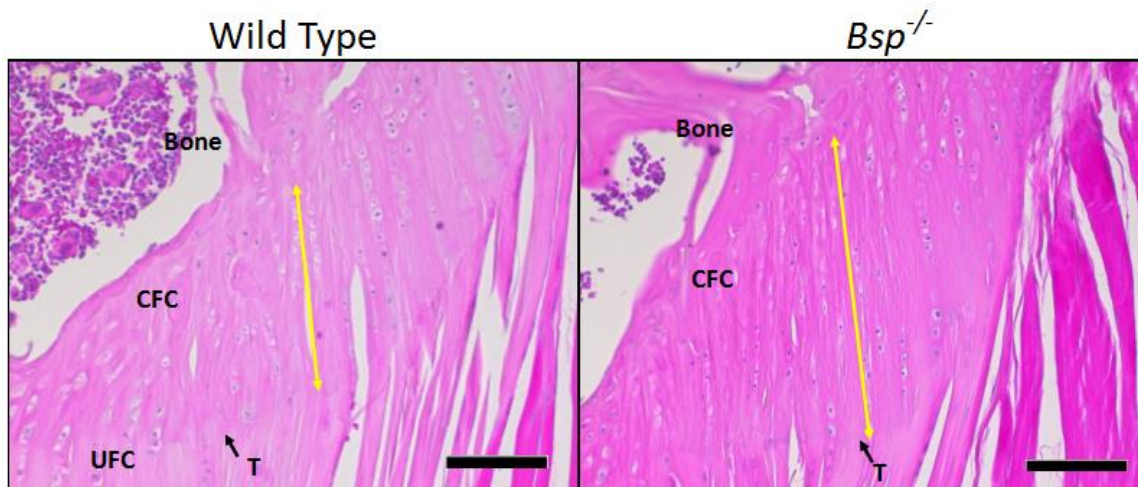
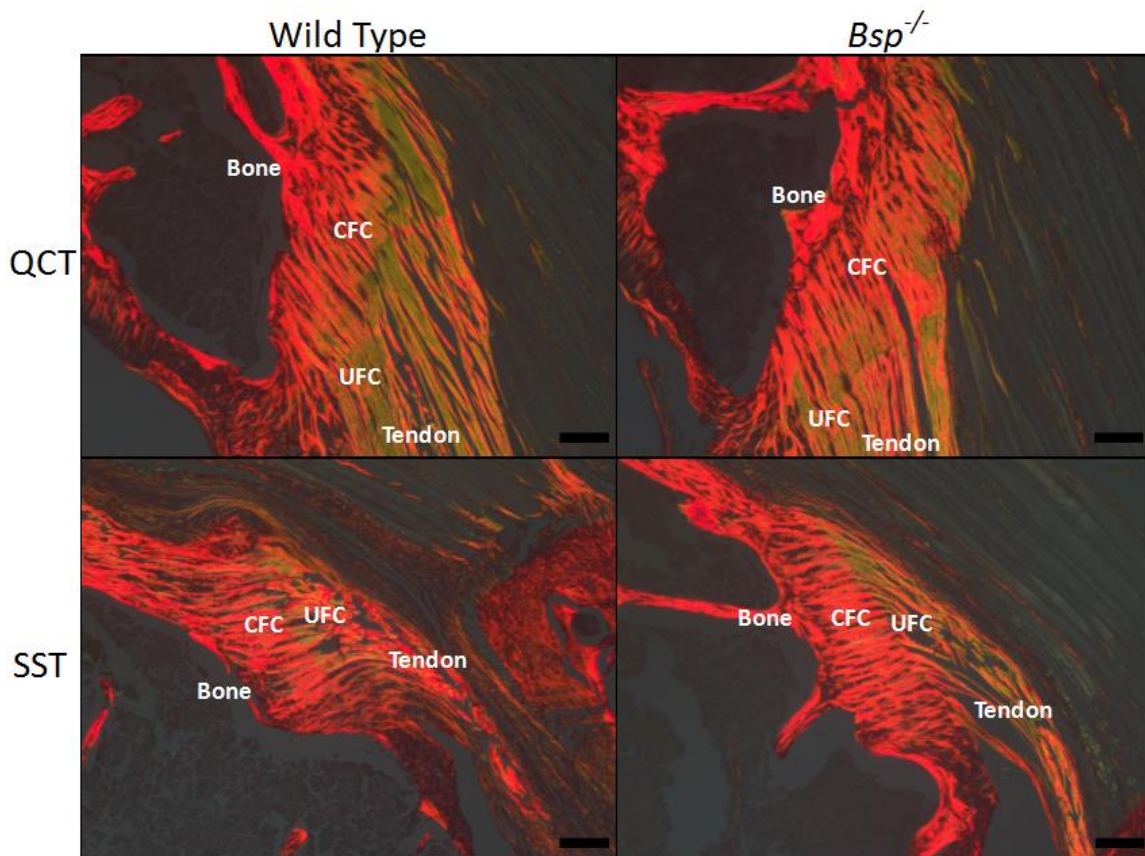


Table 1. CFC lengths of 15 week and 14 month old wild type and *Bsp*^{-/-} QCT

entheses. CFC length was measured by drawing three transverses from tidemark to bone in the orientation of the collagen fibers per individual mouse by two blinded observers and averaged. Average CFC lengths from wild type and *Bsp*^{-/-} mice were compared against each other using a two-tailed, unpaired, parametric t-test. Statistical analysis indicated significant differences ($p < 0.05$) between genotypes within age groups.

CFC Length (μm)	Wild type	<i>Bsp</i> ^{-/-}
15 weeks (n=5)	178.8 \pm 15.5 μm	229.1 \pm 17.5 μm
14 months (n=3)	182.9 \pm 23.7 μm	259.3 \pm 17.5 μm

Figure 3.4 At 14 months of age no differences in collagen organization are observed between wild type and *Bsp*^{-/-} mice. Picrosirius red staining of the QCT and SST enthesis of 14 month old male wild type and *Bsp*^{-/-} mice (n=3). Collagen fibres (bright objects) are well ordered in both wild type and *Bsp*^{-/-} entheses. CFC: calcified fibrocartilage, UFC: uncalcified fibrocartilage, bar = 100 μ m



3.4.2 Age 14 and 21 days

General morphology of the QCT and SST enthesis of 14 and 21 day old wild type and *Bsp*^{-/-} mice was assessed via hematoxylin and eosin (H&E) staining (Fig. 3.5 and 3.6). No gross morphological differences are apparent between wild type and *Bsp*^{-/-} entheses. No tidemark is present in the H&E stains of these time points. At 14 days post-natal the cartilaginous anlage of the patella is just beginning to mineralize, and while the attachment point of the quadriceps tendon can be identified, von Kossa staining indicates that this region of the patella has not mineralized yet (Fig. 3.7). Mineral has reached the edge of the SST enthesis at 14 days of age but has not yet extended into the developing fibrocartilage (Fig. 3.7). At 21 days post-natal lamellar bone is beginning to form in the patella with some individual mice displaying more than others. A small band of mineral is present in the SST enthesis fibrocartilage (Fig. 3.8). Picrosirius red staining indicates that collagen content and organization is normal (Fig. 3.9 and 3.10). IHC using antibodies against OPN and BSP was performed on the murine SST and QCT enthesis at 14 and 21 days post-natal (Fig. 3.11-3.14). BSP and OPN are restricted to the mineralized tissues at these time points and a thin band of BSP (weakly stained) and OPN can be seen adjacent to the bone in the SST enthesis, representing the developing mineralization front. Neither SIBLING proteins are present in the developing QCT enthesis at these time points.

Figure 3.5 No gross morphological differences are apparent in the entheses of 14 day-old wild type and *Bsp*^{-/-} mice. General morphology of the QCT and SST entheses of 14 day old male and female wild type and *Bsp*^{-/-} mice was assessed by standard hematoxylin and eosin staining (n=5). Bar = 100 μ m

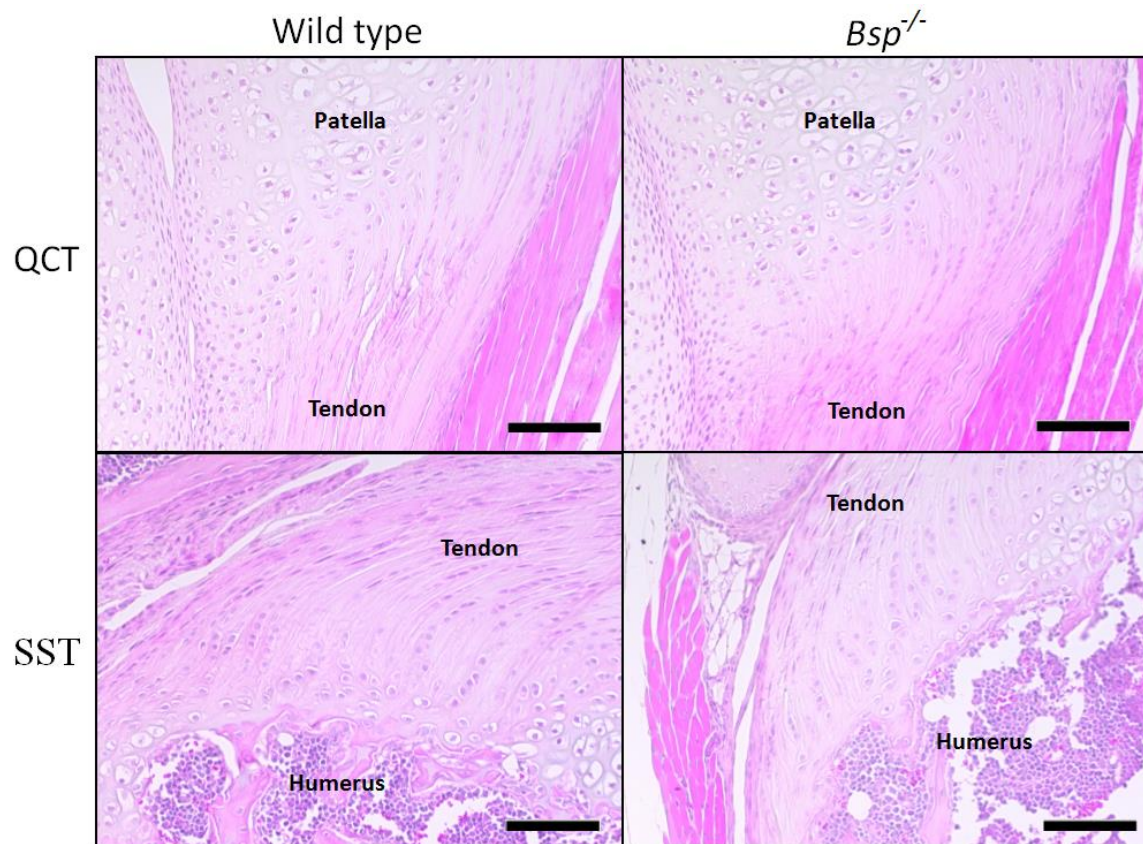


Figure 3.6 No gross morphological differences are apparent in the entheses of 21 day-old wild type and *Bsp*^{-/-} mice. General morphology of the QCT and SST entheses of 21 day old male wild type and *Bsp*^{-/-} mice was assessed by standard hematoxylin and eosin staining (n=5). Bar = 100 μ m

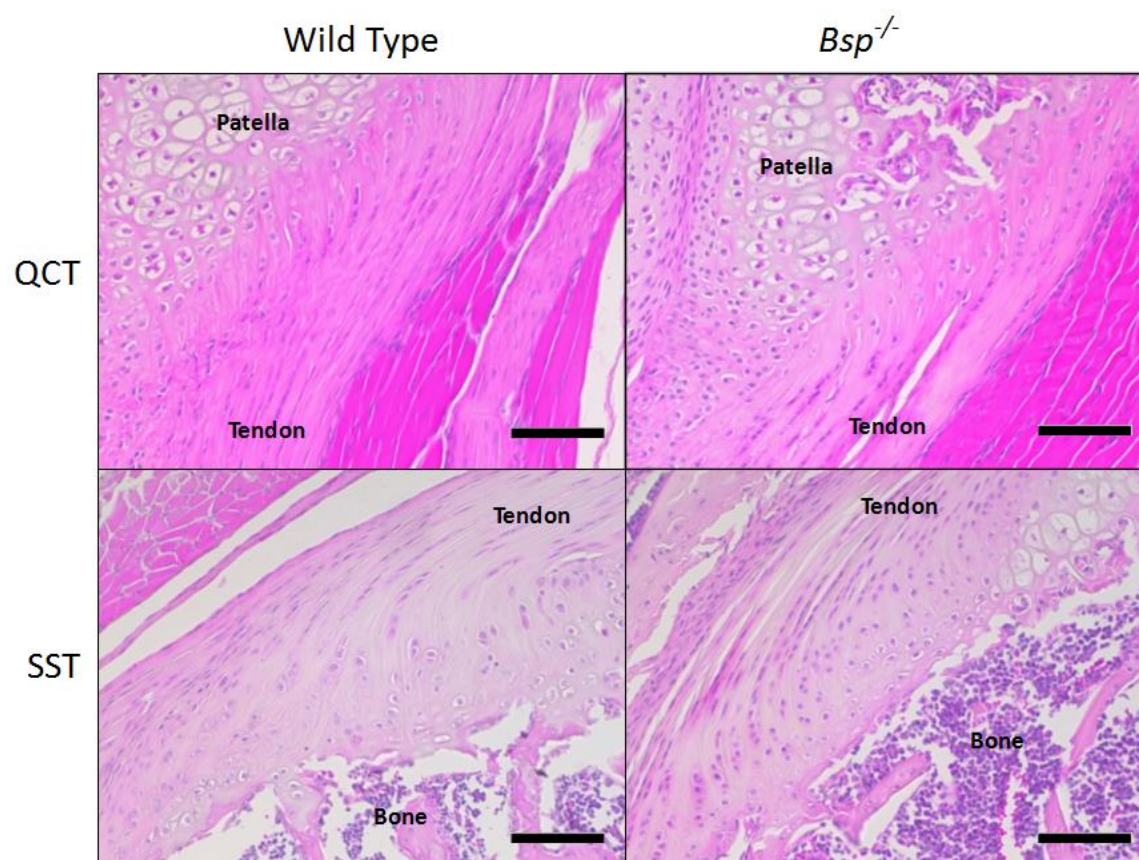


Figure 3.7 Mineral is not present in the entheses of 14 day-old wild type and *Bsp*^{-/-} mice. Whole tissue von Kossa staining was performed on the QCT and SST entheses of 14 day old male and female wild type and *Bsp*^{-/-} mice (n=5). Mineral deposition is represented in black. Sections are counterstained with toluidine blue. Bar = 100 μ m

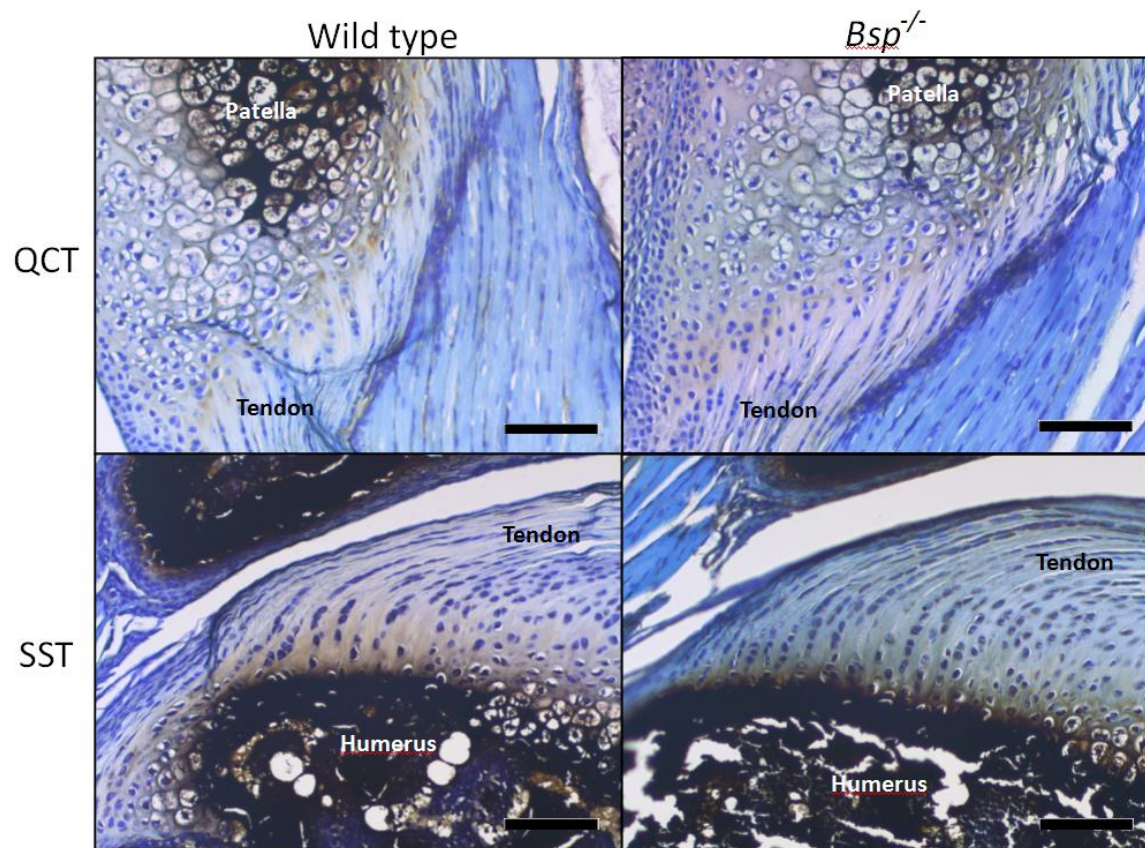


Figure 3.8 Mineral is not present in the QCT entheses of 21 day-old wild type and *Bsp*^{-/-} mice however small amounts are present in the SST entheses. Whole tissue von Kossa staining was performed on the QCT and SST entheses of 21 day old male wild type and *Bsp*^{-/-} mice (n=5). Yellow circle demarcates the enthesis. Mineral deposition is represented in black. Yellow arrows indicate early sites of mineral deposition in the enthesis. Sections are counterstained with toluidine blue. Bar = 100 μ m

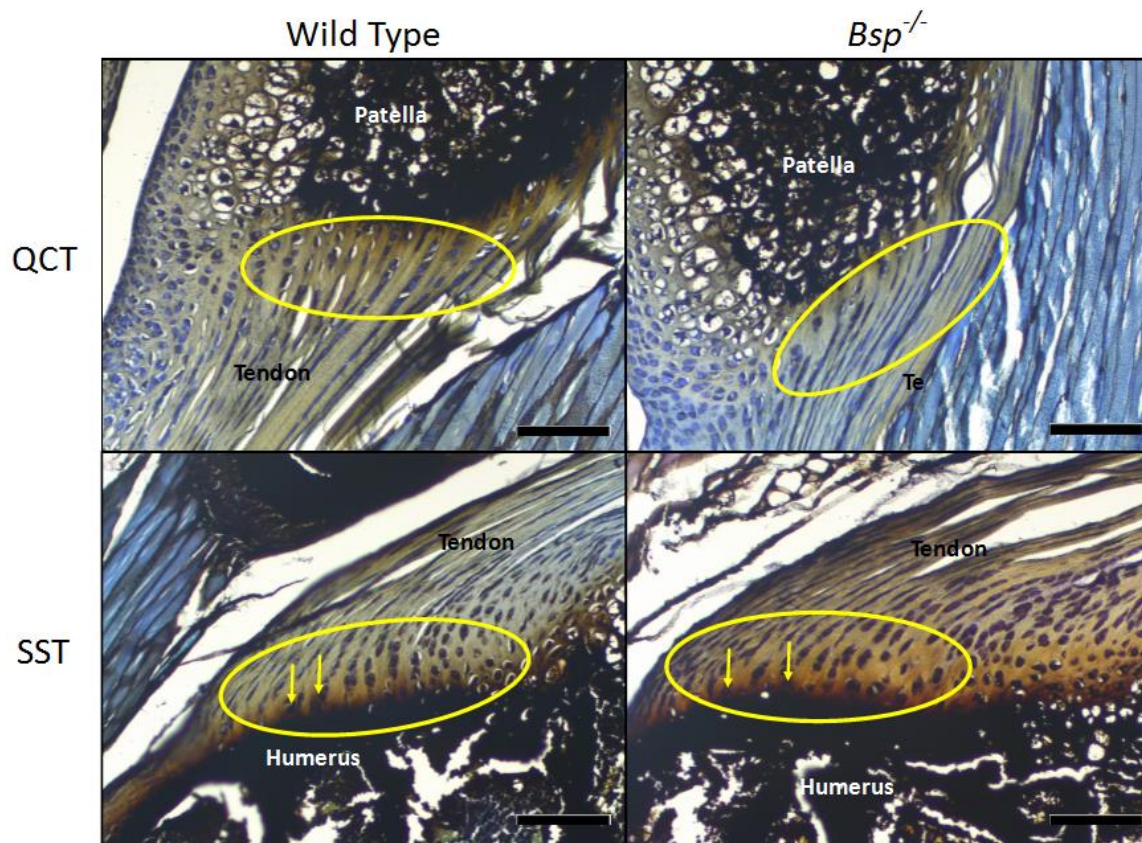


Figure 3.9 At 14 days of age no differences in collagen organization are observed between wild type and *Bsp*^{-/-} mice. Picrosirius red staining of the QCT and SST entheses of 14 day old male and female wild type and *Bsp*^{-/-} mice (n=5). No apparent differences in the organization of collagen fibers (bright red/green) are present in wild type and *Bsp*^{-/-} entheses. Bar = 100 μ m

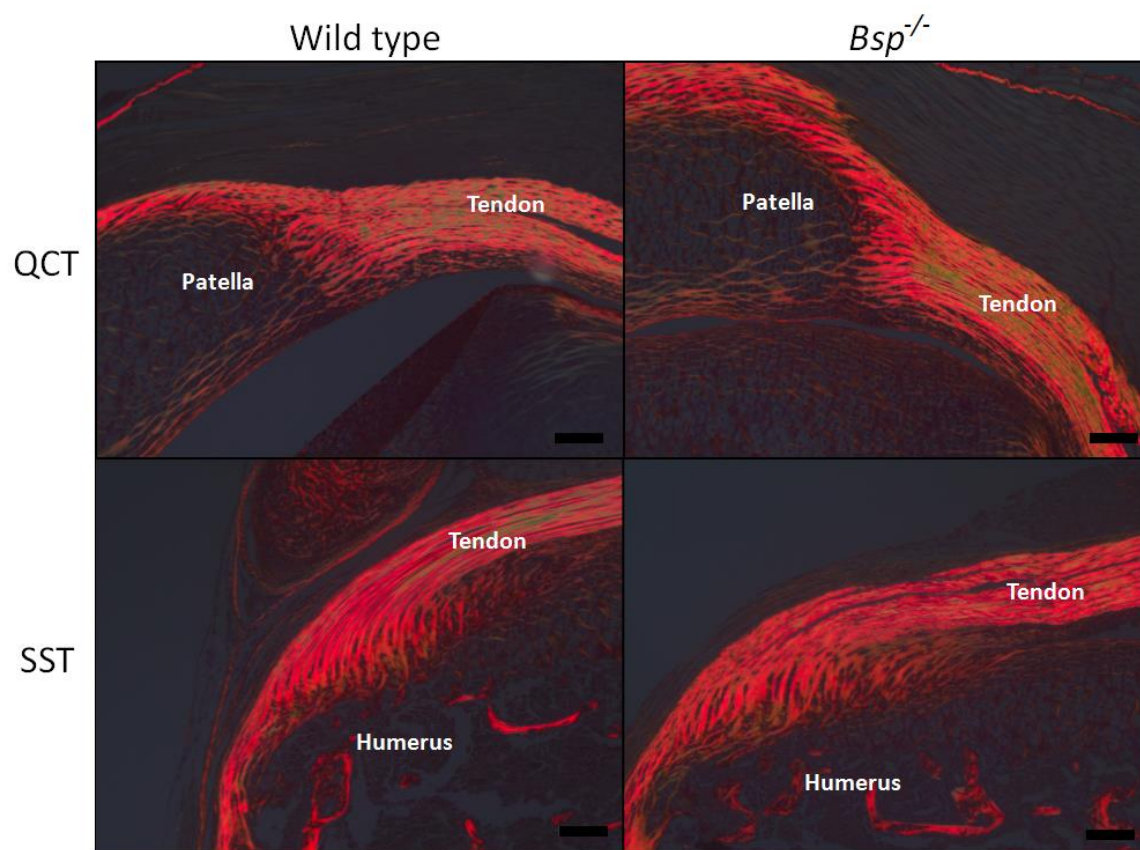


Figure 3.10 At 21 days of age no differences in collagen organization are observed between wild type and *Bsp*^{-/-} mice. Picrosirius red staining of the QCT and SST entheses of 21 day old male wild type and *Bsp*^{-/-} mice (n=5). No apparent differences in the organization of collagen fibers (bright red/green) are present between wild type and *Bsp*^{-/-} entheses. Bar = 100 μ m

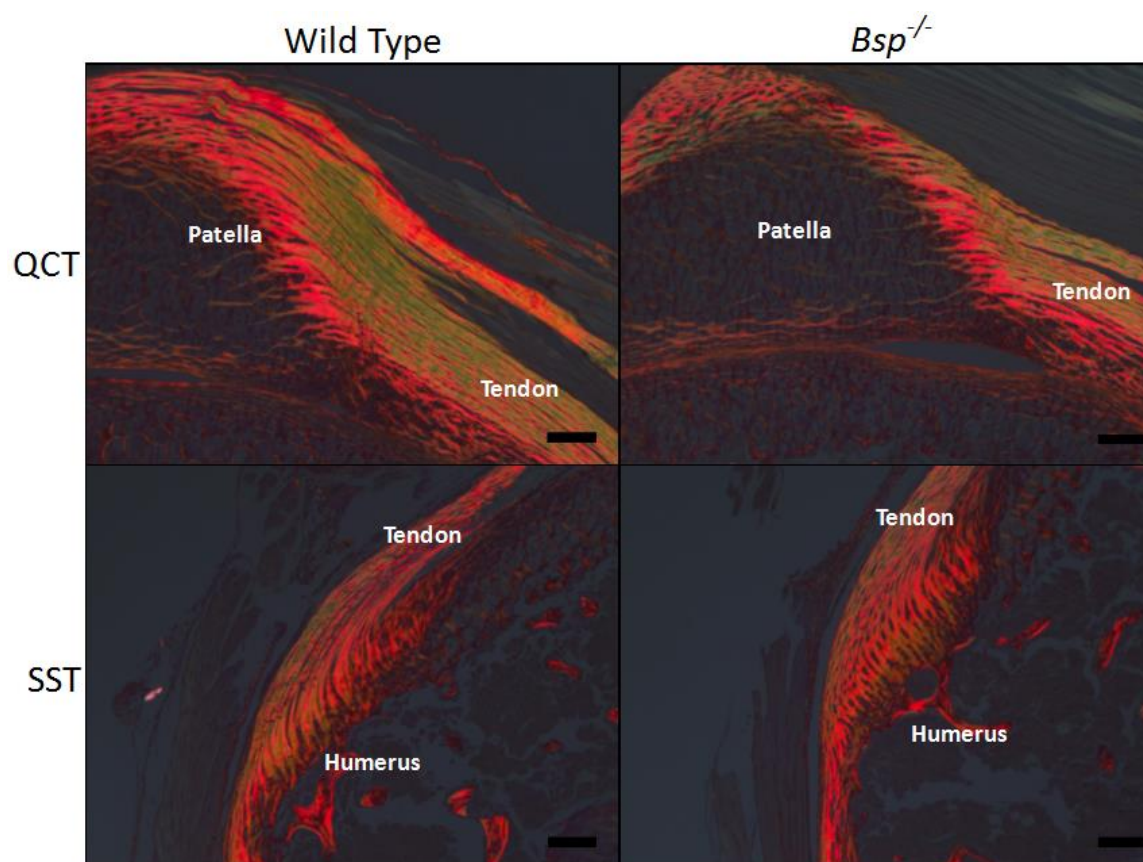


Figure 3.11 BSP is not present in the entheses of 14 day old wild type and *Bsp*^{-/-} mice.

Immunohistochemistry using anti-BSP antiserum was performed on the QCT and SST entheses of 14 day old male and female wild type and *Bsp*^{-/-} mice (n=5).

Diaminobenzidine staining (brown) indicates the presence of BSP protein. Bar = 100 μ m

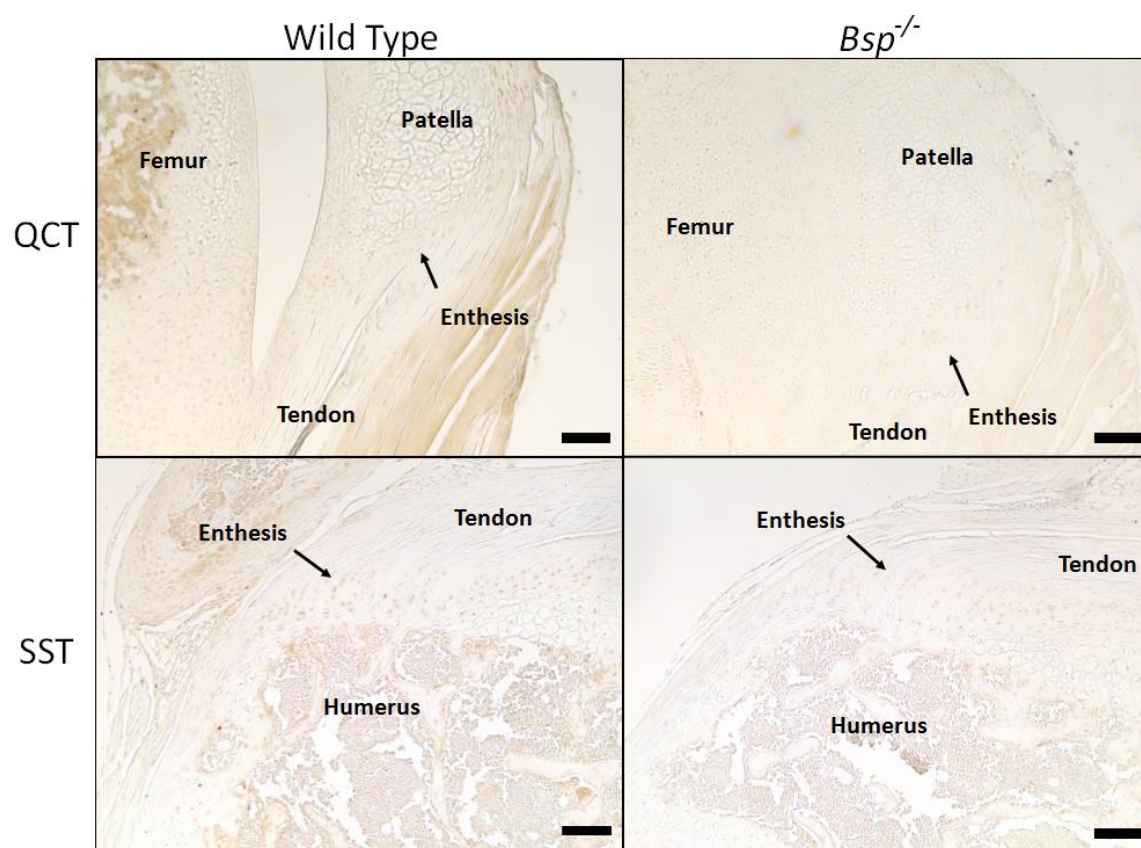


Figure 3.12 BSP is localized to mineralized regions in 21 day old wild type mice.

Immunohistochemistry using anti-BSP antiserum was performed on the QCT and SST entheses of 21 day old male wild type and *Bsp*^{-/-} mice (n=5). Diaminobenzidine staining (brown) indicates the presence of BSP protein. Bar = 100 μm

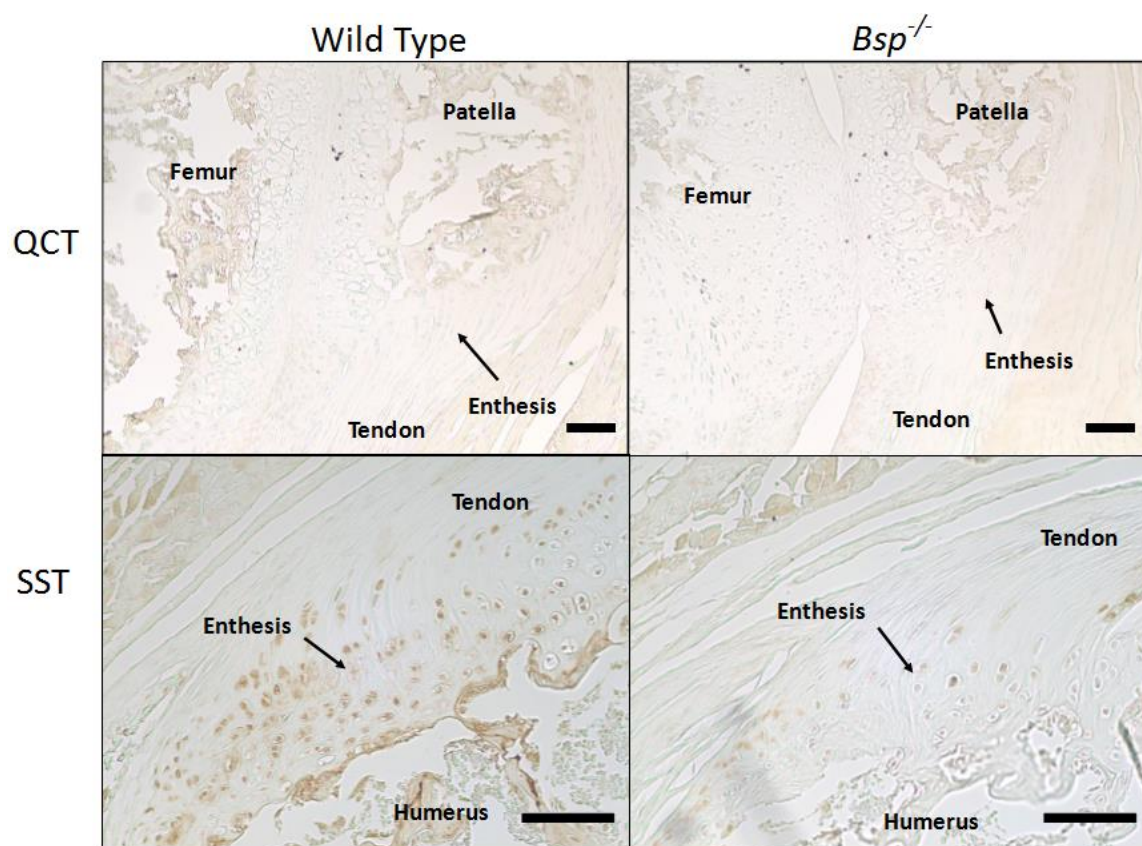
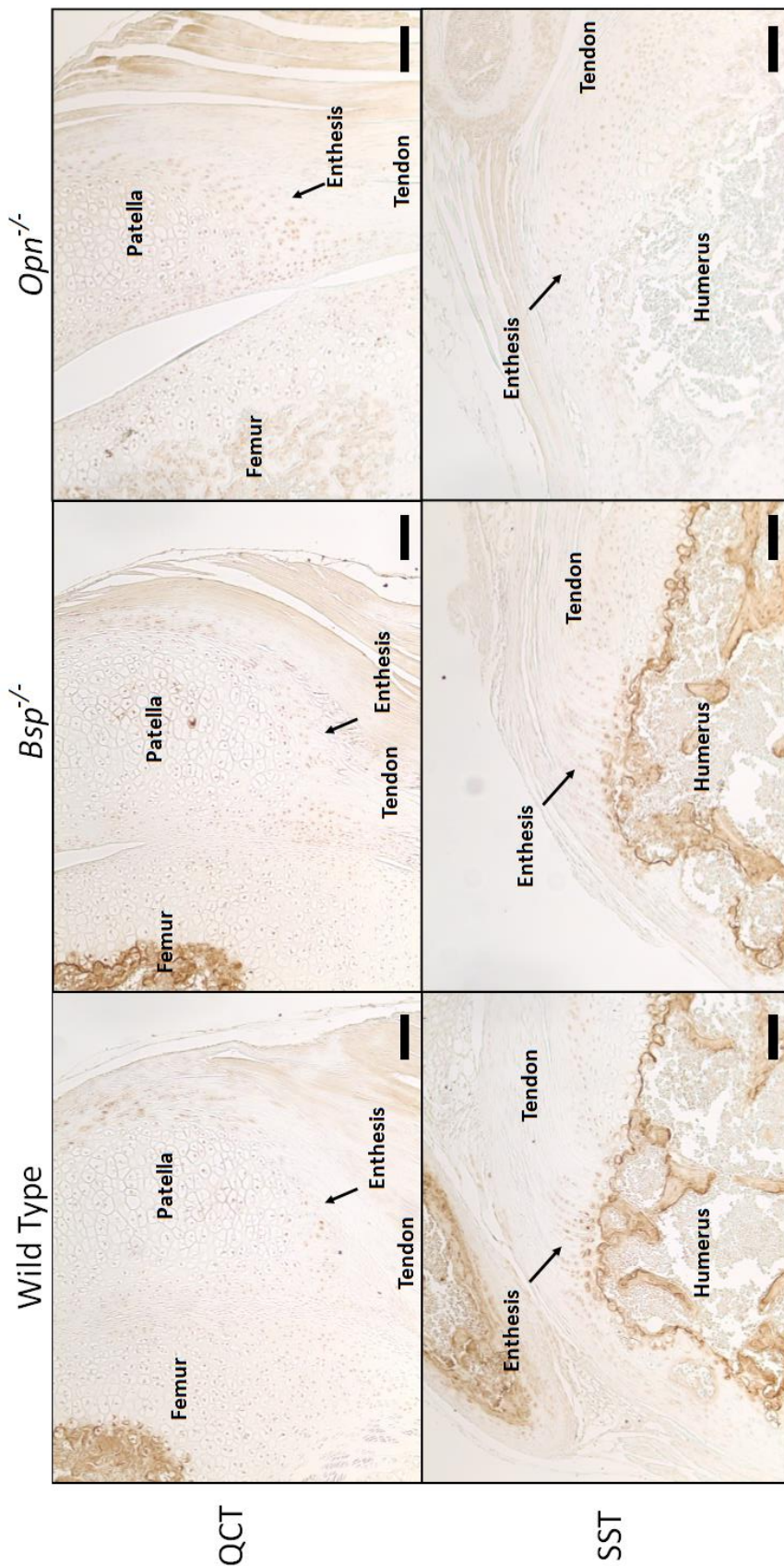


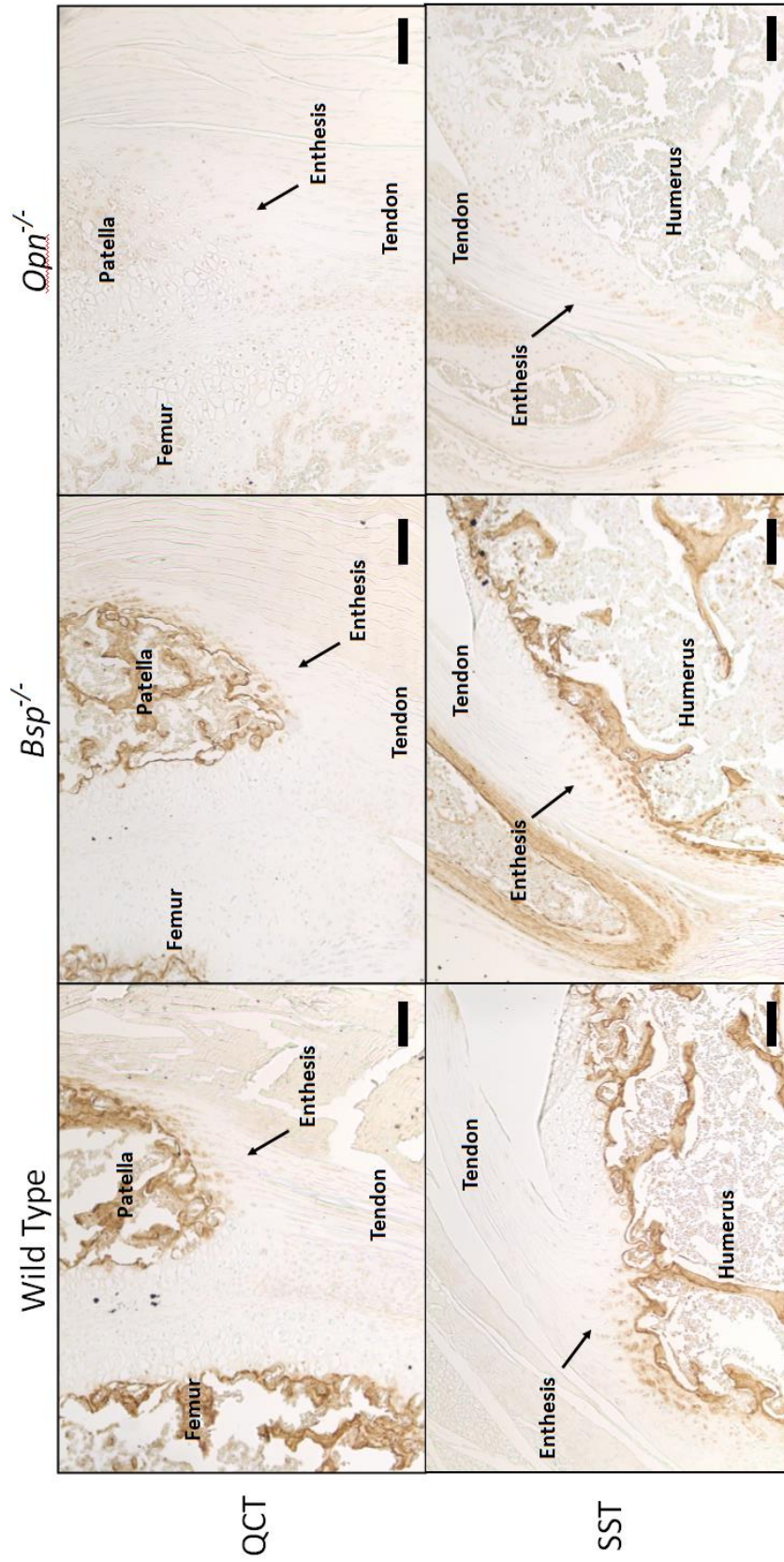
Figure 3.13 OPN is not present in the entheses of 14 day old wild type and *Bsp*^{-/-} mice. Immunohistochemistry using anti-OPN antiserum was performed on the QCT and SST enthesis of 14 day old male and female wild type, *Bsp*^{-/-} and *Opn*^{-/-} mice (n=5). Diaminobenzidine staining (brown) indicates the presence of OPN protein. Bar = 100 μ m



QCT

SST

Figure 3.14 OPN is localized to mineralized regions in 21 day old wild type and *Bsp*^{-/-} mice. Immunohistochemistry using anti-OPN antiserum was performed on the QCT and SST enthesis of 21 day old male wild type, *Bsp*^{-/-} and *Opn*^{-/-} mice (n=5). Diaminobenzidine staining (brown) indicates the presence of OPN protein. Bar = 100 μm



3.5 Discussion

In order to further elucidate the role of BSP in the fibrocartilaginous enthesis, a histological characterization of the BSP null enthesis was performed in mice of 14 days, 21 days and 14 months of age. At 14 days BSP and OPN protein are not present in the QCT and SST entheses in wild type animal. At 21 days small amounts of BSP and OPN appear to be present near the bone in the SST enthesis, while no positive staining is observed in the QCT enthesis. Little change was observed in the general morphology, mineral deposition, collagen organization and OPN protein localization of *Bsp*^{-/-} mice. At 14 months of age immunohistochemical staining indicates no differences in the staining patterns of BSP and OPN from that observed at 15 weeks of age, and collagen organization remains unaffected by loss of BSP at age 14 months. Interestingly, the CFC of the QCT enthesis is further lengthened beyond measurements from 15 weeks of age, suggesting a dysregulation in the growth of this tissue in the absence of BSP.

3.5.1 14 months

In captivity, mice live to two to three years of age. At the age of 14 month the only notable abnormality in the *Bsp*^{-/-} mouse enthesis is the extension of the CFC observed in the QCT enthesis. As previously noted this phenotype was first observed at 15 weeks of age, however the increase in CFC length is larger at 14 months of age. Wild type CFC length remains the same from 15 weeks to 14 months of age, suggesting that this tissue is fully mature by 15 weeks with outward growth of the mineralization front ceasing at some point prior. The increase in length of the *Bsp*^{-/-} enthesis suggests that the

mineralized region continues to expand in the absence of BSP. BSP has traditionally been described as a promoter of mineralization, for which there is strong *in vitro* evidence (Hunter and Goldberg, 1993). However, in this instance BSP appears to be acting as a regulator of mineral growth, modulating the extent to which the mineralization front in the CFC extends outwards from the bone.

An analysis of the mineral content at the tidemark in the 14 month old *Bsp*^{-/-} mouse by Raman spectroscopy is warranted, as the mineral gradient at 14 months may be steeper still. Unfortunately Raman spectroscopy could not be conducted on 14 month old animals at this time as the animals used in this study were taken from a preserved archive of mice maintained by our laboratory. While animals kept in this fashion are suitable for histology, Raman spectroscopy requires fresh tissue, which could not be generated in a timely manner due to the age of the animals.

Future investigations at this time point should include mechanical studies on the *Bsp*^{-/-} QCT as it may provide insight as to the functional significance of the lengthened CFC. Mathematical and mechanical modelling suggest that alterations in the length of the CFC in the magnitudes observed at this time point may result in weakening of the tendon-bone insertion due to the enlarged regions of presumably stiffer tissue, and if further abnormalities are present in the gradient region it may exacerbate the tendon defect further (Genin et al., 2009).

3.5.2 14 and 21 days

Due to BSP's role in mineralizing tissues, the apparent similarities in growth plate development and enthesis development, and the deficiencies identified in endochondral ossification in the *Bsp*^{-/-} mouse, it was hypothesized that BSP may play a role in enthesis development and mineralization. Furthermore, it was hoped that phenotypes caused by a loss of BSP would be more apparent during development. Entheses develop post-natally (Zelzer et al., 2014), and a mineral gradient is apparent in the SST enthesis as early as 14 days postnatal (Schwartz et al., 2012). By 21 days the developing SST enthesis begins to resemble the morphology of the mature enthesis when examined histologically (Schwartz et al., 2012). Based on this knowledge, time points of 14 and 21 days of age were chosen for study. No developmental characterization of the mineral content of the developing murine QCT enthesis has been described.

In the fibrocartilaginous enthesis, BSP and OPN appear to be restricted to sites of mineralization. BSP and OPN's absence in the extracellular matrix (ECM) of the 14 day old SST and QCT entheses is not surprising as these structures are not mineralized at this time point. Due to the lack of BSP in wild type tissues at 14 days of age, it is to be expected that the *Bsp*^{-/-} mouse does not display an enthesis phenotype when examined histologically at this time point. At 21 days post-natal, mineral is just beginning to be deposited in the developing enthesis fibrocartilage in the SST, however no differences are apparent in general morphology, mineral deposition or collagen organization between wild type and *Bsp*^{-/-} mice, consistent with our observations in mice 15 weeks and 14 months of age. The mineralization front in the patella has not yet expanded into the QCT enthesis fibrocartilage by 21 days of age, and as such, neither BSP nor OPN are present

in wild type tissue. Unsurprisingly, no differences are apparent in 21 day old *Bsp*^{-/-} QCT morphology.

Further characterization of the developing *Bsp*^{-/-} enthesis is needed to elucidate BSP's role in enthesis development. A histological characterization at 28 days post-natal is suggested, since at this time point mineral deposition in enthesis fibrocartilage is likely occurring. Further time points moving toward 15 weeks of age could also be assessed in order to determine at what age the *Bsp*^{-/-} CFC length begins to outpace wild type tissue.

A major shortcoming in the histological analysis of BSP within enthesis tissue is the BSP antibody's unfortunate affinity for cells located in uncalcified fibrocartilage, as well as muscle tissues. Our original IHC protocol used on 15 week old mice from our previous study and the 14 month old mice shown here, is effective in demonstrating BSP staining in the ECM. Intense brown staining is present in the CFC ECM of wild type animals while no ECM staining is observed in control *Bsp*^{-/-} entheses. Cells located in the UFC however stain positive in both wild type and *Bsp*^{-/-} mice, indicating that the BSP antiserum possesses some nonspecific binding activity. In the 15 week and 14 month old mice we were interested in showing that BSP is present in the ECM, and as cellular nonspecific staining is a common problem in IHC stains, this issue was not addressed at these time points. In the analysis of the 14 and 21 day old animals, where little mineral is present and uncalcified regions of fibrocartilage are more abundant, nonspecific cellular staining was much more evident. At these time points we were interested in whether BSP protein could be detected in the ECM and the cells of the developing enthesis, which would eventually become the CFC, however the non-specific staining prevented us from adequately addressing this question. A new protocol was developed for both BSP and

OPN antisera, which was intended to reduce the amount of nonspecific cellular staining. The altered protocol was effective in reducing nonspecific staining in OPN antiserum, however this protocol was less effective for the BSP antiserum, since it drastically reduced the staining intensity of both specific staining in bone and nonspecific cellular staining. Indeed, the BSP research field in general lacks an effective anti-BSP antibody. While numerous biotech companies claim to provide anti-BSP antibodies, none so far have produced an antibody that adequately meets the demands of all of the researchers in the field.

To conclude, these studies have shown that loss of BSP results in an increased lengthening of the CFC of the QCT entheses in 14 month old mice beyond what was observed in 15 week old animals. This observations suggests a defect in the regulation of CFC growth in the QCT entheses in the absence of BSP. All other parameters measured in 14 month old mice remained unaffected by the loss of BSP. During development, BSP and OPN are not present in 14 day old murine entheses. In 21 day old entheses small amounts of these proteins may be present in the SST entheses, but are absent in the QCT entheses reflecting the amount of mineral present in entheses studied at these times. This observation suggests that BSP and OPN are restricted to mineralized sites in the entheses. Further characterization at 28 and 42 days post-natal is warranted to uncover BSP's role in entheses development and mineralization.

3.6 References

- Baht, G.S., Hunter, G.K., Goldberg, H.A., 2008. Bone sialoprotein–collagen interaction promotes hydroxyapatite nucleation. *Matrix Biol.* 27, 600–608.
- Benjamin, M., McGonagle, D., 2001. The anatomical basis for disease localisation in seronegative spondyloarthropathy at entheses and related sites. *J. Anat.* 199(Pt 5), 503–26.
- Bianco, P., Fisher, L.W., Young, M.F., Termine, J.D., 1991. Expression of bone sialoprotein (BSP) in developing human tissues. *Calcif. Tissue Int.* 49(6), 421–6.
- Bouleftour, W., Boudiffa, M., Wade-Gueye, N., Bouët, G., Cardelli, M., Laroche, N., Vanden-Bossche, A., Thomas, M., Bonnelye, E., Aubin, J., 2014. Skeletal Development of Mice Lacking Bone Sialoprotein (BSP)-Impairment of Long Bone Growth and Progressive Establishment of High Trabecular Bone Mass. *PLoS One* 9, e95144.
- Chen, J., Shapiro, H., Sodek, J., 1992. Developmental expression of bone sialoprotein mRNA in rat mineralized connective tissues. *J. Bone Miner. Res.* 7, 987–997.
- Fisher, L., Fedarko, N., 2003. Six Genes Expressed in Bones and Teeth Encode the Current Members of the SIBLING Family of Proteins. *Connect. Tissue Res.* 44, 3340.
- Ganss, Kim, R.H., Sodek, 1999. Bone Sialoprotein. *Crit. Rev. Oral Biol. Med.* 10, 79–98.
- Genin, G.M., Kent, A., Birman, V., Wopenka, B., Pasteris, J.D., Marquez, P.J., Thomopoulos, S., 2009. Functional grading of mineral and collagen in the attachment of tendon to bone. *Biophys. J.* 97, 976–85.
- Holm, E., Aubin, J.E., Hunter, G.K., Beier, F., Goldberg, H.A. 2015. Loss of bone sialoprotein leads to impaired endochondral bone development and mineralization. *Bone* 71, 145–54.
- Hunter, G.K., Goldberg, H.A., 1993. Nucleation of hydroxyapatite by bone sialoprotein. *Proc. Natl. Acad. Sci. U.S.A.* 90, 8562–5.
- Schwartz, A.G., Pasteris, J.D., Genin, G.M., Daulton, T.L., Thomopoulos, S., 2012. Mineral distributions at the developing tendon enthesis. *PLoS One.* 7, e48630.
- Vandenbergh, J.G., 1967. Effect of the presence of a male on the sexual maturation of female mice. *Endocrinology* 81, 345–349.
- Zelzer, E., Blitz, E., Killian, M., Thomopoulos, S., 2014. Tendon- to- bone attachment: From development to maturity. *Birth Defects Res. C Embryo Today* 102, 101–12.

CHAPTER FOUR

GENERAL DISCUSSIONS AND CONCLUSIONS

4.1 Summary and Perspectives

Fibrocartilaginous entheses are transitional structures that connect tendons and ligaments to bone and contain a region of fibrocartilage with a mineralized component. Prior to these studies, mineral-associated proteins present in the calcified fibrocartilage (CFC) of the enthesis remained essentially uncharacterized and the mechanism by which mineral is deposited in enthesis fibrocartilage left unidentified. Bone sialoprotein (BSP) is an extracellular matrix protein commonly found in mineralizing tissues and has potent hydroxyapatite nucleating, collagen binding and cell signaling properties (Goldberg and Hunter, 2012). BSP has recently been implicated in the connection of periodontal ligament to the root of the tooth (Foster et al., 2013). The studies reported in this thesis have identified the presence of the mineral associated proteins BSP and OPN in the calcified tissues of the murine fibrocartilaginous enthesis in adult animals. Furthermore, it was shown that the loss of BSP results in abnormalities in the CFC of the quadriceps tendon (QCT) enthesis. Specifically, the CFC of the QCT enthesis in adult mice is elongated, and this elongation increases with age. Mineral content within the CFC was found to be comparable between *Bsp*^{-/-} and wild type mice, as demonstrated by Raman spectroscopy and microCT. Collagen organization in the enthesis was not affected by the loss of BSP at any time point measured, in contrast to the phenotype observed in the periodontal ligament (Foster et al., 2013). During development, OPN and BSP are restricted to the mineralized regions of the enthesis. By 21 days of age, small amounts of mineral, along with BSP and OPN, can be detected in the fibrocartilage of the developing supraspinatus tendon (SST) enthesis. However, no phenotype is observed in the entheses of *Bsp*^{-/-} mice at this time point, in line with observations in the adult animal. In the QCT

entheses, mineral is not yet present in the entheses fibrocartilage by 21 days post-natal and as such, BSP and OPN are not present at this time point and no phenotype is observed in the *Bsp*^{-/-} mouse.

BSP has long been thought to be a promoter of mineralization, and there is strong *in vitro* evidence for its hydroxyapatite nucleating properties (Hunter and Goldberg, 1993). Phenotypes in the *Bsp*^{-/-} mouse such as delays in early mineralization in the long bones (Bouleftour et al., 2014; Holm et al., 2015); defects in bone repair after injury (Malaval et al., 2009); and acellular cementum deficiencies (Foster et al., 2013), are small, but also point towards BSP being a promoter of mineralization. The phenotype observed in the *Bsp*^{-/-} entheses, however, suggests a different role for BSP in this tissue. The extension of the QCT CFC indicates that more mineral, not less, is present in the *Bsp*^{-/-} fibrocartilaginous entheses. BSP's expression at sites where mineralization is actively occurring has long been established (Bianco et al., 1991), and BSP is particularly abundant at mineralization fronts in bone (Bianco et al., 1993). Recently it was shown that active mineralization in the entheses occurs in a narrow band of Indian hedgehog (IHH) producing cells at the tidemark and that there is little turnover in entheses fibrocartilage once formed (Dyment et al., 2015). Thus it seems likely that BSP is active at the tidemark. It would appear that at the entheses mineralization front, BSP is acting as a regulator of mineralization, controlling mineral deposition at this site to ensure that the tissue is the appropriate size and the mineral gradient at the tidemark is properly formed. A delicate balance between pro- and anti-mineralization factors must occur at the tidemark, and the phenotypes observed in the *Bsp*^{-/-} fibrocartilaginous entheses suggest that BSP is one of possibly a number of factors active at this site. In BSP's absence, the

balance is disrupted, with other pro-mineralization factors compensating for BSP, driving excess mineralization at the tidemark.

4.2 Limitations of Research and Future Directions

4.2.1 *Phenotypic differences in different entheses and the role of muscle loading*

A curious observation of these studies is that while alterations are present in the mineralized tissues of the QCT enthesis, there is an apparent lack of a phenotype in the SST enthesis. It is reasonable to assume that because both are fibrocartilaginous entheses, loss of BSP would result in the same phenotypic observations in both structures. However, in fibrocartilaginous entheses there are factors beyond biological and genetic ones that influence the structure's development.

The role of mechanical factors in the development of the tissues of the musculoskeletal system are well established (Galloway et al., 2013; Gkiatas and Lykissas, 2015), and the role of mechanical cues in the enthesis has been analyzed as well. In entheses that display a large change in insertional angle during joint movement, a larger region of uncalcified fibrocartilage (UFC) is observed (Benjamin and McGonagle, 2001; Benjamin and Ralphs, 1998). Since this enthesis zone is more pliable than either tendon or the CFC, researchers have hypothesized that the increased amount of UFC aids in smooth movement of the joint during its total range of movement. Gao and Messer suggest that the size of the CFC is determined by the tensile load that the enthesis is under at puberty (Gao and Messner, 1996). When the shoulder muscles of newborn mice are paralyzed with botulinum toxin, decreased mineralization near the SST enthesis in the

bone was observed at 21 days of age and fibrocartilage failed to form at the insertion (Thomopoulos et al., 2007).

Since the genetic factors at the QCT and SST entheses in the *Bsp*^{-/-} mouse are the same, the anatomical location and function of these entheses must be considered. The muscles attached to the QCT are some of the largest and most powerful muscles in the body, in both mice and humans. Located on the anterior surface of the femur, they are involved in the extension of the leg and are used extensively during locomotion. The QCT inserts directly into the back of the patella rather than obliquely or by wrapping around another anatomical feature. As such, the tensile force on the QCT enthesis under load is large and the insertional angle is small. In contrast, the supraspinatus muscle is located in the shoulder and its contraction drives the initiation of abduction of the arm at the shoulder joint. The muscle is smaller than the quadriceps muscles and produces loads of a lower magnitude. Furthermore the SST makes contact with bone at an oblique angle, wrapping around the head of the humerus before inserting at the SST enthesis. As such the nature of the loads in the QCT and SST entheses are quite different, and these differences may be the cause of the discrepancies in phenotypes observed in the *Bsp*^{-/-} mouse. In order to investigate the interplay between muscle load and BSP's regulatory role in enthesis development, paralysis experiments, such as those described above, on the lower limbs of *Bsp*^{-/-} mice should be considered.

4.2.2 *Establishing the expression of BSP in the enthesis*

While these studies have established the presence of BSP and OPN protein in the enthesis, the question of whether these proteins are expressed in the enthesis remains

unanswered. Fibrochondrocytes of the enthesis have much in common with the chondrocytes of the growth plate (Zelzer et al., 2014), and BSP expression in hypertrophic chondrocytes has been demonstrated via *in situ* hybridization experiments (Bianco et al., 1991). It seems reasonable that the fibrochondrocytes of the CFC are the source of the BSP and OPN identified in the matrix. However, observations in 14 and 21 day old mice indicate that BSP and OPN are restricted to mineralized tissues in the enthesis, if present, and to bone, with no matrix staining present in the regions of the enthesis that have not yet become mineralized. BSP and OPN have a high binding affinity for hydroxyapatite (HA) (Goldberg et al., 2001), and as such, BSP and OPN could be expressed exogenously and become localized to the CFC by virtue of their acidic domains rather than being expressed endogenously within the tissue.

In hopes of determining if BSP is expressed by enthesis fibrochondrocytes, real time quantitative PCR (qPCR) experiments were attempted but were ultimately unsuccessful. In order to harvest mRNA from enthesis fibrochondrocytes for qPCR analysis, a laser capture microdissection (LCM) procedure was employed to specifically isolate fibrochondrocytes from the enthesis and avoid contamination with cells from bone and/or tendon. The LCM apparatus is a standard optical microscope equipped with a high power cutting laser and a low power catapult laser. It allows a user to examine a histological section and select specific regions to excise with the cutting laser. The excised specimen is then catapulted into a collection tube by the catapult laser for subsequent analysis.

LCM is traditionally used on soft tissues to isolate specific cell types for qPCR analysis. Working with a mineralized tissue such as the enthesis present unique

challenges. Traditional histological analysis of mineralized tissue involves a lengthy decalcification process. The protocol used by our laboratory immerses tissue in high molarity EDTA for 3 weeks at 37 °C. Due to the unstable nature of RNA molecules, cryosectioning of fresh tissue prior to LCM is required to acquire sufficient mRNA yields for qPCR analysis. This necessitated the development of a method to section through solid patellae quickly to preserve RNA integrity while maintaining the structure of the tissue, so that the enthesis could be easily identified and excised during LCM. To overcome this obstacle we utilized a blade made of tungsten carbide, which is much harder than traditional stainless steel blades, which allowed us to cleanly cut fresh patellar sections without tearing the tissue. Although this method was ultimately not useful for obtaining RNA from enthesal tissue, it was critical to facilitate our Raman spectroscopy studies, which also required fresh, undecalcified tissue sections.

qPCR functions on the premise that the amount of RNA present in a sample is proportional to the number of PCR cycles the sample must undergo before reaching a critical threshold (CT) in which the PCR amplification becomes exponential. Data returned from qPCR analysis on enthesis fibrochondrocytes yielded CT values in the range of 30-40 PCR cycles, well beyond the range which is considered reliable (generally 25 cycles or lower). This data indicates that very little to no RNA was present in our qPCR reactions, indicating a poor yield from the LCM extraction protocol. When considering the nature of the tissue under study and the process used, low RNA yield is understandable. Fibrocartilage in general is a hypocellular tissue, with each CFC section taken containing perhaps 40 cells. Several sections per individual were pooled together for qPCR analysis, however this did not appear to ameliorate the issue. Furthermore,

tissue used in this study was taken from animals 15 weeks of age. At this age the fibrochondrocytes of the CFC are mature and are not likely to strongly express matrix genes, and so BSP and OPN mRNA are likely sparse in these cells to begin with. This study highlights the many obstacles and difficulties present in conducting gene expression experiments on the mineralized tissues of the enthesis. Liu *et al.* did successfully perform qPCR analysis via LCM on enthesis fibrocartilage, however in this study tissue was taken from a developing enthesis in juvenile mice (age 14 days) and no mineralized tissue was present at this time (Liu et al., 2013). *In situ* hybridization is another commonly used technique to detect the presence of specific RNA molecules in tissues and our laboratory is currently pursuing experiments of this nature on enthesis fibrocartilage to establish BSP and OPN expression there.

4.2.3 Other potential mineralization factors in the enthesis

In line with other mineralized tissues, excluding acellular cementum, loss of BSP in the enthesis does not cause a gross inability to form calcified tissue in the enthesis. Biomineralization is a complex and multifactorial process with a great deal of functional redundancy between the different players that regulate mineralization. Here we have identified two mineral associated proteins in the enthesis, and partially characterized the role of one factor involved in the formation of the CFC. In order to have a more complete understanding of the mechanism and regulatory network that controls formation of enthesis CFC, additional mineralization factors must be identified.

One potential candidate is dentin matrix protein 1 (DMP1), a fellow member of the SIBLING family with similar properties to BSP. Originally thought to be specific to

dentin, DMP1 has been identified in bone, cartilage and cementum as well (D'souza et al., 1997; Feng et al., 2003; George et al., 1995; Hirst et al., 1997; Macdougall et al., 1998). DMP1 possesses an RGD integrin-binding motif (Kulkarni et al., 2000), and has been reported to bind collagen in the hole zones (He and George, 2004), and promote mineral deposition. Under some conditions DMP1 can act as a nucleator of HA formation (He et al., 2003); however, under other conditions it can act as an HA inhibitor (Silverman and Boskey, 2004). Thus, there is still controversy in the field regarding the role of DMP1 in mineralization. During the course of the studies outlined in this thesis, DMP1's presence in enthesis fibrocartilage was probed as well. Immunohistochemistry revealed inconsistent results for DMP1 localization, with some entheses strongly staining for DMP1, while others stained weakly and in some no staining at all was detected. The presence or absence of staining did not correspond with BSP genotype and surprisingly, different entheses taken from the same mouse displayed different staining results. Further investigation is required to elucidate the reasons accounting for DMP1's erratic staining pattern in the enthesis.

Another potential mineralization factor in the enthesis is asporin, so named because it is a member of the small leucine-rich repeat proteoglycan family which includes decorin and biglycan, and because it possesses a contiguous sequence of aspartate (Asp) residues in its N-terminal domain (Henry et al., 2001). Asporin binds type I collagen, which is competitively inhibited by decorin, indicating that the two proteins occupy the same binding site (Kalamajski et al., 2009). Asporin's poly D sequence appears to possess calcium-binding properties (Kalamajski et al., 2009), similar to the properties conferred to BSP and OPN by their acidic domains (Goldberg et al., 2001). In

osteoblast cell culture, addition of asporin to culture media results in an increase in mineral nodule formation and expression of the osteoblastic cell markers osterix and Runx2, as shown by qPCR (Kalamajski et al., 2009). In a study of smoothen (Smo) knock-out mice, Liu *et al.* identified *Aspn* mRNA in developing enthesis fibrocartilage using RNAseq and qPCR. In mice in which the *Smo* gene is ablated (*Smo*^{-/-}), enthesis fibrocartilage fails to mineralize and RNAseq and qPCR analysis indicate that there is a 3.9 fold reduction in *Aspn* expression in *Smo*^{-/-} enthesis fibrocartilage (Liu et al., 2013). Clearly asporin plays some role in the mineralization process of enthesis fibrocartilage however further studies are required, as the presence and localization of asporin protein in the enthesis has not yet been established.

Ultimately it is hoped that the search for factors and molecules that regulate mineral deposition and enthesis development will lead to advances in enthesis repair, specifically in tissue engineering. Numerous cell, growth factor and biomaterial based implants and grafts have been developed in an attempt to regenerate the complex transitional zones of the enthesis, however none so far have successfully created a biocompatible material with the same mechanical properties of the native enthesis (Lu, 2013). Currently, the major hurdle in clinical translation of these therapies is successful integration of the graft into the existing musculoskeletal system. Given its cell binding properties and its apparent role in the regulation of the formation of the CFC, BSP may ultimately prove to be a useful molecule in the reattachment of tendons and ligaments into bone.

4.3 Conclusions

These studies have identified the SIBLING proteins BSP and OPN in the CFC of the murine fibrocartilaginous enthesis, showing for the first time the presence of these mineral associated proteins in the enthesis. The enthesis phenotype of mice that lack BSP was examined in order to elucidate the role of BSP in enthesis fibrocartilage. In the absence of BSP, the growth of the CFC appears to be dysregulated in the QCT enthesis, which continues to increase in size well into adulthood. In the absence of BSP, the body may compensate with an increase in the cross-sectional area of tendons in the *Bsp*^{-/-} mouse. Due to the known properties of BSP, it may still be involved at the mineralization front of the fibrocartilaginous enthesis where it likely contributes to a complex network of proteins which act to control the growth of the CFC and regulate mineral deposition in the enthesis. As such, BSP may ultimately prove to be a useful molecule in the reattachment of tendons and ligaments into bone.

4.4 References

Benjamin, M., McGonagle, D., 2001. The anatomical basis for disease localisation in seronegative spondyloarthropathy at entheses and related sites. *J. Anat.* 199(Pt5), 503-26.

Benjamin, M., Ralphs, J.R., 1998. Fibrocartilage in tendons and ligaments--an adaptation to compressive load. *J. Anat.* 193 (Pt 4), 481–94.

Bianco, P., Fisher, L.W., Young, M.F., Termine, J.D., Robey, P.G., 1991. Expression of bone sialoprotein (BSP) in developing human tissues. *Calcif. Tissue Int.* 49(6), 421-6.

Bianco, P., Riminucci, M., Bonucci, E., Termine, J.D., Robey, P.G. 1993. Bone sialoprotein (BSP) secretion and osteoblast differentiation: relationship to bromodeoxyuridine incorporation, alkaline phosphatase, and matrix deposition. *J. Histochem. Cytochem.* 41, 183–91.

Bouleftour, W., Boudiffa, M., Wade-Gueye, N., Bouët, G., Cardelli, M., Laroche, N., Vanden-Bossche, A., Thomas, M., Bonnelye, E., Aubin, J., 2014. Skeletal Development of Mice Lacking Bone Sialoprotein (BSP)-Impairment of Long Bone Growth and Progressive Establishment of High Trabecular Bone Mass. *PLoS One.* 9, e95144.

D'souza, R.N., Cavender, A., Sunavala, G., Alvarez, J., Ohshima, T., Kulkarni, A.B., MacDougall, M., 1997. Gene expression patterns of murine dentin matrix protein 1 (Dmp1) and dentin sialophosphoprotein (DSPP) suggest distinct developmental functions in vivo. *J. Bone Miner. Res.* 12(12), 2040-9.

Dyment N.A., Breidenbach A.P., Schwartz A.G., Russell R.P., Aschbacher-Smith L., Liu H., Hagiwara Y., Jiang R., Thomopoulos S., Butler D.L., Rowe D.W., 2015 GDF5 Progenitors Give Rise To Fibrocartilage Cells That Mineralize Via Hedgehog Signaling To Form The Zonal Entesis. *Dev. Biol.* doi: 10.1016/j.ydbio.2015.06.020 [Epub ahead of print].

Feng, J.Q., Huang, H., Lu, Y., Ye, L., Xie, Y., 2003. The Dentin matrix protein 1 (Dmp1) is specifically expressed in mineralized, but not soft, tissues during development. *J. Dent. Res.* 82(10), 776-80.

Foster, B.L., Soenjaya, Nociti, F.H., Holm, Zerfas, P.M., Wimer, H.F., Holdsworth, D.W., Aubin, J.E., Hunter, G.K., Goldberg, H.A., Somerman, M.J., 2013. Deficiency in Acellular Cementum and Periodontal Attachment in Bsp Null Mice. *J. Dent. Res.* 92, 166–72.

Galloway, M.T., Lalley, A.L., Shearn, J.T., 2013. The role of mechanical loading in tendon development, maintenance, injury, and repair. *J. Bone Joint Surg. Am.* 95, 1620–8.

- Gao, J., Messner, K., 1996. Quantitative comparison of soft tissue-bone interface at chondral ligament insertions in the rabbit knee joint. *J. Anat.* 188 (Pt 2), 367–73.
- George, A., Silberstein, R., Veis, A., 1995. In situ hybridization shows Dmp1 (AG1) to be a developmentally regulated dentin-specific protein produced by mature odontoblasts. *Connect. Tissue Res.* 33(1-3), 67-72.
- Gkiatas, I., Lykissas, M., 2015. Factors Affecting Bone Growth. *Am. J. Orthop.* 44(2), 61-7.
- Goldberg, H.A., Warner, K.J., Li, M.C., Hunter, G.K., 2001. Binding of bone sialoprotein, osteopontin and synthetic polypeptides to hydroxyapatite. *Connect. Tissue Res.* 42(1), 25-37.
- Goldberg, H.A., Hunter, G.K., 2012. Functional domains of bone sialoprotein. In: Goldberg M., ed. *Phosphorylated extracellular matrix proteins of bone and dentin*. Vol. 2. Oak Park (IL): Bentham Science Publishers. p. 266–282.
- He, G., George, A., 2004. Dentin matrix protein 1 immobilized on type I collagen fibrils facilitates apatite deposition in vitro. *J. Biol. Chem.* 279(12), 11649-56.
- He, G., Dahl, T., Veis, A., George, A., 2003. Nucleation of apatite crystals in vitro by self-assembled dentin matrix protein 1. *Nat. Mater.* 2(8), 552-8.
- Henry, S.P., Takanosu, M., Boyd, T.C., Mayne, P.M., 2001. Expression Pattern and Gene Characterization of Asporin a Newly Discovered Member of the Leucine-Rich Repeat Protein Family *J. Biol. Chem.* 276, 12212–12221.
- Hirst, K.L., Simmons, D., Feng, J., Aplin, H., Dixon, M.J., 1997. Elucidation of the sequence and the genomic organization of the human dentin matrix acidic phosphoprotein 1 (DMP1) gene: exclusion of the locus from a causative role in the pathogenesis of dentinogenesis imperfecta type II. *Genomics* 42(1), 38-45.
- Holm, E., Aubin, J.E., Hunter, G.K., Beier, F., Goldberg, H.A. 2015. Loss of bone sialoprotein leads to impaired endochondral bone development and mineralization. *Bone* 71, 145-54.
- Hunter, G.K., Goldberg, H.A., 1993. Nucleation of hydroxyapatite by bone sialoprotein. *Proc. Natl. Acad. Sci. U.S.A.* 90, 8562–5.
- Kalamajski, S., Aspberg, A., Lindblom, K., Heinegård, D., Oldberg, Å., 2009. Asporin competes with decorin for collagen binding, binds calcium and promotes osteoblast collagen mineralization. *Biochem. J.* 423(1), 53-9.

Kulkarni, G.V., Chen, B., Malone, J.P., Narayanan, A.S., 2000. Promotion of selective cell attachment by the RGD sequence in dentine matrix protein 1. *Arch. Oral Biol.* 45(6), 475-84.

Liu, C.F., Breidenbach, A., Aschbacher-Smith, L., Butler, D., Wylie, C., 2013. A Role for Hedgehog Signaling in the Differentiation of the Insertion Site of the Patellar Tendon in the Mouse. *PLoS One* 8, e65411.

Macdougall, M., Gu, T.T., Luan, X., Simmons, D., Chen, J. 1998. Identification of a novel isoform of mouse dentin matrix protein 1: spatial expression in mineralized tissues. *J. Bone Miner. Res.* 13(3), 422-31.

Malaval, L., Monfoulet, L., Fabre, T., Pothuau, L., Bareille, R., Miraux, S., Thiaudiere, E., Raffard, G., Franconi, J.-M., Lafage-Proust, M.-H., Aubin, J., Vico, L., Amédée, J., 2009. Absence of bone sialoprotein (BSP) impairs cortical defect repair in mouse long bone. *Bone* 45(5), 853-61.

Silverman, L., Boskey, A.L., 2004. Diffusion systems for evaluation of biomineralization. *Calcif. Tissue. Int.* 75(6), 494-501.

Thomopoulos, S., Kim, H., Rothermich, S., Biederstadt, C., Das, R., Galatz, L., 2007. Decreased muscle loading delays maturation of the tendon enthesis during postnatal development. *J. Orthop. Res.* 25, 1154–63.

Zelzer, E., Blitz, E., Killian, M., Thomopoulos, S., 2014. Tendon- to- bone attachment: From development to maturity. *Birth Defects Res. C Embryo Today.* 102, 101–12.

APPENDIX A

Statement of Permission for the Use of Animals for Experimental Research.

All animal experimentation was performed in compliance with the animal use protocol 2008-092. This protocol is held by Dr. Harvey Goldberg, a principal investigator at the Schulich School of Medicine and Dentistry and the Department of Biochemistry at the University of Western Ontario, London, Ontario, Canada.



2008-092::5:

AUP Number: 2008-092

AUP Title: Functional Characterization of Bone Sialoprotein Using the BSP-null Mouse

Yearly Renewal Date: 11/01/2013

The YEARLY RENEWAL to Animal Use Protocol (AUP) 2008-092 has been approved, and will be approved for one year following the above review date.

1. This AUP number must be indicated when ordering animals for this project.
2. Animals for other projects may not be ordered under this AUP number.
3. Purchases of animals other than through this system must be cleared through the ACVS office.
Health certificates will be required.

REQUIREMENTS/COMMENTS

Please ensure that individual(s) performing procedures on live animals, as described in this protocol, are familiar with the contents of this document.

The holder of this Animal Use Protocol is responsible to ensure that all associated safety components (biosafety, radiation safety, general laboratory safety) comply with institutional safety standards and have received all necessary approvals. Please consult directly with your institutional safety officers.

Submitted by: Kinchlea, Will D
on behalf of the Animal Use Subcommittee

APPENDIX B

Statement of Permission for the Use of Published Materials (Figure 1.2)

Dear Mr Marinovich

We hereby grant you permission to reprint the material below at no charge **in your thesis, in print and on the University of Western Ontario web site** subject to the following conditions:

1. If any part of the material to be used (for example, figures) has appeared in our publication with credit or acknowledgement to another source, permission must also be sought from that source. If such permission is not obtained then that material may not be included in your publication/copies.
2. Suitable acknowledgment to the source must be made, either as a footnote or in a reference list at the end of your publication, as follows:
“This article was published in Publication title, Vol number, Author(s), Title of article, Page Nos, Copyright Elsevier (or appropriate Society name) (Year).”
3. Your thesis may be submitted to your institution in either print or electronic form.
4. Reproduction of this material is confined to the purpose for which permission is hereby given.
5. This permission is granted for non-exclusive world **English** rights only. For other languages please reapply separately for each one required. Permission excludes use in an electronic form other than as specified above. Should you have a specific electronic project in mind please reapply for permission.
6. This includes permission for the Library and Archives of Canada to supply single copies, on demand, of the complete thesis. Should your thesis be published commercially, please reapply for permission.

Kind regards

Steph Norton :: Rights Associate :: Global Rights :: **ELSEVIER**

T: **+44 (0)1865 843325** :: F: **+44 (0)1865 853333**

E: s.norton@elsevier.com

CURRICULUM VITAE

Ryan Marinovich

UNIVERSITY EDUCATION

Candidate for Master of Science- Biochemistry **2013 - Current**

The University of Western Ontario, London, ON

Bachelors of Medical Science, Honours Specialization in the Biochemistry of Infect and Immunity, with distinction **2013**

The University of Western Ontario, London, ON

HONOURS, SCHOLARSHIPS AND AWARDS

Dean's Honour List **2010 - 2013**

- Awarded in recognition of academic success during the 2010, 2011, 2012 and 2013 academic terms

The University of Western Ontario Entrance Award of Distinction **2009 – 2010**

- Received a \$1,500 scholarship: Achieved an entering average above 85%

Graduate Teaching Assistant Award **2014-2015**

- Received a \$500 award: Selected based on merit and student feedback. One of 20 given per annum

RESEARCH-BASED HONOURS, SCHOLARSHIPS AND AWARDS

Western Graduate Research Scholarship **2014, 2015**

- \$4,500 annual scholarship awarded to graduate students entering with and maintaining a minimum 80% average

Biochemistry Undergraduate Summer Research Program**2012**

- \$6,000 studentship awarded by the biochemistry department at the University of Western Ontario to 2nd and 3rd year students to participate in the research program of a faculty member during the summer.
- Awarded to 15 students out of 69 applications selected by professors in the department based on marks, applications and references.

RESEARCH EXPERIENCE

Masters in Biochemistry Graduate Student**September 2013 – Current***Goldberg Lab, Schulich School of Medicine and Dentistry, London, ON*

- **Project title:** The Role of Bone Sialoprotein in the Tendon-Bone Insertion

Fourth Year Thesis Student**Fall 2012 – Spring 2013***Shilton Lab, Schulich School of Medicine and Dentistry, London, ON*

- **Project title:** Cloning and Purification of SecA1 and SecA2 from *Mycobacterium tuberculosis*

Biochemistry Undergraduate Summer Research Program**Summer 2012***Shilton Lab, Schulich School of Medicine and Dentistry, London, ON*

- **Project title:** *In vitro* Translocation Assay for *Escherichia Coli* SecA

PUBLICATIONS

Works in Preparation

1. **Ryan Marinovich**, Yohannes Soenjaya, Gregory Wallace, Andre Zuskov, Andrew Dunkman, Brian Foster, Vida Lam, Amin Rizkalla Frank Beier, Martha Somerman, David Holdsworth, Lou Soslowsky, Francois Laguné-Labarhet, Harvey A. Goldberg¹. The role of bone sialoprotein in the tendon-bone insertion.

PRESENTATIONS & ABSTRACTS

Canadian Connective Tissue Conference

June 2014

London, ON

- Prepared an abstract and presented a poster titled, "The Role of Bone Sialoprotein at the Tendon-Bone Insertion"

Canadian Connective Tissue Conference

May 2015

London, ON

- Gave an oral presentation entitled "The Role of Bone Sialoprotein in the Tendon-Bone Insertion"

TEACHING EXPERIENCE

Teaching Assistant: Biochemistry 3380G - Biochemistry Laboratory **2014-2015**

The University of Western Ontario, London, ON

Teaching Assistant: Biochemistry 2288A - Biochemistry and Molecular Biology for Foods and Nutrition **Fall 2014**

The University of Western Ontario, London, ON